Thesis for the Degree of Doctor of Philosophy

Cellulose nanofiber film coating for enhancing fruit preservation

과일 보관성 향상을 위한 셀룰로오스 나노파이버 필름 코팅

August 2021

Seoul National University
Department of Biosystems & Biomaterials Science and Engineering

Kwak, Hojung

Cellulose nanofiber film coating for enhancing fruit preservation

Advised by Prof. Hyun, Jinho

Submitting a Ph.D. Dissertation of Agriculture
May 2021

Seoul National University
Department of Biosystems & Biomaterials
Science and Engineering

Kwak, Hojung

Confirming the Ph.D. Dissertation written by
Kwak, Hojung

July 2021

Chair	Lee, Ki Hoon
Vice Chair	Hyun, Jinho
Examiner	Ki, Chang Seok
Examiner	Kwak, Seon-Yeong
Examiner	Yun, Kyusik

Abstract

Cellulose nanofiber film coating for enhancing fruit preservation

Department of Biosystems & Biomaterials Science and Engineering

Seoul National University

Hojung Kwak

Cellulose pulp is nanofibrillated through carboxymethylation (CM) and grinding process, and the prepared cellulose nanofiber (CNF) is applied to the surface of fruits to enhance their storage period and freshness. CM-CNF forms ionic crosslinks through electrostatic interaction with divalent cations. The networked film structure improves mechanical properties and exhibits a gas barrier effect. As the CM time is increased, the diameter of CNFs is decreased, the surface area is increased, and the degree of substitution is increased. As the degree of substitution increased, the negative charge at the CM-CNF surface is increased, and an electrostatic repulsive force is formed between the CM-CNFs. For this reason, the dispersibility and colloidal stability of the CM-CNF suspension solution are improved. The high dispersibility of CM-CNF is crucial in improving transparency and physical properties of the film during production process. The addition of magnesium and calcium ions improves the tensile strength of the CM-CNF film by cross-linking, and reduces the hydrophilicity of the film by reducing the ionic carboxyl groups. The CM-CNF film with reduced hydrophilicity decreases water vapor permeability in a high-humidity environment.

The improvement of fruit storability with CM-CNF film is confirmed by applying it to strawberries which are non-climacteric fruits, and bananas which are climacteric fruits. Because ripening of fruit proceeds through respiration, it is important to prevent the inflow of oxygen required for respiration and the evaporation of moisture inside the fruit. The CM-CNF film significantly reduces the amount of carbon dioxide generated in the respiration process by blocking the inflow of oxygen required for respiration of fruits, and suppresses weight loss by preventing moisture

evaporation of fruits. The improvement of fruit storability can be confirmed by observing the delayed firmness, and the change of total soluble solids and acidity of the fruit. Fruits coated with CM-CNF film have a reduced ripening rate and remain fresh for a relatively long time.

Keyword: Cellulose nanofiber (CNF), Carboxymethylation, Electrostatic interaction, Food preservation.

Student Number: 2017-32983

Table of Contents

List of Figures

I. Introduction

Currently, as the problem of food shortage is emerging, various efforts are made worldwide to solve the problem by improving the storability of fresh food [1-3]. As one of the methods to solve this problem is through improving storage properties by coating a polymer film on the surface of food is being actively studied by researchers [4,5]. Such polymer film can reduce external impact by coating on the food surface. In addition, it prevents the movement of water, gas and solutes to improve the storage properties of food [6-8]. In particular, the demand for food films derived from natural polymers is increasing [9,10]. Natural polymer materials can be more easily decomposed than conventional petroleum-derived films and have the advantage of reducing environmental pollution [11,12]. Also, high availability in nature, and characteristic of being able to manufacture a film suitable for the properties of food by using various derivatives [13-15]. The polymer film materials for food that have all these advantages and features will help improve the application range of natural polymer materials.

Cellulose nanofiber (CNF) is a major component in most plants and microalgae and is produced by some bacteria [16, 17]. Therefore, it is easy to obtain raw materials and has eco-friendly characteristics [18,19]. Furthermore, the thickness and shape of CNF can be controlled through chemical and physical processes [20-22]. In addition, when dried the film is transparent and

has very low gas permeability [23-25]. Through these advantages, CNF is attracting attention as an excellent food polymer film material and reinforcing agent. W. Wang et al. produced a film for food by compounding CNF and gelatin through the electrostatic interaction [26]. Also, glycerol was used as a plasticizer, and the effect of improving the physical properties and barrier properties of the film was confirmed. Furthermore, T. Wang et al. used CNF as a binder to produce a food film by complexing Zein, Pectin, and Precipitated Calcium Carbonate (PCC) [27]. Zein, Pectin and PCC are dispersed in CNF to form a single layer, which was then spray coated with the wax. The surface of the film was super hydrophobic, and the barrier properties were improved. Moreover, K. Zhao et al. complexed with CNF through electrostatic interaction with alginate and chitin [28]. It was confirmed that the physical properties of the film were changed according to the change in the film manufacturing method, and the blending method had a higher effect than the layer by layer method. Through the above studies, it was found that CNF was mixed with various polymers to improve film properties and barrier properties. However, there was a limitation in that the manufacturing process that make it very complicated and a large amount of material was consumed. In addition, it was difficult to evaluate the effectiveness because there was no application test suitable for the characteristics of the actual food.

In this study, a food film in which CNF and divalent cation (DC) were

complexed through electrostatic mutual bonding was attempted. It was aimed at improving the physical properties and barrier properties of the film and simplifying the manufacturing process. In addition, the prepared film was applied to fresh food such as fruit, vegetable, and dairy product to evaluate the degree of improvement in storability. First of all, carboxymethylation of CNF was performed in order to improve the dispersibility of the solution phase and increase the transparency. After optimizing the carboxymethylation reaction time, a negative charge was introduced on the surface of CNF. Thereafter, CNF hydrogels were fabricated through electrostatic interaction with magnesium and calcium ions and dried to evaluate the film properties and barrier properties. The applicability test was conducted by selecting strawberry, which is a non-climacteric fruit, and banana, which is a climacteric fruit. In addition, it was attempted to compare the degree of browning of banana peels by mixing red cabbage extract. Currently, the application of CNF is being analyzed in various ways in the food industry. As a representative material of natural polymers, CNF is attracting attention because it is eco-friendly and can be used in various ways. Through the above study, CNF film have shown great potential for its applicability in the food industry.

II. Literature survey

2.1. Background of enhancing the food preservation

Food preservation is a storage method for long-term storage of food. By conserving food, human societies can promote and enhance food security through stable food storage [29,30]. It can also reduce the impact of food production on the environment [31]. For this reason, food preservation has long been developed in various ways. It is important to survey the background of food preservation for acquiring the point of food preservation film.

2.1.1. Importance of food preservation

Through the flow of history, it is found that food preservation was essential for supporting the human life. There are three reasons why the food preservation is important in human life.

1. Food preservation could be protected from spoilage of bacteria, fungi and other types. In other words, it could be prevented human from infection related to bacteria, fungi and other types of organism [32]. Infection through foods is one of the fatal hazards to humans, especially when eating food that has been degraded by bacteria [33]. To prevent these risk factors, food processing, storage and packaging have been developed for a long time [34]. Food preservation is a basic step to maintain human life.

2. Food preservation allows humans to achieve a nutritional balance. Humans are required to provide balanced nutrition for the entire period of their lives in order to live a healthy life. The supply of vitamins and minerals, including essential nutrients, can be supplemented by food intake. If the food preservation period is short, humans can become nutritionally unbalanced. In addition, the human immune system is weakened and the average life span is shortened [35]. Food preservation is one of the important factors in improving the average life span of humans. Therefore, it is expected that there will be a rapid development of technical and economic factors in the future.

3. Food preservation stabilizes food prices and maintains economic stability. Food is an essential element in human life, and it allows us to achieve a

balance through the laws of supply and demand [36]. In particular, the instability of food prices is one of the important causes of rising inflation. If such instability continues, it can adversely affect economic development and pose a threat to the country. Therefore, in order to satisfy the continuous demand, the commodity value of food is one of the important factors that increase the price of food. Due to these economic reasons, the development of food preservation methods has rapidly developed into the modern society [37].

2.1.2. Traditional methods of food preservation

The widely known food preservation method is wax coating on the surface of food. It was applied in china in the 12th century for retain the water contents and respiration rate [38,39]. Lemon and citrus was coated with beeswax and stored because of its short shelf life [40]. The first developed film “Yuba” for food preserving was shown in japan in the 15th century [41,42]. It was produced by boiling soy milk proteins on the pan and then air dried a day [43]. In 16th century England, a method of coating the surface with a lard was introduced to maintain the freshness of meats [44]. It was known as “larding” until now. It has advantage to prevent spoiling the bacteria, yeast and fungi in the surface of meats [45]. Hot melt paraffin waxes were commercial storage method that was noted in the United States since the 1930s [46,47]. It helped to enhance the shelf life of citrus fruits. Paraffin waxes was spread in the fruit surface suppresses the evaporation of the moisture. And also, it is not absorbed into the human body but is ejected by excretion activity in the digestive system [48]. In the 1950s, oil-in-water emulsions with carnauba wax were advanced [49,50]. It was extracted from the parm tree leaves in the Brazil [51]. It also applied for enhancing the shelf life of fresh fruits and vegetable. In the 20th century, various application of food preservation is commercially applied. There are few examples with casings for sausages, chocolate coatings for fruits [52,53]. Various attempts have long been made to preserve food. Food is essential to prolong the human

life, so the efforts to be made to improve preservation will continue in the future.

2.2. Food presevation film

Recently, researchers are paying attention to food presevation film as one of the modern industrial techniques to increase the shelf life of fresh food. This is because it has distinct advantages over traditional non polymeric packaging [54]. It is able to be eaten, without the need to throw and unpack the film, which is important advantage of being biodegradable and environmental friendly. In particular, natural polymers favor to conduct with high stability and degradability. The materials of food preservation film are typically used polysaccharides, proteins, and lipids [55].

2.2.1. Materials for fabricating food preservation film

Polysaccharides are long-chain polymers consisted of mono or disaccharide repeating units linked by glycosidic bonds [56]. It is easy to get and cheap. It can act as a gas barrier due to its low gas permeability [57]. However, water vapor transmission rate is relatively higher than other materials of food preservation film, so it needs to be supplemented [58].

Starch is a polymer of D-glucopyranosyl consisting of linear chain (amylose) and branched chain (amylopectin). It is odorless, tasteless, colorless, non-toxic, biologically absorbable and semi-permeable to CO_2 and O_2 [59,60]. On the other hands, food preservation film based on starch should require plasticizers to enhance their flexibility. And It has too high hydrophilicity surface to protect from water vapor.

Chitin is second most abundant natural polymer [61,62]. Chitosan is derived from chitin by deacetylation on the alkali condition. Chitosan is able to form films without the addition of additives, exhibits great air permeability, relatively excellent mechanical properties and protect to spoilage of bacteria, yeast and molds [63]. Chitosan coatings are usually applied in vegetable and fruit such as strawberries, cucumbers, as an antimicrobial coating on apples, pears, peaches and plums as gas barriers.

Cellulose and its various derivatives are significant natural materials for acquisition of food preservation film [64]. It is most abundant natural polymers Highly crystallized Methyl cellulose (MC), hydroxypropyl methyl

cellulose (HPMC) Hydroxypropyl cellulose (HPC), and CMC have excellent film forming properties [65]. Films are typically odorless and tasteless and flexible. And also are high transparent with resistant to moisture and gas transmission [66,67].

Proteins are random copolymers with linear chain built up to 20 different monomers. The formation of protein films involves denaturation of protein initiated by heat, solvents or change in pH, followed by association of peptide chains through new intermolecular interaction [68]. Proteins have excellent film forming properties and good adherence to hydrophilic surfaces. It also provided relatively good barriers to O_2 and CO_2 [69].

Gelatin is one of major components of vertebrate skin, bone and connective tissue. It is possible to attained from hydrolysis of fibrous insoluble protein and collagen [70]. It has high contents of glycine, proline and hydroxyproline. Gelatin based films can be fabricated with 20-30% gelatin, 10-30% plasticizers and 40-70% water followed by drying the gelatin [71,72].

Soy proteins is globular protein that is isolated from soybean. It is possible to fabricate film formation on heated soymilk [73]. It is very brittle to apply as a film and needs a high proportion of plasticizers [74]. It was composited with cellulose nanofiber [75], chitin [76], and montmorillonite [77].

Corn zein is relatively hydrophobic because of high content of non-polar amino acids. Zein has good film forming properties and also can be applied for production of biodegradable films [78]. Zein films are also brittle and

require plasticizer for enhancing the flexibility [79]. Zein films have the ability to decline the ratio of weight loss and firmness loss and delay color change of foods [80].

The lipid coating is traditional method to increase shelf life of foods. It is able to block evaporation of moisture and water vapor. It is caused to improve surface appearance of various foods; fruits, vegetables, meats [81,82].

Triglyceride is constructed by ester crosslinking of fatty acids with glycerol Mono and di triglycerides [83]. It is insoluble in water. Unsaturated fatty acid is able to decrease melting point and increase moisture transfer rate. Therefore, it is important to regulate the balance between saturated fatty acid and unsaturated fatty acid [84,85].

2.2.2. Manufacture process of food preservation film

It is necessary that film solution coated on the surface of food uniformly. S This is because preservation will continue for a long time only when the whole food is protected. Therefore, the manufacturing process is one of the things that needs to be carefully considered depending on the characteristics of the food.

Dipping is the most noted methods to fabricate of food preservation film [86]. As shown in Fig. 1A, the coating is fabricated by dipping on the precursor solution directly. It is important to evaluate the properties such as viscosity, density and surface tension as well as food withdrawal speed.

Brushing method for the application of film solution to fresh vegetable and fruits (Fig. 1B). It has more efficiency to apply fresh foods than the wrapping or dipping method [87]. However, the thickness of film is not uniform and hardly to evaluate repeatability.

Spraying is conventional method in food industry. It is used when coat forming solution is relative low viscosity (Fig. 1C). Spraying system are able to fabricate a fine spray with drop size up to 20μm [88].

Panning is used to apply various layers of film onto hard surface of food, spherical particles in a batch process (Fig. 1D). For example, coating for confectionery centers. (Peanuts or almonds)

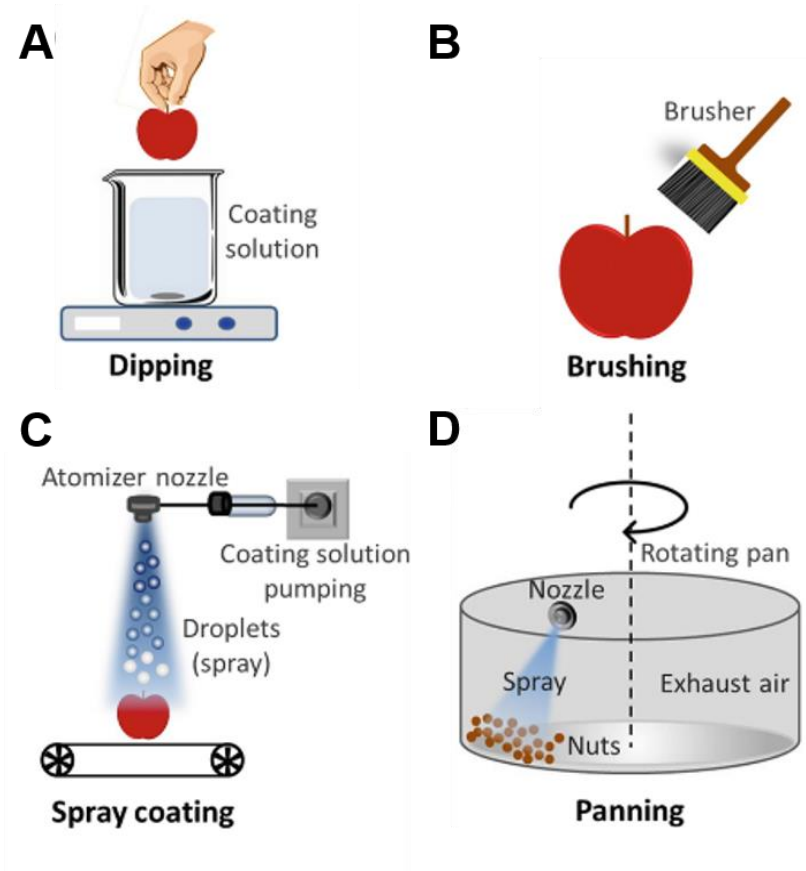

Fig. 1 Schematic images of coating methods for food preservation. A) Dipping method for coating on the surface of foods. B) Brushing method of entire surface of foods. C) Spray coating with atomizer nozzle for covering with surface of foods. D) Panning method for coating on the core (nuts or almonds) with spraying nanosized particles [89].

2.3. Cellulose

Cellulose is an organic component with the formula $(C_6H_{10}O_5)_n$ and also It is a polysaccharide consisting of a linear chain of thousands of β(1→4) linked D-glucose units [90]. It is the most abundant natural polymer on earth. The cellulose content of cotton fiber is about 90%, that of wood is 40–50%, and that of dried hemp is approximately 50% [91]. There are two types of natural cellulose, cellulose I, with structures Iα and Iβ. Cellulose produced by algae and bacteria is consist of Iα, while cellulose of higher plants has mainly component of Iβ [92]. Cellulose in regenerated cellulose fibers is cellulose II. The transformation of cellulose I to cellulose II is irreversible reaction, suggesting that cellulose II is more stable than cellulose I. With various chemical treatments it is possible to produce the structures cellulose III and cellulose IV [93]. It is one of essential properties to evaluate the degree of polymerization (DP) and chain length. The chemical formula of cellulose where n is represented the DP and the number of glucose groups. Cellulose from wood pulp generally has between 400 and 1800 units; cotton and other plant fibers as well as bacterial cellulose have chain lengths ranging from 800 to 10,000 units. [94]. Cellulose has component of fibers with crystalline and amorphous regions. These fibers can be fabricated by mechanical treatment of cellulose pulp, which is assisted by chemical oxidation or enzymatic treatment [95]. Cellulose can be treated with strong acid to hydrolyze the

amorphous fiber regions, thereby producing short and rigid cellulose nanocrystals about 80 nm in length [96]. These are of high interest due to their self-assembly into cholesteric liquid crystal, [97] production of hydrogels or films, [98] use in superior thermal and mechanical properties

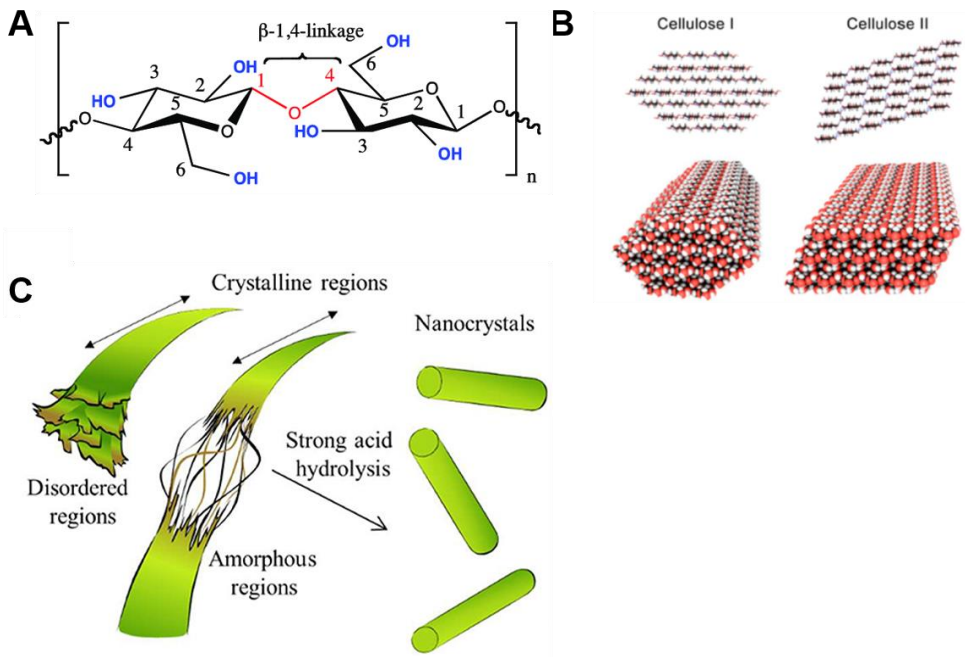

Fig. 2 Images of cellulose structures A) The molecular structures of cellobiose with β-1,4 linkage B) The 3D structure of cellulose I and cellulose II that modified the with chemical reaction [99]. C) The conceptual cellulose nanofiber structure of the crystalline and amorphous regions [100].

2.3.1. Cellulose nanofiber (CNF)

Cellulose nanofiber is linear polymer, which determine their high stiffness and strength due to the extensive intermolecular and intramolecular hydrogen bonding between molecules [101,102]. And it is a material composed of nano-sized cellulose fibers with high aspect ratio. Generally, thickness are 5–20 nanometers with a wide range of lengths [103]. It is pseudo-plastic and exhibits thixotropy, the property of gels or fluids that are viscous under normal conditions, but become less viscous when shaken or agitated [104]. When the shearing forces are removed the gel regains much of its original state. The fibers are isolated from any cellulose containing source including wood-based fibers through high-pressure, high temperature and high velocity impact homogenization, grinding or microfluidization [105].

2.3.2. Optimization to prepare CNF

CNF can be obtained from a variety of biomass resources, including wood, sugarcane bagasse, and Bacteria [106]. Most plant-derived CNFs are mixed with a variety of substances, with the exception of using bacteria, which are difficult to mass-produce (Fig. 3A). For this reason, CNFs are typically manufactured through mechanical processes. This is because substances such as hemicellulose and lignin are strongly bound [107]. Grinding is one of the representative methods for crushing CNFs (Fig. 3B). The fiber is nanosized using a rapidly rotating grinding stone. Because pulp receives a strong shear force as it passes through the grinder, repeating the process yields CNFs of 5-100 μm thickness [108]. However, it is not easy to use in industries due to limited capacity. High pressure homogenizer systems are widely used to overcome limitations (Fig. 3C). It is suitable for mass production process by making cellulose suspension and making strong force impression. However, since energy consumption is extremely high at 30000-70000 kWh/ton, research is needed to overcome the shortcomings [109]. Chemical pretreatment can be the answer to these circumstance. There is a way to hydrolyze cellulose fibers into acids or enzymes before mechanical processing. It also uses TEMPO-mediated oxidation or carboxymethylation to promote fibrillation [110].

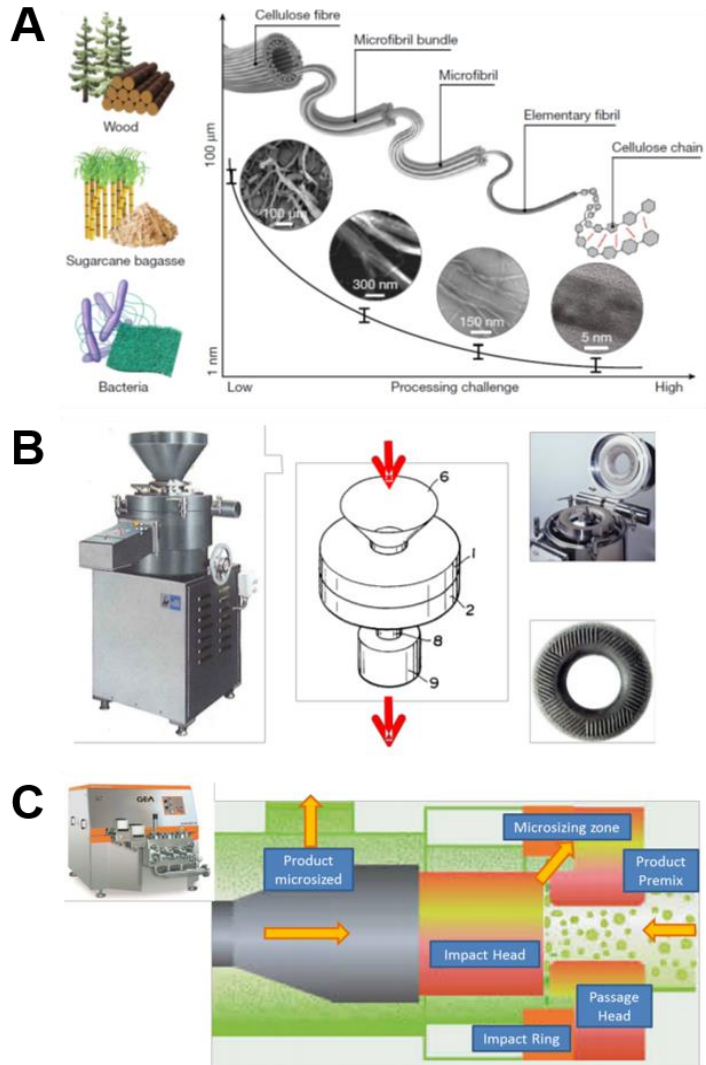

Fig. 3 A) Images of top-down process of fabrication of CNF with wood, sugarcane bagasse and bacteria [111]. B) Grinding process of CNF with parts of grinding stone. C) The mechanism of high pressure homogenizing process [112].

2.3.3. Carboxymethylation of CNF

The carboxymethylated reaction is to replace the -OH group with -CH_2COOH group in a reaction with chloroacetic acid, modifying the anionic to surface of cellulose fiber (Fig. 4). Mercerization is carried out using NaOH as pretreatment [113]. It is reduced to -O group by NaOH. The cellulose fiber is swollen by electrostatic repulsion [114]. Chloroacetic acid penetrates between the fibers and modifies the carboxymethyl group. The modification of carboxymethyl group are able to be reduced the number of grinding treatments because the fiber becomes nanosized [115]. In particular, the thickness of the fiber can be adjusted according to the time of carboxymethylation, so it can be manufactured according to the application. However, it is possible to manufacture more transparent and strong film [116].

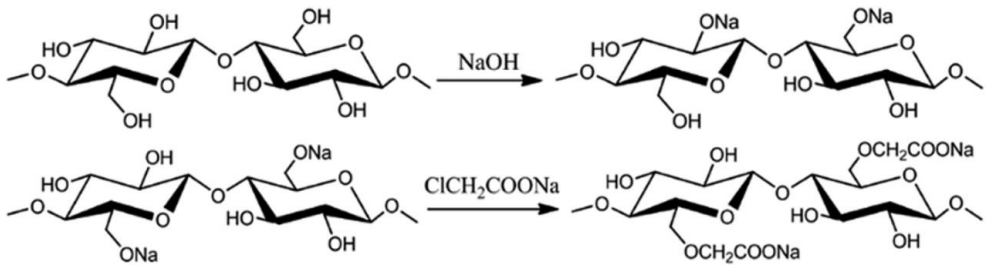

Fig. 4 The mechanism of carboxymethylation of CNF. The fiber is mercerized with sodium hydroxide. And It is swollen by water molecules into the interfibrillar space. The CNF is modified with carboxymethyl group under the chloroacetic acid with boiled condition [117].

2.4. CNF film for enhancing food preservation

2.4.1. The suitability of CNF as material of food preservation film

The food preservation film improves storage by coating the surface of the food. CNF is one of the best substances to meet various conditions. It has high transparency, high flexibility and strong mechanical properties, so supplementary materials such as plasticizer and additional are not forced [118]. And it is possible to produce eco-friendly film with simple process. CNF has excellent barrier properties. The film is formed by overlapping the fiber a reduced air permeability. The senescence process occurs through respiration on the surface of fruits and vegetables. Also, acidification promotes when meat or oil comes into contact with oxygen. As such, most foods change their condition and deteriorate in quality when they come into contact with air. Therefore, excellent barrier properties are one of the important factors when considered to choice the material for producing food preservation film [119]. And also, the CNF film is easy to remove on the surface of food. It is easy to handle because it swells quickly when it comes into contact with water.

Most foods protected by the food preservation film are stored in the refrigerator. Therefore, food preservation film must function in the environment of the refrigeration room. The environment in the refrigeration room is generally about 4°C and the relative humidity is 60%. CNF-derived film is one of the easiest materials to use in a cold room environment. This is

because CNF film does not change at refrigeration temperature unless the relative humidity rises rapidly. Therefore, it is important to measure the change in barrier properties with changes in relative humidity.

2.4.2. Electrostatic interaction with metal ion

Electrostatic interactions enhance the properties of CNFs, and allow for a variety of advantages [120]. Carboxymethyl groups are negative under the aqueous solutions. Therefore, it can be combined with various cations on the solution (Fig. 5A). In particular, strong bonds are formed by divalent cations (DC). CNF combines with DCs in wet state to produce hydrogels (Fig. 5B). Hydrogels have various properties depending on their binding forces with DCs (Fig. 5C). Properties are controllable, so suitable materials can be made easily. Controlling the fiber size is important because the surface area becomes larger as the fiber thickness of the CNF becomes thinner (Fig. 5D). In other words, the nanofibrillated CNF has more opportunities to interact with the DC.

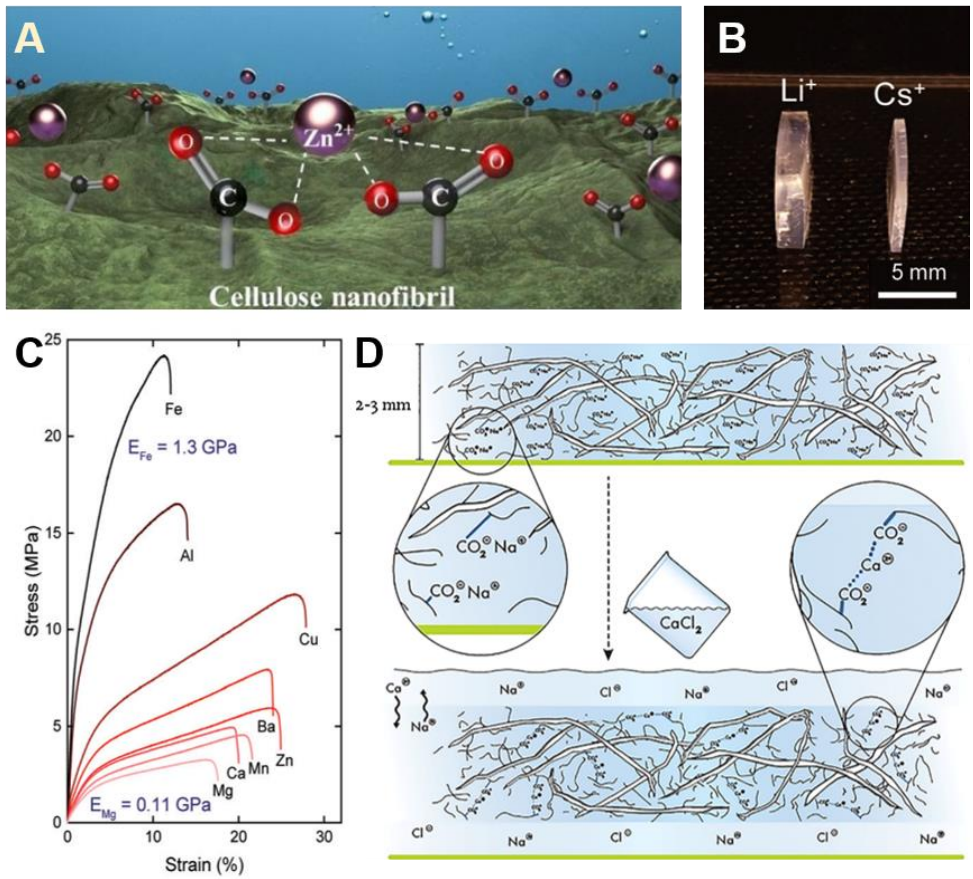

Fig. 5 A) Electrostatic interaction between carboxymethyl group of CNF and Zn^{2+} ion [121]. B) The difference of swelling property of CNF hydrogel between Li^{+} ion and Cs^{+} ion [122]. C) The tensile strength of CNF among the multivalent cations [123]. D) The mechanism of electrostatic interaction of Ca^{2+} ion with CNF [124].

2.5. Functional additives in film

There are variant functional additives in food preservation film. In particular, natural extracts are popularly analyzed to researchers. It has advantage to enhance food preservation with biodegradable and eco-friendly.

The anthocyanin components include delphinidin-3-glucoside, cyanidin-3-glucoside, and gerberin-3-glucoside in mulberries [125]. As shown in Fig. 6A, anthocyanin has been used to prepare intelligent films. The blended film could process the oxidation of heat-sensitive anthocyanin.

The curcumin is one of popular additives blended the food preservation film (Fig. 6B). It is an extract from turmeric that possesses the properties of antibacterial, anti-fungal, and antioxidant [126]. These properties could decrease microbial growth on the fruit surface while also diminishing oxygen and accelerating CO_2 in the environment which helps to preserve the freshness of the fruit.

Pomegranate (Punica granatum L.) is well-known efficacy in protection and remedy of cardiovascular diseases, and it is also contained significant healthy properties such as anticancer, antioxidant, and antimicrobial activity [127]. Pomegranate peel is known of source of phenolic compounds included, ellagic acid, lignins, catechin, epicatechin, and ellagitannins. Pomegranate peels are generally wasted without regard for their valuable properties [128].

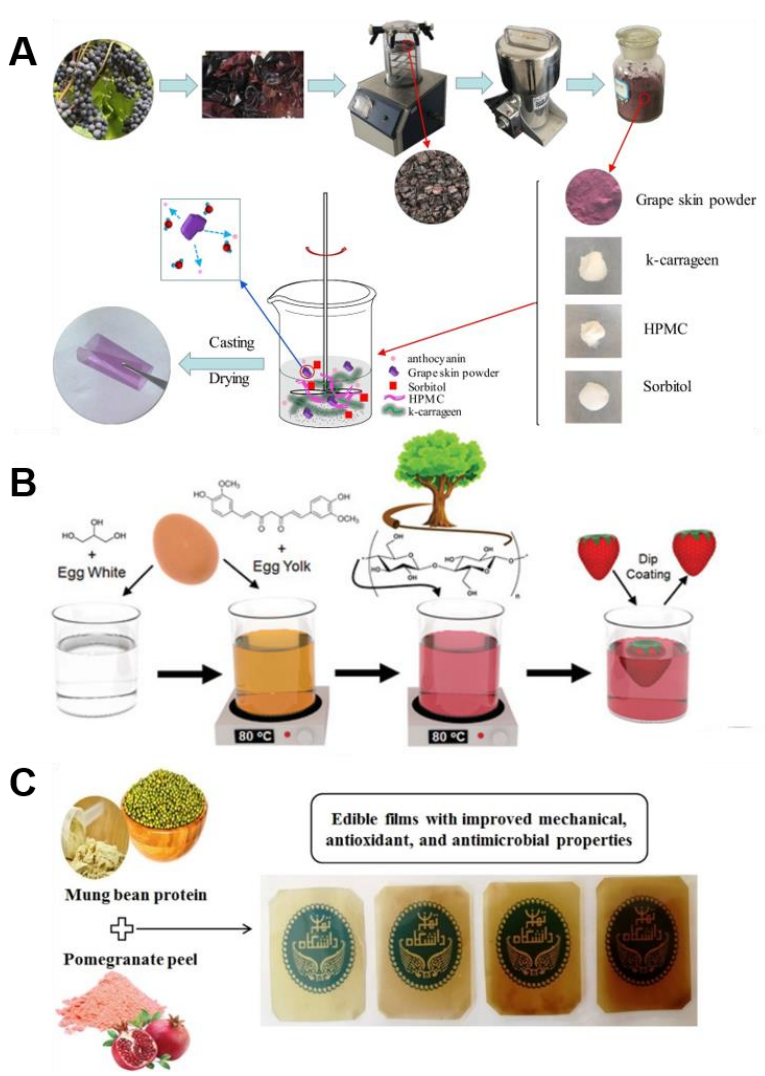

Fig. 6 A) Schematic images of CMC film composited with a κ-carrageenan and ATC [129]. B) Schematic illustration of the nanocomposite synthesis and dip-coating process on fruits. Egg albumen and glycerol are mixed in DI water, which is heated, and egg yolk and curcumin are added stepwise into the solution [130]. C) The food preservation film fabricated with mung bean protein and pomegranate peel [131].

III. Materials and methods

3.1. Materials

Never-dried bleached eucalyptus kraft pulp (79.4 % ± 0.6 % cellulose, 18.8 % ± 0.2 % hemicellulose and very little amount of lignin and byproducts) was supplied by Moorim P&P (Ulsan, Korea) [132]. Strawberries (Korean Seolhyang, Fragaria × anananssa Duch.) and bananas (Musa × paradisiaca) and red cabbage (Brassica oleracea var. capitata f. rubra) were bought in a local market. Methanol (99.5 %, Samchun, Seoul, Korea), ethanol (anhydrous 99.9 %, Samchun, Seoul, Korea), isopropanol (99.5 %, Samchun, Seoul, Korea), sodium hydroxide (98 %, Samchun, Seoul, Korea), chloroacetic acid (≥99.0 %, Sigma-Aldrich, St. Louis, MO, USA), NaCl (≥99.0 %, Sigma-Aldrich, St. Louis, MO, USA), $MgCl_2$ (anhydrous ≥98.0 %, Junsei, Saitama, Japan), $CaCl_2$ (anhydrous ≥97.0 %, Sigma-Aldrich, St. Louis, MO, USA), 1,1-Diphenyl-2-picrylhydrazyl (Free radical ≥97.0 %, TCI, Tokyo, Japan), L-tyrosine (≥98.0 %, Sigma-Aldrich, St. Louis, MO, USA), tyrosinase from mushroom (lyophilized powder, ≥1000 unit/mg solid, Sigma-Aldrich, St. Louis, MO, USA)

3.2. Preparation and characterization of CNF coating solution

Never-dried bleached eucalyptus kraft pulp used as starting raw materials. First of all, the pulp fibers were beaten using a laboratory valley beater about 30 min. For carboxymethylation and nanofibrillation, the following process was carried out using beaten pulp. The wet pulp (dry weight, 70 g) was solvent-exchanged to ethanol. It was immersed in isopropanol / methanol (3200 ml:800 ml) solution with sodium hydroxide (11.2 g). And then it was heated at 65 °C under continuous stirring for 60 min. The reaction was initiated by the addition of 14 g of monochloroacetic acid and the pulp slurry was stirred for 90 min about 700 rpm. These CM-CNF was solvent-exchanged using distilled water at pH 7.0 and passed through a grinder (Super Masscolloider, Masuko Sangyo Co., Ltd., Japan) to produce the CM-CNF precursor solution. The operation speed was 1,500 rpm and the gap distance of grinder stones were 100 μm. The final concentration of the pulp suspension was about 1.5 %, respectively [133].

3.2.1. Carboxylate contents

The carboxyl group content of the carboxymethylated pulp was determined using the ionic conductivity method. This method describes the analysis of the total acidic content of pulp fiber, and the term of the total acid group was replaced by carboxyl group content. Briefly, 1 g of carboxymethylated pulp in sodium form was converted to the proton form until all acid groups received H^+ as counter-ions and then titrated with 0.01 mol/l NaOH. The total

amount of the carboxyl group and degree of substitution was calculated according to Equation (1) and (2):

$$\text{Carboxyl group content (mmol/g}^{-1}) = \frac{C_{NaOH} \times V_{NaOH}}{w} \quad (1)$$

$$\text{Degree of substitution (\%)} = \frac{162 \times C_{NaOH} \times V_{NaOH}}{\text{w} - 80 \times C_{NaOH} \times V_{NaOH}} \times 100 \quad (2)$$

Where C_{NaOH}, V_{NaOH}, and w are the concentration of the NaOH solution, the volume of the NaOH solution consumed at a flat area, and the oven-dry weight of the sample, respectively.

3.2.2. Zeta-potential

The zeta-potential values of CNF suspensions were measured by zetasizer Nano ZS90 (Malvern Instrument, U.K.). The concentrations of CNF according to the degree of substitution were 0.1 %.

3.2.3. Fourier Transform Infrared Spectroscopy (FTIR)

The chemical structure of dried CM-CNF films was characterized by Fourier transform infrared spectroscopy (FTIR) (Nicolet iS5, Thermo Fisher Scientific, Waltham, MA, USA). Scanning was carried out in the range from 500 to 4000 cm^{-1} with 32 scans at a resolution of 4 cm^{-1}.

3.2.4. Transmission electron microscopy (TEM)

Nanoscale images of CM-CNFs were obtained using a transmission electron microscope (TEM, JEM1010, JEOL, Tokyo, Japan). The CM-CNF suspension was dropped on a glow-discharged carbon copper grid and the fibers were negatively stained with a 10 μl uranyl acetate solution (1% w/v).

The dimension of CM-CNFs was analyzed using the ImageJ program (1.52a NIH, Bethesda, Maryland, USA).

3.2.5. X-Ray Diffraction analysis (XRD)

The XRD pattern was analyzed X-ray Diffractometer (D8 ADVANCE with DAVINCI, Bruker, Berlin, Germany) with CuKα radiation (1 - 1.5418 Å) at 40 kV and 40 mA. The 2theta range was 5° to 40° with scan speed of 1 sec/step. The crystallinity index (CI) of CM-CNF was calculated according to equation (3):

$$\text{CI}\ (\%) = \frac{(I_{002} - I_{am})}{I_{002}} \times 100 \qquad (3)$$

Where I_{002} and I_{am} are the peak intensities of crystalline and amorphous regions, respectively [134].

3.2.6. Thermal gravimetric analysis (TGA)

TGA samples were characterized using a simultaneous TGA analyzer (SDT, TA instruments, New castle, DE, USA). About 25 mg of the film was positioned on the microbalance located inside the furnace. The test was carried out from 35°C up to 550°C with a heating rate of 10°C/min in a nitrogen atmosphere [135].

3.3. Fabrication of CNF film

3.3.1. Dip coating process

The CM-CNF solution was used as the coating material at 1% (w/w) (Fig. 7). Before dipped into the CM-CNF soltion, fuits were rinsed in D.I. water. Fruits were dipped into the CM-CNF solution. And then, it was dipped into the DC solution directly. DC solution was prepared with 2% of NaCl, $MgCl_2$, and $CaCl_2$ solution. It was used as a cross-linking agent. And then these were dipped into the DC cross-linking agent for 7 min. All the samples were dried at 25 °C overnight.

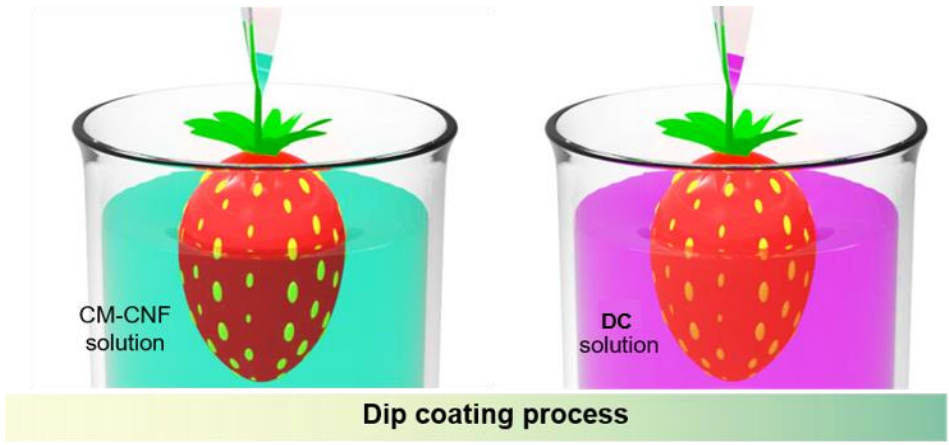

Fig. 7 Schematic image of dip coating process of fruit using CM-CNF and DC solution.

3.3.2. Concentration of cations

CM-CNF/$CaCl_2$ film was fabricated with different concentration of cation solution (0, 1, 2, 3, 4, and 5 %) The tensile strength of the films (1 cm×2 cm×30 μm) was investigated using a universal testing machine (UTM, GB/LRX Plus, Lloyd, West Sussex, UK) fitted with a 10 N load cell. Strain speed of the samples was 2 mm/min.

3.3.3. Soaking time

To approximately determine the soaking time of CM-CNF hydrogel in an aqueous solution with DC, it was calculated by the following equation (4) [136]:

$$t\ (s) = \frac{4 \times H^2}{\pi^2 \times D} \qquad (4)$$

Where H is half of the thickness and D is diffusion coefficient. And then the films were dried 24hr in ambient condition.

3.3.4. Scanning Electron Microscopy (SEM)

The surface morphology of CM-CNF/DC films was observed with field emission scanning electron microscopy (FE-SEM, SUPRA 55 V P, Carl Zeiss, Oberkochen, Germany). The films were dried overnight in a desiccator cabinet at 20 ℃. Platinum was sputtered onto the surface of CM-CNF/DC films at 20 mV for 160 s, and was visualized with a voltage of 2 kV.

3.4. Physical properties of CNF film

3.4.1. Rheological property

CM-CNF hydrogels with NaCl, $MgCl_2$, and $CaCl_2$ were prepared and cut into the shape of circular disk (0.8 cm diameter, 0.1 cm thichkness). Then, the hydrogel specimens were immersed in PBS buffer for 24 h. The rheological behavior of hydrogels was analyzed using a digital rheometer (MARS Ⅲ, Thermo Scientific, Newington, NH, USA). Shear strain sweep oscillatory rheometry was performed using a parallel plate geometry (8 mm) with a gap size of 800 μm under 0.001% to 0.1% strain range [137].

3.4.2. Fourier Transform Infrared Spectroscopy (FTIR)

The chemical structure of dried CM-CNF/DC films was characterized by Fourier transform infrared spectroscopy (FTIR) (Nicolet iS5, Thermo Fisher Scientific, Waltham, MA, USA). Scanning was carried out in the range from 500 to 4000 cm^{-1} with 32 scans at a resolution of 4 cm^{-1}.

3.4.3. Thickness

The thickness of the CM-CNF films was determined by imaging the side view of three different samples with a digital microscope. (Inverted microscope, CELENA®S, Anyang, Korea) Each sample was measured three times in a random area.

3.4.4. Density

The inverted microscopy was used to measure the film thickness for each

sample average of three different films measured at three random points measured at room temperature. The sample was (5cm x 5cm) weight three times. The density was calculated by using the following equation (5):

$$\text{Density (g/cm}^3\text{)} = \frac{M}{V} \qquad (5)$$

Where M is mass (g) and V is volume (cm^3) of the film.

3.4.5. Moisture contents

About 30 μm thick CM-CNF films were cut into 5 cm×5 cm size for the measurement of moisture content. It was completely dried in the oven at 120 °C overnight. It was calculated by the following equation (6):

$$\text{Moisture content} = \frac{(M_i - M_f)}{M_i} \times 100 \qquad (6)$$

Where M*i* is the initial mass and M*f* is the final mass of the film, all in grams. The sample was 5cm x 5cm (n=3).

3.4.6. Transmittance

Optical transmittance was measured in UV/Vis spectrophotometer (OPTIZEN POP, Mecasys, USA), range from 400 nm to 800 nm. Each sample were cut into 1 cm x 1 cm. it was detached into side of 1ml plastic cuvette cell.

3.4.7. Tensile strength

The tensile strength of the films (1 cm×2 cm×30 μm) was investigated using a universal testing machine (UTM, GB/LRX Plus, Lloyd, West Sussex, UK) fitted with a 10 N load cell. Strain speed of the samples was 2 mm/min.

3.5. Barrier properties of CNF film

3.5.1. Contact angle

Static contact angles of the films were measured by a contact angle analyzer (Drop shape analyzer, DE/DSA 100, KRUSS, Germany) using the syringe dropping at room temperature in air (about 5 μm per D.I. water drop). Three different positions on the films were measured and the average value was calculated to determine the static contact angle.

3.5.2. Water vapor pressure (WVP)

The water vapor permeability (WVP) was measured based on the ASTM E96/E96M-05 standard method. Film samples were mounted between the top and the lid of permeability cup (Φ = 60 mm, Height = 20 mm, made of aluminum) with ~28.26 cm^2 effective area filled with silica gel as desiccant. The weight of the assembled permeability cup was measured immediately and then placed in the atmospheric condition for 24 h. The weight change of CM-CNF, CM-CNF/NaCl, CM-CNF/$MgCl_2$ and CM-CNF/$CaCl_2$ films was measured under the 50 %, 85 %, and 98 % RH at 23 °C. Water vapor transmission rate (WVTR) and WVP were calculated by the following Equations (7) and (8) [138]:

$$\mathrm{WVTR}\ \left(\mathrm{g/m^2 \cdot s}\right) = \frac{\Delta \mathrm{W}}{\mathrm{Area \cdot time}} \qquad (7)$$

$$\mathrm{WVP}\ \left(\mathrm{g/m \cdot Pa \cdot s}\right) = \frac{\mathrm{WVTR \cdot L}}{P_{sat} \times \Delta \mathrm{RH}} \qquad (8)$$

Where ΔW was the weight of the water vapor passing through film, L film thickness, P_{sat} water vapor saturation pressure at 23 °, and ΔRH (%) percentage relative humidity gradient.

3.5.3. Thermal imaging

The control and coated strawberries were stored in the refrigerator (≈ 4 ℃) for 24 h, and taken out right before the thermography measurement. Thermography was performed in the insulating room which was automatically controlled at constant 23 °C and RH 60%. Thermographs were captured for 60 min with 10 min intervals. Thermographs of the samples were recorded using infrared camera (Ti55FT, Fluke, Everett, WA, USA). The camera rendered the thermographs using constant emissivity of 1. The experimental data was acquired with SmartViewTM 3.0 software.

3.6. Extraction and characterization of RC extract

3.6.1. Extraction of RC extract

The extraction and quantification of RC extract were carried out according to the method described by Francis [139]. 10 g of red cabbage sample was added in falcon tube, 30 mL of acidified ethanol (85 mL of ethanol and 15 mL of 1.5 mol L^{-1} HCl) was added and implemented to constant agitation for 1 h. The supernatant was separated by filter manually. And also, It was dried in the vacuum desiccator at overnight [140].

3.6.2. Total anthocyanin contents (TAC)

TAC was calculated using a spectrophotometric differential pH method, according to Rapisarda et Al. [141], with a few modifications. Two lyophilized samples of 500 mg were treated with 10 ml of buffer solution, pH 1.0 (125 ml of 0.2 M KCl and 375 ml of 0.2 M HCl), and 10 ml of buffer solution, pH 4.5 (400 ml of 1 M sodium acetate, 240 ml of 1 M HCl and 360 ml of water), respectively. The mixture was homogenized and centrifuged twice at 4 °C at 5000g for 15 min. The supernatant was collected and its absorbance was read at 510 nm. TAC was determined by the following equation (9):

$$\text{TAC (mg/g)} = \frac{\text{A}}{\varepsilon \times \text{L}} \times MW \times DF \times \frac{v}{w} \times 10^3 \qquad (9)$$

Where the terms in parentheses indicate the difference between the absorbance value at 510 nm at pH 1.0 and 4.5 solutions, respectively.

Molecular weight was the molecular mass of cyanidin-3-glucoside chloride, its molar absorptivity (ε) was 24,825 at 510 nm, and DF is the dilution/concentration factor related to the sample weight, the extract volume and the yield of the process of lyophilization. Each sample was analyzed in triplicates.

3.6.3. Color distance

The film color distance was determined by colorimeter (TES-135A, TES, Taipei, Taiwan). The values of L^* (lightness), a^* (red – green) and b^* (yellow–blue) parameters were recorded to evaluate color changes with concentration of RE. Tests were performed in triplicate and the total color difference was calculated according to the equation (10):

$$\Delta E^* = \sqrt{\Delta L^{*2} + \Delta a^{*2} + \Delta b^{*2}} \qquad (10)$$

The CNF- RE film was cut 5×5 cm with different concentration of RE.

3.6.4. DPPH assay

The antioxidant activity of the RE solutions were determined using a DPPH assay [142]. This was achieved by mixing 3.8 mL of a standard DPPH methanol solution (0.004 %) with 0.2 mL of the samples in different concentrations. The radical quenching potency of the RE solutions and ascorbic acid as a standard material were also measured at different concentrations (10, 20, 40, 80, 160 and 200 μL/mL). A DPPH standard solution was used as a control sample. The absorbance (Ab) values were

analyzed at 517 nm and DPPH radical quenching was calculated according to the equation (11):

$$\text{DPPH assay} = \frac{Ab_{DPPH} - Ab_{sample}}{Ab_{DPPH}} \times 100 \qquad (11)$$

3.6.5. UV protection

The UV protection of Rhodamine B (RhB) solution in the presence of photocatalyst (TiO_2) under high-pressure mercury lamp (150 W) was conducted to evaluate the UV-shielding performance of films. Briefly, 25 mg of TiO2 and 50 mL of RhB solution (1×10^{-5} M) were mixed for complete dispersion. Prior to irradiation, the suspension was stirred in the dark for 30 min at ambient temperature to reach adsorption/desorption equilibrium. The films were used to cover the mouth of the beaker before UV irradiation. The distance between of the lamp and the film was about 10 cm. The photocatalytic degradation of RhB solution was carried out under constant stirring. At given intervals (t), 1 mL of the suspension were collected and centrifuged to remove the photocatalyst. The absorbance of RhB at 552 nm was measured by spectrophotometer. The UV-protecting performance was calculated as below equation (12):

$$I\ (\%) = \frac{A_t}{A_0} \times 100 \qquad (12)$$

Where A_0 is the initial absorbance of RhB solution without UV radiation and A_t is the absorbance of the remaining RhB solution protected with film under UV radiation.

3.6.6. Cell proliferation test

NIH 3T3 fibroblast cells (1.5×10^6 cells/ml) were seed on the CNF- RE film. The produced structures were cultured in medium consisting of DMEM with 4.5 g/l glucose, L-glutamine, sodium pyruvate, and 10 % FBS. The film se in the composite hydrogels were cultured in a humidified 5 % CO^2 incubator at 37 °C for one or seven days. For investigation of cell proliferation, the printed constructs were washed once with PBS and incubated with alamarBlue® (Invitrogen) solution for 4 h at 37 °C. The alamarBlue® fluorescence was assayed at 540 nm (excitation) and 590 nm (emission) using a microplate reader (Synergy HT, BioTek, Winooski, VT, USA).

3.7. Application – Climacteric / Non-climacteric fruits

3.7.1. Weight change

Fruits were weighted at the beginning of the experiment after air drying and thereafter each day during the storage days. Weight loss was expressed as the percentage loss of the initial total weight. For each measurement, 3 fruits corresponding to each treatment were used. The weight change was calculated by using the following equations (13):

$$\text{Weight change (\%)} = \frac{(M_i - M_f)}{M_i} \times 100 \qquad (13)$$

Where M*i* is the initial mass and M*f* is the final mass of the fruits. It was expressed by fraction of the original weight (%)

3.7.2. Firmness

Firmness of Strawberries was measured using a penetrometer. The CT-3 texture analyzer (Brookfield Co., Middleborough, MA, USA) was used for firmness measurement. Fruit firmness (N) was measured at the equatorial plane of the fruit using a flat probe of 100 mm diameter at a speed of 2 mm s^{-1} and a strain of 5 mm [143].

3.7.3. Respiration rate

Respiration rate was determined by using the static methods. Five strawberries were placed in 1L Nalgene polypropylene jars with a septum in the lid for sampling gas. The jars were stored at room temperature. Gas sampling was carried out after 2 hours with 1 cc syringes by means of a needle

connected to a gas chromatography (YL 6400, Younglin Instrument, Seoul, Korea). Three replicates were performed for each sample. The respiration rate was calculated by using the following equations (14):

$$\text{Respiration rate } (\text{ml}\cdot CO_2\cdot \text{kg}^{-1}\cdot \text{h}^{-1}) = \frac{(\Delta\ CO_2)}{100} \times V_{\text{headspace}} \times \frac{1000}{m} \times \frac{60}{t} \quad (14)$$

Where ΔCO_2 is the difference between the initial and final concentration of CO_2, $V_{\text{headspace}}$ is the empty volume of the jar (ml), m is mass of strawberries and t is sampling time (min) [144].

3.7.4. Total soluble solids (TSS)

After firmness analysis, strawberries were cut into small pieces, wrap with gauze and squeezed in plastic squeezer. To determine soluble solids, 0.3 ml of squeezed juice was added to a refractometer prism. The results were expressed in Percentage of soluble solids (%)

3.7.5. Total acidity (TA)

After TSS analysis, strawberries juice was added to an acidometer. The one millimeter of juice was dropped to acidometer with the samples were three replicated. The results were expressed in Percentage of acidity (%)

3.7.6. Tyrosinase inhibition assay

Tyrosinase inhibition assays were performed with minor modifications [145]. Tyrosinase (1000 U/mL) from mushroom solution was prepared at a concentration of 100 U/mL in phosphate buffer solution, pH 6.5. Tyrosinase mushroom solution (150 µL) and phosphate buffer solution at pH 6.5 (300 µL)

were mixed with 0-3 % concentration of RE extract (0.8 mg). The mixture was then incubated at 25 ℃ for 5 min before adding 300 µL of 2.5 mM L-tyrosine solution, and the reaction was measured at 475 nm. The percentage of inhibition of tyrosinase activity was calculated under equation (15):

$$\text{Inhibition (\%)} = \frac{A-B}{A} \times 100$$

Where A represents the difference in the absorbance of the control sample, and B represents the difference in the absorbance of the test sample.

3.8. Statistical analysis

All experiments were carried out in triplicates and the average results were shown as mean ± standard deviation. Statistical analysis of the results was performed using a one-way analysis of variance (one-way ANOVA) with Tukey mean analysis. It was performed using IBM SPSS statistics version 25 (SPSS inc., Chicago, IL, USA).

IV. Results and discussion

4.1. Characterization of carboxymethylated CNF coating solution

The characteristics of CNFs were evaluated by measuring carboxymethylation time about 0, 30, 60, 90, and 120 minutes to determine suitable coating solution. The ion conductivity, carboxylate content and degree of substitution were measured according to the carboxylation reaction time. It was attempted to derive an appropriate carboxylation reaction time through these experiments.

An ionic conductivity method was used to measure the carboxyl contents and degree of substitution of the CNF. Carboxymethylation can be controlled by pretreatment reaction time [146]. Fig. 8A shows the titration curve of ionic conductivity with carboxymethylated pulp. The ionic conductivity decreases with the addition of sodium hydroxide. This is because the rapid decrease in conductivity reaches neutrality with the addition of initial hydrochloric acid. The plateau section is formed by the carboxymethyl group of carboxymethylated CNFs. Therefore, the total amount of carboxyl can be quantified by the amount of sodium hydroxide consumed in a plateau section. As shown in Fig. 8B, the sample of 0min calculated using equation (1) was 9.12 μmol/g. As reaction time increased, so did the carboxyl content. This is because the presence of a negative charge on the fiber's surface varies with or

without reaction time. The pretreatment reaction time was 289.47 μmol/g for 30 minutes, 462.77 μmol/g for 60 minutes, 602.35 μmol/g for 90 minutes, and 622.33 μmol/g for 120 minutes. And also calculated the degree of substitution of CNF using equation (2). The pretreatment reaction time was 4.56 % for 30 minutes, 8.23 % for 60 minutes, 10.87 % for 90 minutes, and 11.37 % for 120 minutes (Fig. 8C). Consequently, both degree of substitution and carboxyl content increased in proportion to the pretreatment reaction time. In addition, it was confirmed that there was no significant difference in the reaction time over 90 minutes.

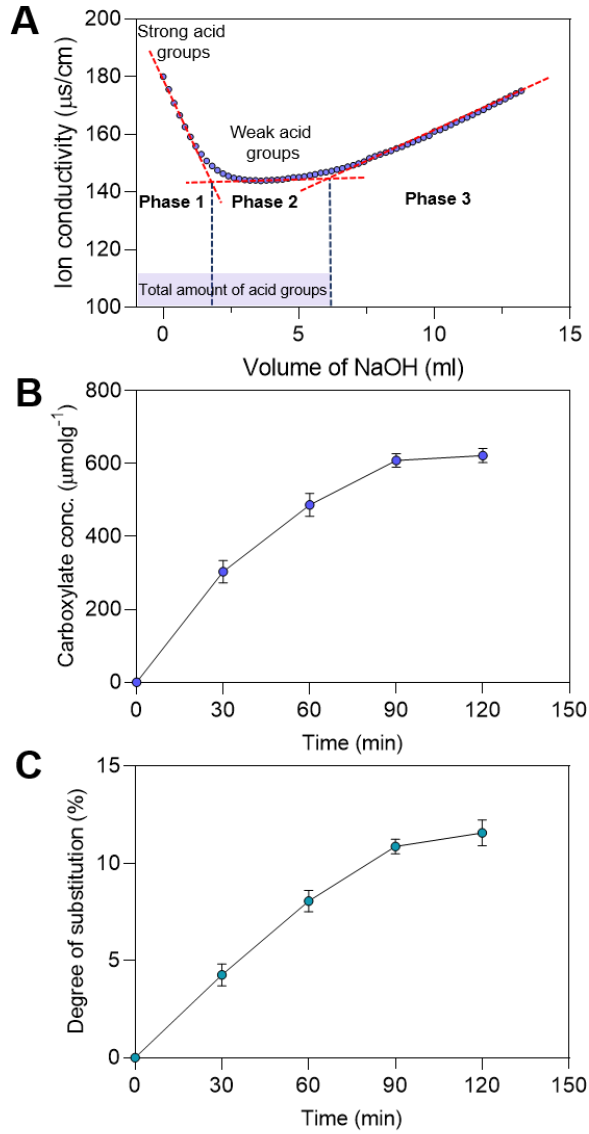

Fig. 8 A) Ionic conductivity titration curve by consuming NaOH solution. B) The carboxylate concentration of pulp cellulose by reacting pretreatment with monochloroacetic acid. C) The percentage of degree of substation with reacting pretreatment. (n=3)

The surface charge of the CNF was analyzed using a zetasizer (Fig. 9A). Pulp solutions with carboxymethylation time are prepared as samples. The pretreatment reaction time was -30.23mV for 0 minutes, -37.37 mV for 30 minutes, -43.51 mV for 60 minutes, -50.93 mV for 90 minutes, and -53.33 mV for 120 minutes. As the carboxymethylation time increased, the zeta potential gradually decreased due to the negative charge in the carboxymethyl group. The result of zeta potential supports why carboxyl content and Degree of substitution increase with reaction time. In addition, it was confirmed that the reaction time in more than 90 minutes is less efficient.

The FT-IR spectrum of the CNF film according to the carboxy content of CNF was confirmed (Fig. 9B). The peak of untreated CNF is indicated by water absorbed by the fibers at 1649 cm^{-1} [147]. As carboxymethylation proceeded, the carboxyl content of CNF increased, resulting in a gradual increase in the carboxyl peak assigned to 1598 cm^{-1}. The repulsion between the nanofibers was formed due to the surface charge of carboxymethyl groups.

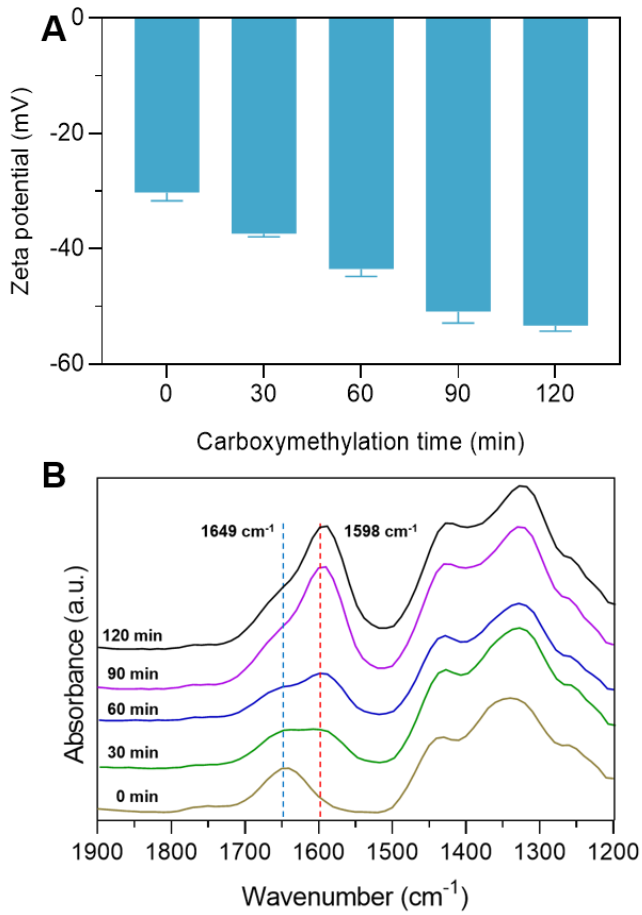

Fig. 9 A) Zeta potential of carboxymethylation of CNF with pretreatment reaction. (n=3) B) The change of FTIR spectrum according to carboxylation time.

The TEM was taken to measure the thickness of the fiber over carboxylation time. It was confirmed that the thickness of the fiber decreases as the carboxylation time increases. Through these results, carboxylation had the effect of nanosizing the fiber to widen the surface area. It was hard to measure the thickness of CNF for 0 min. The pretreatment reaction time was 51.23 nm for 30 minutes, 27.45 nm for 60 minutes, 8.31 nm for 90 minutes, and 8.05 nm for 120 minutes (Fig. 10).

These results confirm that the longer the reaction time, the more uniform the thickness of the fibre can be obtained and the more homogeneous the film can be manufactured. Also, the difference in fiber thickness was not significant after 90 minutes.

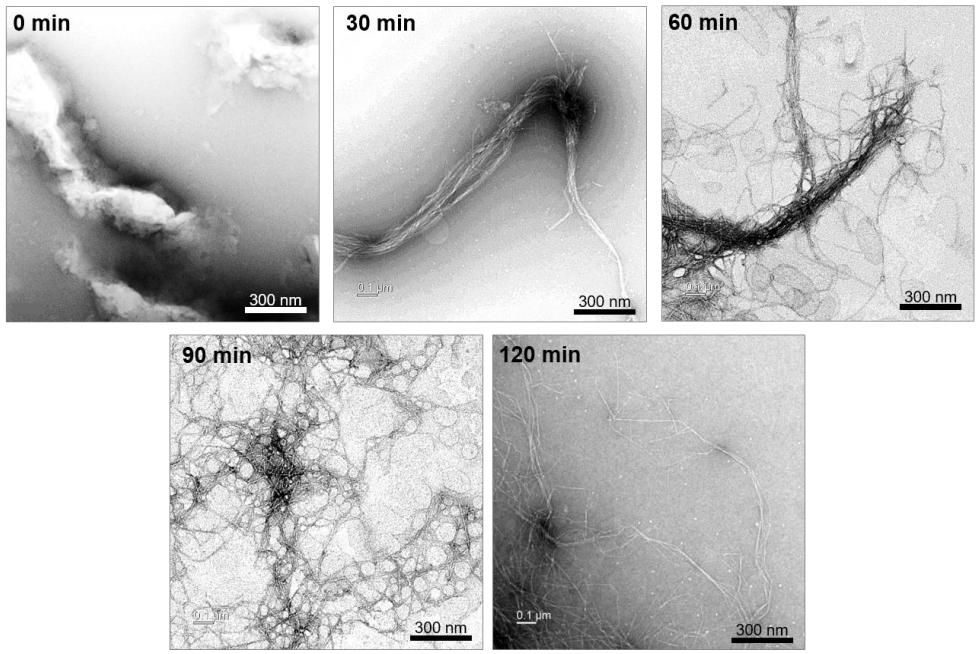

Fig. 10 The TEM image of CNF pulp with pretreatment of carboxy-methylation. The TEM images of pretreatment reaction for 0 min, 30 min, 60 min, 90 min, and 120 min. The scale bar was 300 nm. And the total percentage of frequency was 100 %. The thickness of CNF was measured by image J program.

XRD patterns were evaluated to identify the effect of the time of carboxymethylation on the crystallinity, which was calculated with deconvoluted graphs by the equation (3). As shown in Figure 11 A-D, CNF exhibited the intense peaks at around 16.2 °, 22.6 °, and 34.3 °. It was reflected on the crystallographic planes of (110), (200), and (040) [148]. It was determined that all the samples were in the crystal structure known as cellulose Iβ [149]. The crystallinity index (CI) of 0 min, 30 min, 60 min and 90 min were 42.79 %, 44.69 %, 48.01 %, and 51.06 %. The results showed a rise in the CI owing to the increase in the time of acid hydrolysis. The sample of 90 min indicated the highest crystallinity at 51.06 %, which demonstrates sharper diffraction with an intense peak at 22.6 ° compared to 0 min, 30 min and 60min. When the carboxymethylation reaction occurs, the fiber is cleaved by the acid hydrolysis. Acid hydrolysis is reacted on the surface of the CNF fiber by the hydromium ion (H_3O^+), which is an intermediate product. Hydromium ions easily penetrate into loose amorphous regions and promote acid hydrolysis [150]. As the carboxymethylation time increases, more amorphous regions are decomposed. Therefore, CI increases in proportion to the carboxymethylation time.

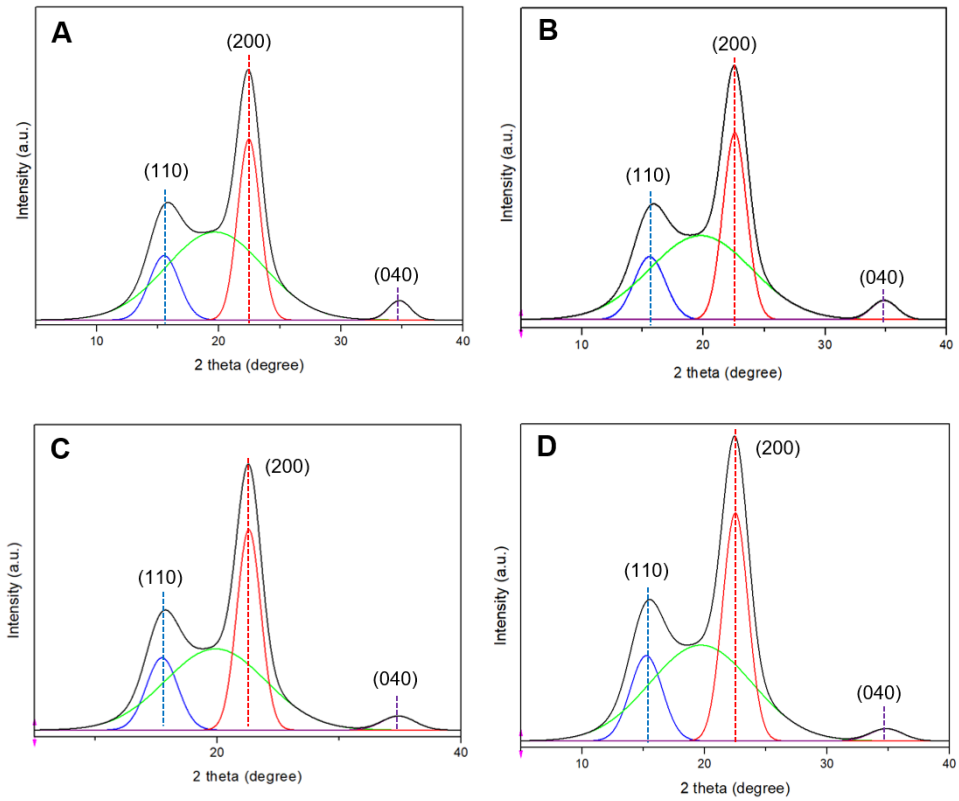

Fig. 11 The XRD peak of CNF by reacting pretreatment with mono-chloroacetic acid. A) 0 min. B) 30 min. C) 60 min. D) 90 min. The peaks were deconvoluted by Origin 8.0 program.

Fig. 12 represent the TGA curves of carboxymethylation time in 0 min, 30 min, 60 min and 90min. There was two-step thermal decomposition behavior. It is also known as a cellulose pyrolysis curve [151]. In the initial degradation stage, the weight loss was analyzed that degradation for all samples 0 min, 30 min, 60 min and 90 min was 4.56, 4.45, 4.51, and 4.53 %. It was caused by the dehydration of water on the surfaces of CM-CNF. The second degradation stage showed under the approximate ranges from 220 °C to 280 °C. The decomposed temperature of 0 min, 30 min, 60 min and 90 min was at 261 °C, 228 °C, 241 °C and 239 °C. It was expected due to the higher surface area of CNF, which more exposure to heat [152]. As shown in Fig. 10, the surface area enlarged as the carboxymethylation time increased. Also, the value of heat transfer was increased when the CI was increases [153]. Because, crystallized cellulose chains were efficient in the pathway to produce better thermal conductivity [153]. As shown in Fig. 11, the CI was increased by proportionate with carboxymethylation time. Totally, enlarged surface area and enhanced CI had an impact on change of second degradation. The char residue for 0 min, 30 min, 60 min and 90 min at near 600 °C were 20.41 %, 26.96 %, 35.08 % and 38.19 %. This result could be explained by the difference in the number of chain end groups [154]. The surface area of CNF fiber enlarged with increasing carboxymethylation time. As the CNF fiber was hydrolyzed for a longer time, more chain end groups were created. As shown in Fig. 8, DS was increased as the carboxymethylation time increased.

In other words, more end groups are substituted with carboxymethyl groups as the reaction time increases. The carbon group of the carboxymethyl group could be formed the char at near 600 °C. Therefore, high char residue was left in proportion to the carboxymethylation time.

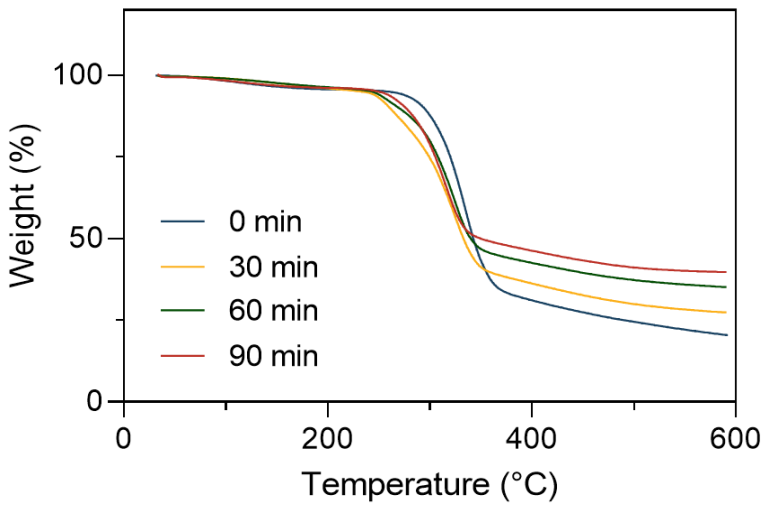

Fig. 12 TGA curves of carboxymethylated CNF in 0 min, 30 min, 60 min and 90 min.

4.2. Fabrication of CNF film

4.2.1. Optimization of concentration of cation solution

It is important to confirm the concentration of the appropriate cation solution. If the concentration of the cation solution is low, the effect of strengthening physical properties is weakened. On the other hand, if the concentration of the cation solution is very high, salt may be precipitated and affect the fruit. A film was prepared by dividing the concentration of $CaCl_2$ solution from 0 to 5%, and tensile strength was measured (Fig. 13). As a result, the tensile strength increased as the concentration of the solution increased. However, there was no statistically significant difference at concentrations above 2%. Through this, it was found that the concentration of the suitable cation solution for preparing the film was 2%. In this experiments, the concentration of all cation solutions was unified at 2%.

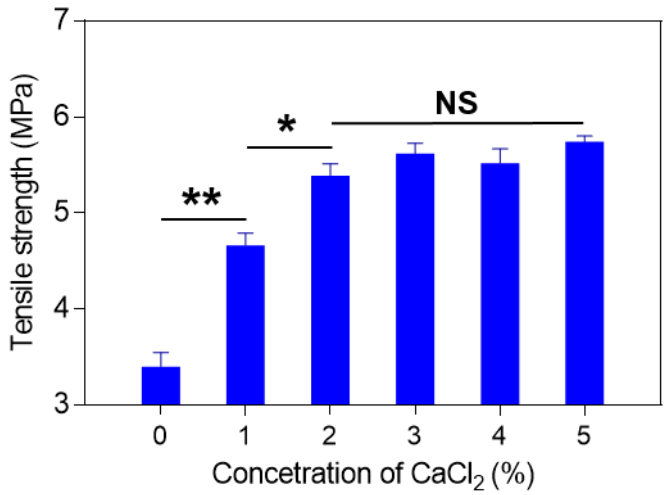

Fig. 13 The tensile strength of the CNF film immersed in $CaCl_2$ solution from 0 to 5% concentration. (n=3), NS indicates no significance, * indicates a p-value of <0.05, ** indicates a p-value of <0.01 and statistical analysis was performed using one-way ANOVA test.

4.2.2. Evaluation of optimized coating condition

It is important to determine the soaking time in the DC solution. If the soaking time is not sufficient, the interaction between CNF and DC will not occur sufficiently. Also, if the soaking time is too long, the processing time will be prolonged. As shown in Figure 14, the carboxymethyl group of CNF binds with DC. CNFs were bound by electrostatic interactions with DCs. The carboxymethyl group has a negative charge stabilized by the cation. The soaking time was calculated using equation (4). The calculated value was about 6.7 minutes. This allowed the integration of all samples used in the experiment with a 7 min soak time.

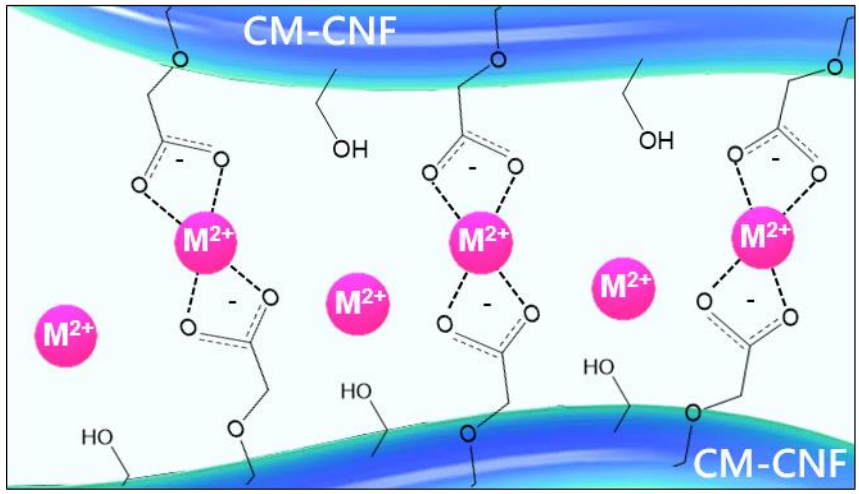

Fig. 14 The schematic image of electrostatic interaction between the carboxymethyl groups on the surface of CMCNF with DC.

The SEM was measured to determine the morphological difference of the film according to soaking. The cross section of the CNF film (Fig. 15 A) and the cross section of the CNF film (Fig. 15 B) contained in the $CaCl_2$ solution were compared. Measurements have shown that samples contained in $CaCl_2$ solutions have tight interactions between fibers. Both samples were found to have layers piled up. However, the samples contained in the $CaCl_2$ solution formed a tight structure between layers. This explains why there was a difference in tensile strength between the two samples. Carboxymethyl groups that are modified on the fiber's surface combine with calcium ions to form more interaction. The interaction formed is believed to have had a mechanical reinforcement effect on the film.

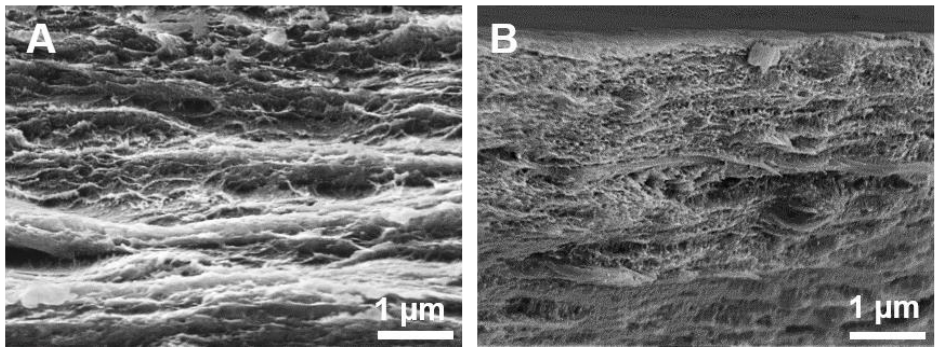

Fig. 15 The SEM images of CM-CNF film A) The cross section image of non-treated CNF film. B) The cross section image of CNF/$CaCl_2$ film.

4.3. Evaluation of CNF film

4.3.1. Physical properties of CNF film

The rheometer was measured to confirm the change of the storage modulus according to the addition of cations (Fig. 16). The concentration of cations was tested and set to 2%. Before drying the film, it was carried out an experiment in the hydrogel state. The storage modulus of CNF was 1252.52 Pa, CNF/NaCl was 1193.16 Pa, CNF/$MgCl_2$ was 1775.53 Pa, and CNF/$CaCl_2$ was 2190.06 Pa. As a result of the experiment, there was no change in the storage modulus of cnf reacted with nacl. This is because Na^+ is a monovalent ion and does not lead to fiber interaction. On the other hand, CNF reacted with $MgCl_2$ and $CaCl_2$ had a significant change in storage modulus. This is because Mg^{2+} ions and Ca^{2+} ions are divalent ions and lead to fiber interaction.

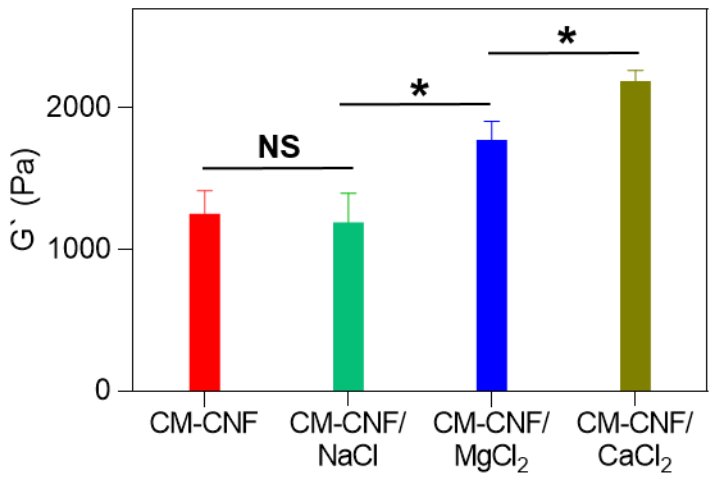

Fig. 16 The storage modulus of CM-CNF hydrogels with cations. (n=3) NS indicates no significance, * indicates a p-value of <0.05, and statistical analysis was performed using one-way ANOVA test.

FTIR was measured to confirm the electrostatic binding of CM-CNF carboxymethyl group and DC (Fig. 17). As shown in the experimental results, CM-CNF film was strongly absorbed at 1598cm^{-1}. This means that the carboxyl group is combined with the hydroxyl group of CNF. In the case of CM-CNF/NaCl film, the position and intensity of CM-CNF film and peak were almost similar as CM-CNF film. Na^{+} cations were found to be relatively weak in the binding with carboxymethyl group due to monovalent cations. On the other hand, CM-CNF/$MgCl_2$ film showed high frequency, shifted to 1632cm^{-1}, and peak size increased. Mg^{2+} cations were divalent cations, and strong electrostatic interaction was formed with carboxymethyl group [155,156]. CM-CNF/$CaCl_2$ film was stronger electrostatic interaction than CM-CNF/$MgCl_2$ film. Separation of peak was observed by interaction. This is due to the large radius of the Ca^{2+} ions (0.99 Å), which have relatively large radius, and are strongly bonded to the carboxyl group than the Mg^{2+} ions (0.66 Å).

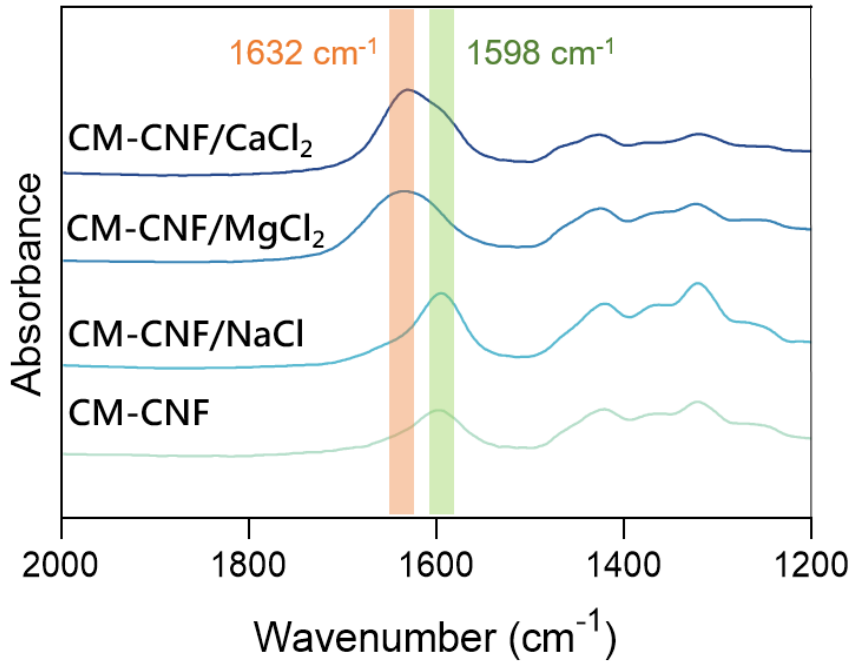

Fig. 17 FTIR spectra to conform interact between carboxymethyl group and cations. The peak was moved to high frequency region when interact with divalent cations. (From 1598 cm^{-1} to 1632 cm^{-1}).

The thickness change of the film was measured when CM-CNF and DC were combined (Fig. 18A). The results showed that the carboxymethyl group was 35.33 ± 3.5 μm, 32.33 ± 4.2 μm, 30.67 ± 2.5 μm and 29.33 ± 4.2 μm respectively, when combined with pristine CM-CNF, Na^{+}, Mg^{2+} and Ca^{2+} ion. This result can be interpreted that the thickness of the film is reduced due to the strong electron interaction and the entanglement of the fiber. DCs are interacted with Interfibrilar hydrogen bond, which prevents water molecules from penetrating between fibers. Density was measured and confirmed (Fig. 18B). The density of film was 1.34, 1.37, 1.44 and 1.50 g/cm^3 when the pristine CM-CNF, CM-CNF/NaCl, CM-CNF/$MgCl_2$ and CM-CNF/$CaCl_2$ were measured (equation 5). Film was compressed strongly because the water molecule could not penetrate between fiber and it was entangled. The previous feature was useful when making the food preservation films because the water content decreases and the swelling phenomenon did not occur. In addition, the penetration of gas becomes more difficult, so that the target product could be efficiently protected. Moisture content was measured to confirm the amount of water content inside the film. DC was added to the pristine CM-CNF, which resulted in a decrease in film thickness and an increase in volume, which was consistent with DC's tendency. The Moisture content of film was 15.32, 14.14, 13.43 and 13.05 % when the Pristine CM-CNF, Na^{+}, Mg^{2+} and Ca^{2+} were added (Fig. 18C, equation 6). The moisture content of film also decreased as the functional group and water molecules

did not combine between fibers. These changes in physical properties were confirmed through changes in the transparency of the film.

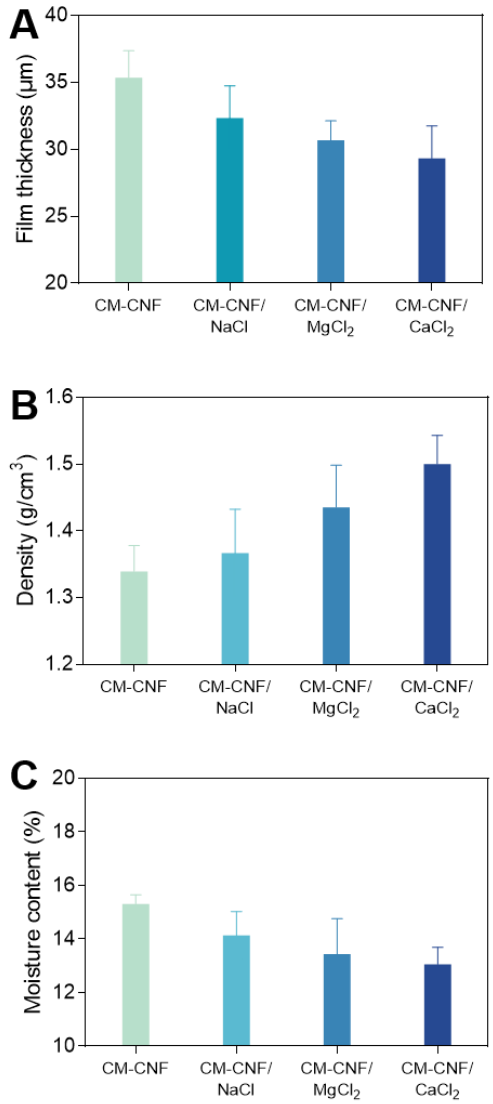

Fig. 18 The physical properties of CNF film A) Thickness B) Density C) Moisture contents. (n=3)

The transparency of the film was reduced as the transmission was changed when the type of cations was changed (Fig. 19A). The pristine CM-CNF film showed more than 81.20 % transmittance at the 650 nm. CM-CNF/NaCl, $MgCl_2$, and $CaCl_2$ films (Fig. 19B) also had a transmission of 76.72 %, 76.49 % and 74.49% at the 650 nm. The cations are entangled with carboxymethyl groups, resulting in the entanglement of the fiber, which leads to a decrease in transmittance. In particular, all results showed that the change of the physical properties of CM-CNF/$CaCl_2$ film was the highest. This result was higher than the same divalent ion, Mg^{2+} ion, which is a film containing the same divalent ion. This phenomenon can be explained by the difference of binding force due to the difference of radius of ion. The radius of Ca^{2+} ion is 0.99 Å, which is larger than Mg^{2+} ion (0.66 Å), which shows relatively higher binding and binding strength because of its large binding force.

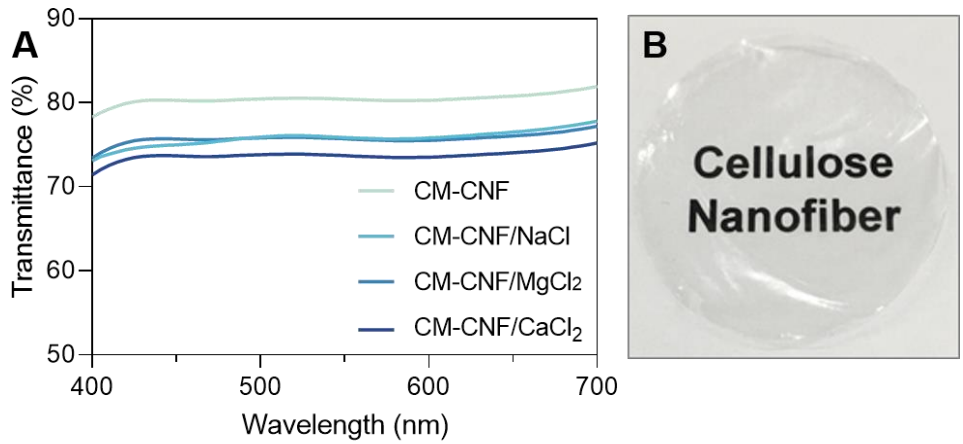

Fig. 19 A) The transmittance of CM-CNF film B) The image of CM-CNF/$CaCl_2$ film.

Tensile strength (TS) is an important factor that protects target products inside the food preservation film, which refers to the power to resist mechanical stress. As shown in Fig. 20, CM-CNF/$CaCl_2$ film has high TS. Pristine CM-CNF film was measured at about 4.15 MPa, and CM-CNF/NaCl, $MgCl_2$, $CaCl_2$ film was 4.41, 4.70, and 5.15 MPa. The strong interaction of carboxyl group and entanglement formation resulted in the enhancement of tensile strength. Through these results, it was confirmed that the property of the pristine CM-CNF film was strengthened. Especially, $CaCl_2$ was expected to strengthen crosslinking agent between CNF fibers. The change in the electrical properties of the film by chemical bonding of cations and CM-CNF affected not only TS but also wettability.

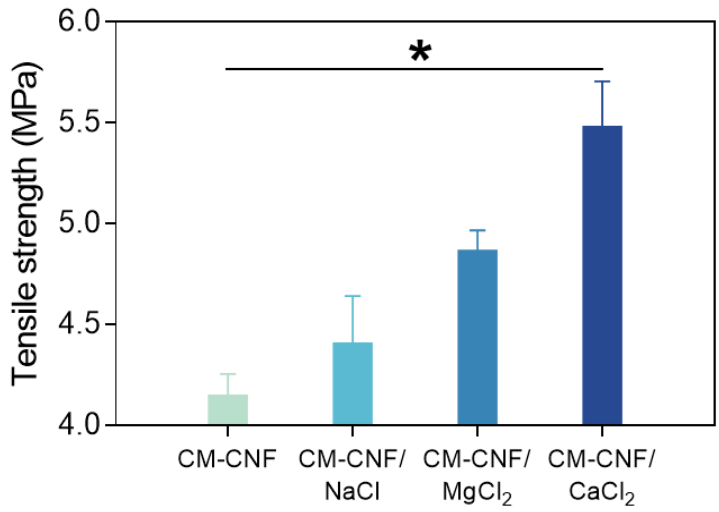

Fig. 20 The tensile strength of CM-CNF film. (n=3) * indicates a p-value of <0.05, and statistical analysis was performed using one-way ANOVA test.

4.3.2. Barrier properties of CNF film

The contact angle for each film was measured and proved (Fig. 21A). The surface of CM-CMF film showed a low contact angle of about 42.7 ° after drop of water drop (Fig. 21B). CNF is basically moisture-permeable and has easy wetness. This is a critical disadvantage as a material of food preservation film. On the other hand, CM-CNF/NaCl, CM-CNF/$MgCl_2$ and CM-CNF/$CaCl_2$ films formed higher contact angles. In particular, CM-CNF/$CaCl_2$ film was confirmed to be 69.7 ° after just dropped the film surface (Fig. 22C). Also, the contact angle of about 56 ° was shown after 1 minute, unlike CM-CNF, which permeated the film inside. The wettability of CM-CNF film was decreased by DC, which helps to improve the preservation of target products.

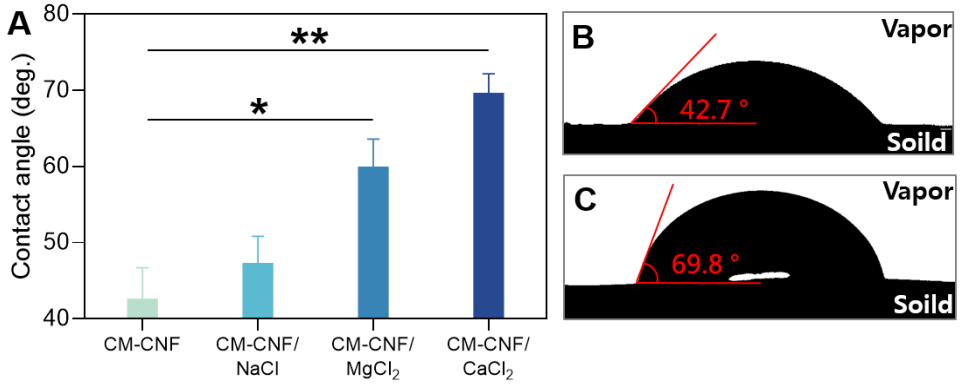

Fig. 21 A) The contact angle of CNF film. * indicates a p-value of <0.05, ** indicates a p-value of <0.01 and statistical analysis was performed using one-way ANOVA test. B) The image of sessile drops of water on CM-CNF film C) The image of sessile drops of water on CM-CNF/$CaCl_2$ film

The results of the WVP value indicated that DC promoted barrier effects. The CM-CNF film was measured at about 9.48 X 10^{-11} g/m·Pa·s, and the WVP value of the film combined with the DC was all lowered (Fig. 22, equation 7, 8). In particular, CM-CNF/$CaCl_2$ was found to be the most effective WVP lowering under 50 % relative humidity conditions at 23 °C (6.46 X 10^{-11} g/m·Pa·s) and this result was predicted to be due to the neutralization of CM-CNF and the increase of hydrophobicity. The hydrophobicity of the film was confirmed by contact angle measurement and the water permeability was also lowered [157]. The inside of the film, which has passed through a lot of moisture, contains more water molecules [138, 158]. It caused in more swollen and weakening the interaction of fibers, eventually losing the barrier properties. CM-CNF/$MgCl_2$ and CM-CNF $CaCl_2$ films inhibited these effects and effectively supplemented the weakness of CM-CNF film without the help of plasticizer. However, the higher the relative humidity, the higher the WVP value of all samples, and the barrier reinforcement effect was small under 98% conditions.

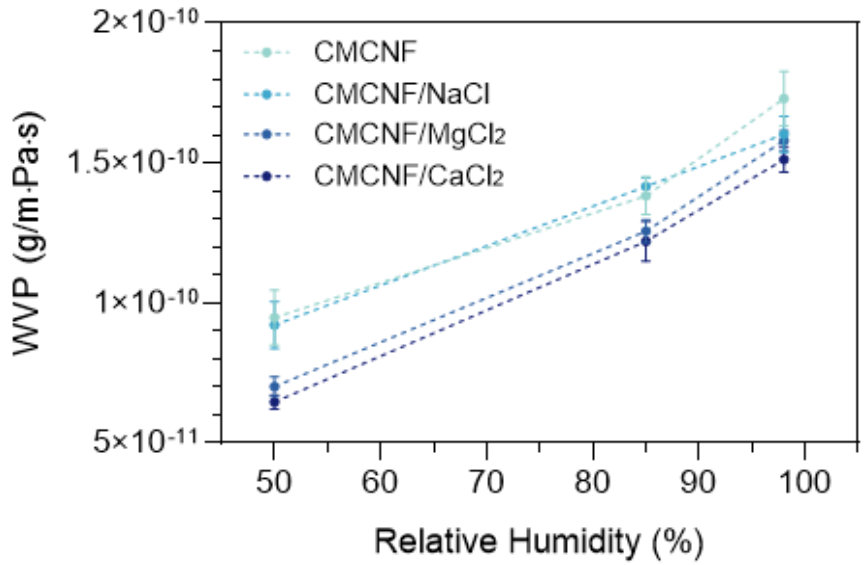

Fig. 22 Water vapor permeability of CM-CNF films at 50, 85, and 98% RH with 23°C.

The CM-CNF coatings could reduce the surface temperature of fruits and keep them in the fresh state longer. The temperature change of strawberries was monitored with thermography upon the exposure of refrigerated strawberries to room temperature (Fig. 23A). It was hard to compare the absolute temperature of the surfaces with thermography due to the continuous change of background temperature. However, it was obvious that the surface temperature of strawberries increased as the exposure time to ambient condition increased. The change of the surface temperature was rapid for the non-treated strawberry compared with CM-CNF coated strawberries (Fig. 23B). The surface temperature of strawberries reached the steady state in 30 min considering that the difference of the surface temperature between strawberries was about 3°C after 30 min and kept for prolonged exposure time.

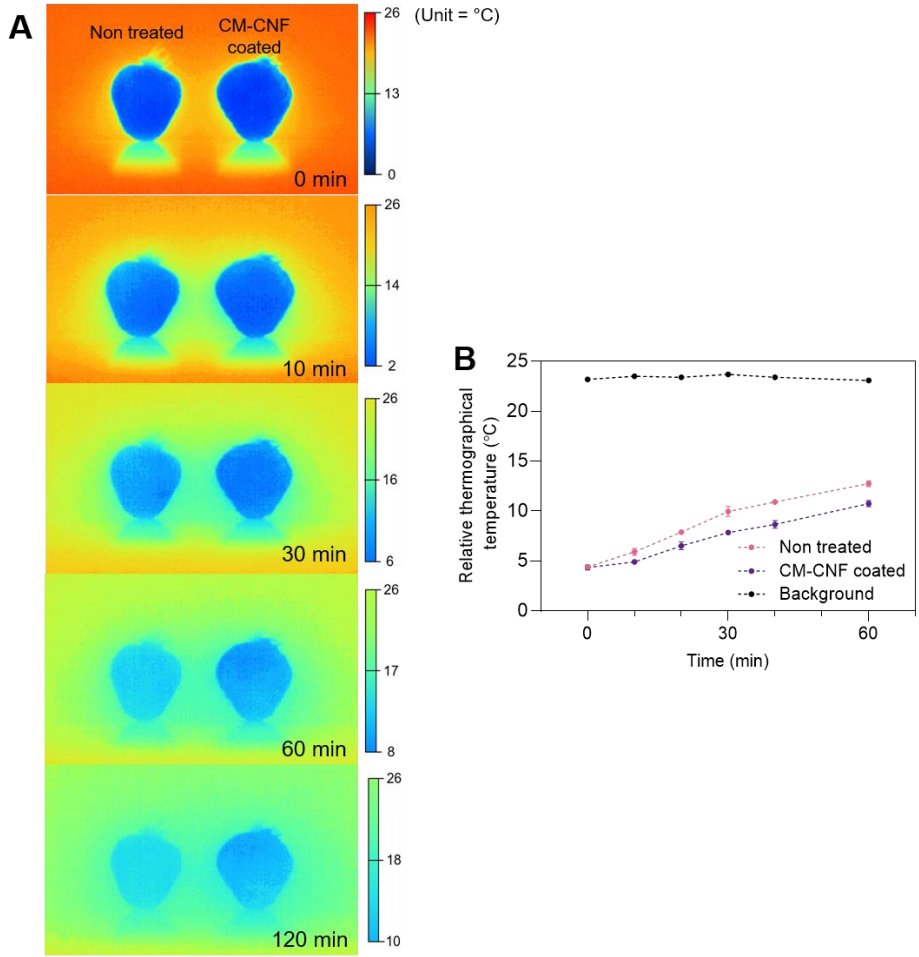

Fig. 23 Effect of CM-CNF coating on the temperature change of strawberry surface. A) Thermograph of strawberries with storage time. B) difference in surface temperature between non-coated and CM-CNF coated strawberries.

Temperature changes were measured in CM-CNF in films soaked in NaCl $MgCl_2$ and $CaCl_2$ solutions (Fig. 24 A, B). Experiments show that it is almost similar to CM-CNF film. It was refrigerated at 4°C and observed at room temperature for about an hour. The non-treated sample and each sample had a temperature difference of about 3 degrees, which was hampered by the CM-CNF film. It has been confirmed that there is no difference by DC solution and it is a phenomenon by CNF. Through this experiment, CM-CNF film shows that it improves the storability of fresh food.

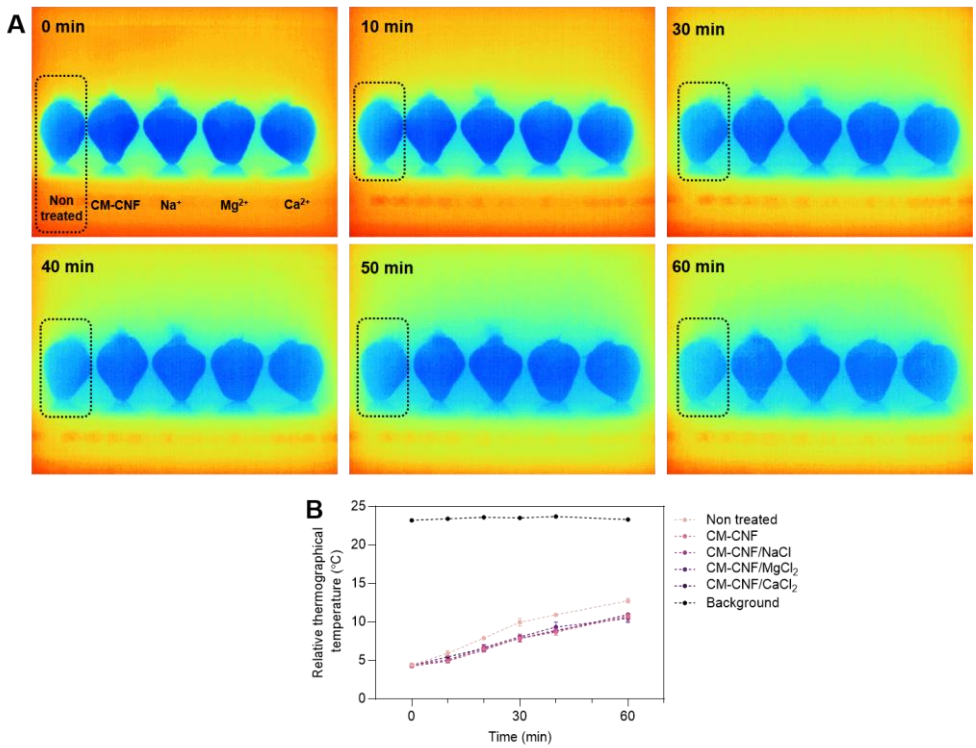

Fig. 24 Effect of variable CM-CNF coating on the temperature change of strawberry surface. A) Thermograph of strawberries with storage time. B) Dependence of film on the surface temperature of strawberry.

4.4. Functionality and Stabilization of CNF- RC extract film

4.4.1. Extraction and characterization of RC extract

Red cabbage extract (RC extract) was extracted by the solvent extration. First, the red cabbage was freeze dried to remove moisture and make it powder. The red cabbage was then melted with ethanol and hydrochloric acid. RC extract was obtained through vacuum filtration and drying. Four conditions were tested to increase extraction efficiency. The experimental conditions were 1. Heating extraction, 2. Solvent extraction, 3. Solvent extraction using freeze-dried red cabbages (Fig. 25, equation 9). Experiments show that total anthocyanin content was 6.87 mg/100 g, 9.98 mg/100 g and 14.01 mg/100 g. Solvent extraction was 1.4 times more efficient than heating. It is also 1.4 times more efficient when extracted using freeze-dried powder. The dry freezing caused the sample to lose moisture and the concentration of solvents to increase the extraction efficiency. Through this experiment, the following experiment processed with RC extract by solvent extraction of freeze dried powder.

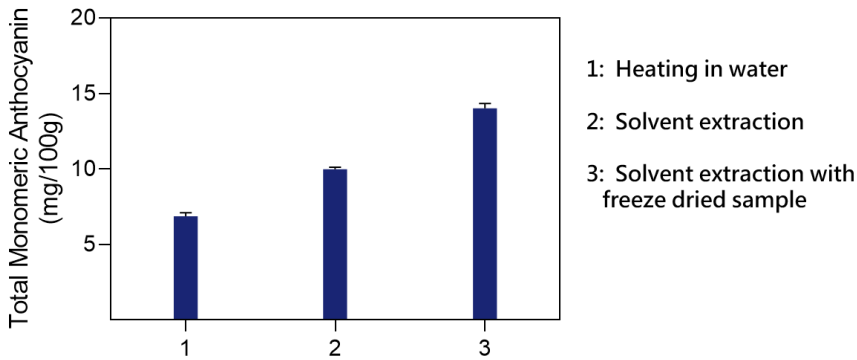

Fig. 25 Total monomeric anthocyanin contents of extracted samples 1. Heating in water. 2. Solvent extraction. 3. Solvent extraction with freeze dried red cabbage. (n=3)

4.4.2. Evaluation of functionality of RC extract

Before evaluating the functionality of RC extract, color variations resulting from addition were measured using a color difference meter (Fig. 26A). RC extract is a natural pigment that can significantly change the color of the film when added to excess. The color range used CIE color space and equation 10 to calculate ΔE by summing the changes in L* (Fig. 26B), a* (Fig. 26C), and b* (Fig. 26D) [159]. The concentration of RC extract was set from 0 to 5, and the color difference of each sample was calculated. Calculations show that lightness gradually decreases and both a* and b* values increase to positive numbers. Calculated by ΔE, a sample of 5 mg/100 g was 22.52 (Fig. 26E). Experiments have confirmed that there is a color change of about 4.82 for each increase in RC extract by 1 mg/100 g.

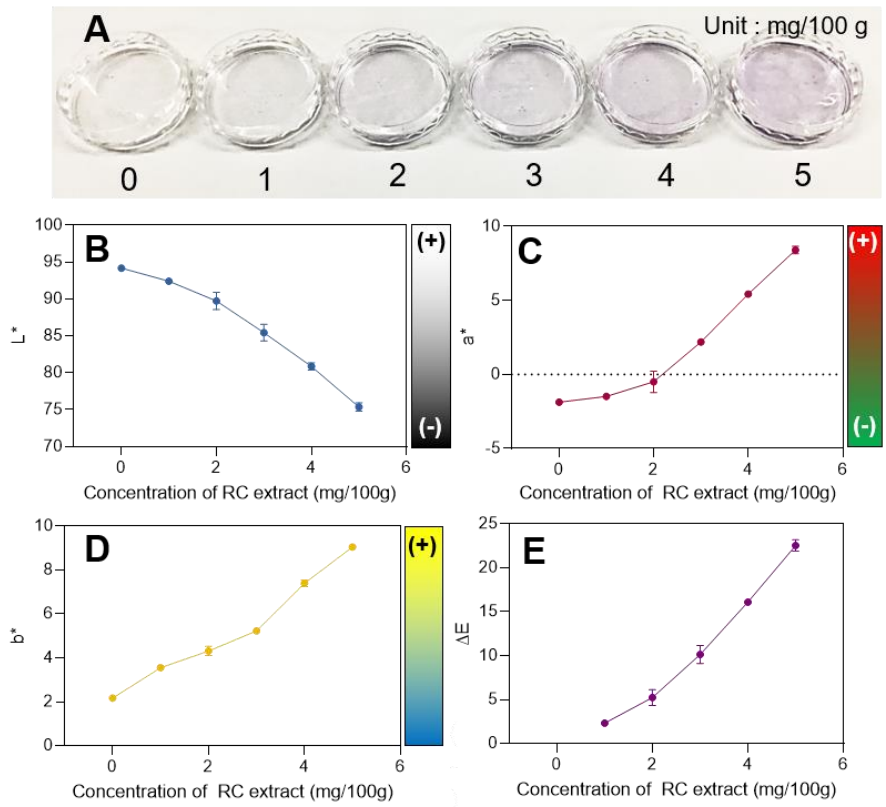

Fig. 26 A) The color distribution of CM-CNF/$CaCl_2$/ RC extracs films by increasing concentration of RC extract from 0 to 5 mg/100 g. B) The CIE color distribution of Lightness* value increasing concentration of RC extract from 0 to 5 mg/100 g C) a* value D) b* value E) ΔE value. (n=3)

RC extract contained natural antioxidant products. RC extract has a ring structure, and if a radical is present, it is scavenged by resonance ring. The N in the middle of DPPH is purple, and when radical is scavenged, it is reduced to NH and yellow (Fig. 27A). To quantify this phenomenon, DPPH (2,2-diphenyl-1-picrylhydrazyl) assay was performed. Using a sample concentration of 1 to 5 mg/100 g, the scavenging rate of DPPH was evaluated. Experiments showed that the higher the concentration of RC extract, the higher the scavenging rate, and in particular, the 5 mg/100 g sample showed a figure of 56.94 % (Fig. 27B, equation 11). This confirmed the antioxidant effect of RC extract.

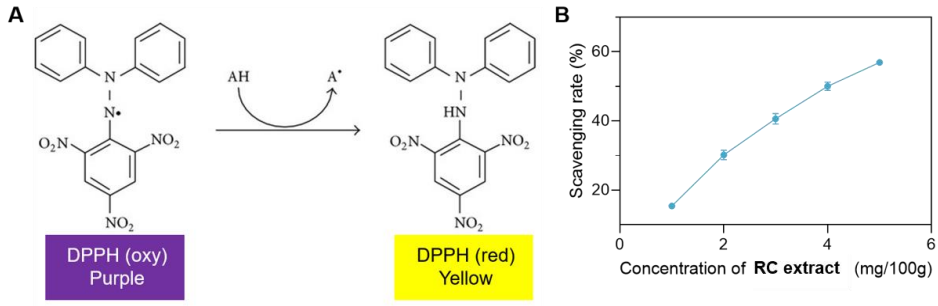

Fig. 27 A) The theory of DPPH assay. The color change by adding RC extract with transform the structure of 2,2-diphenyl-1-picrylhydrazyl. B) The scavenging rate for DPPH by increasing concentration of RC extract. (n=3)

The more RC extract is added to the coating solution, the darker the purple color. As shown in Fig. 28A, B, the transmittance in the visible light region decreased as RC extract concentrations increased. This phenomenon was observed in the ultraviolet range, which showed a significant decrease in ultraviolet penetration. In particular, at 300-340 nm, a strong ultraviolet region, 5 mg/ 100 g concentrations of film penetrated only 23% of ultraviolet light. Compared to CM-CNF film, which has little change in ultraviolet transmittance, the difference was clear. RC extract is also observed in plant leaves, which are known to protect the leaves from the ultraviolet rays of sunlight [160]. Through this, it is expected that the film with RC extract will protect food from ultraviolet light. In particular, if used externally, the effect will be increased. By applying this phenomenon, it could be used in a variety of ways not only in food but also in places for UV protection.

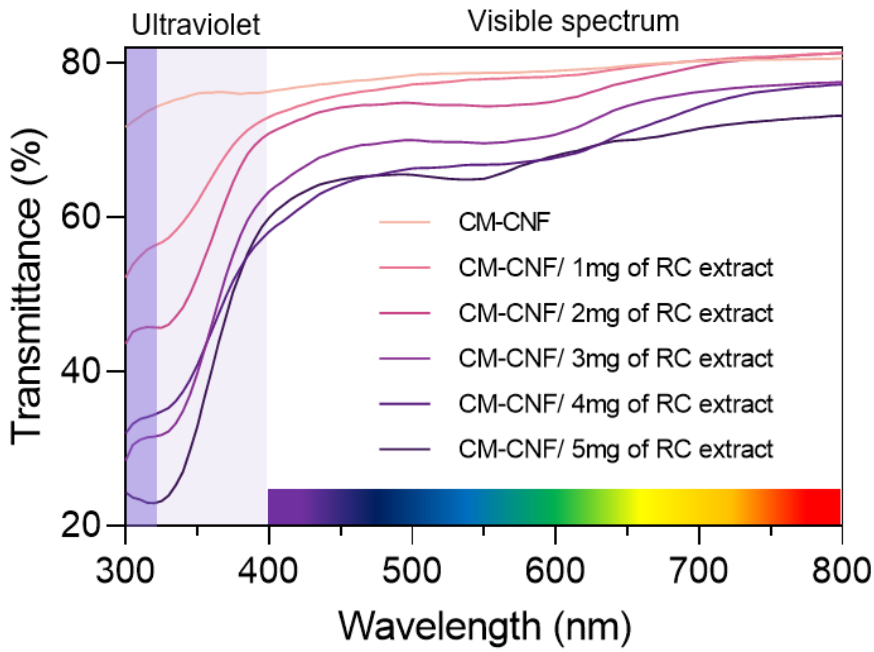

Fig. 28 A) Transmittance of CM-CNF/$CalCl_2$/ RC extract film that wavelength from 300 to 800 nm. B) Wavelength from 300 to 400 nm.

To determine the degree of UV protection, RhB removal was observed using TiO_2 as a photocatalyst. RhB is a reddish dye that is graded by TIO_2, which is excited by ultraviolet light (Fig, 29). The experiment measured absorbance at 10 minute intervals and calculated the color change using equation 12. Experimental results showed that RhB irradiated by CM-CNF film for an hour was approximately 76%. On the other hand, 37% of the film in condition 5mg/ 100 g was graded after an hour. It is believed that RC extract present in the film protects against ultraviolet light and penetrates only relatively low levels of ultraviolet light. Transmitted ultraviolet light activated TiO_2 to form radical and deteriorated RhB. About an hour of experiments have shown that it has more than twice the sunscreen effect. RC extract is thought to have the effect of protecting food from UV rays. This effect can protect food spoilage caused by UV exposure in the cold chain system.

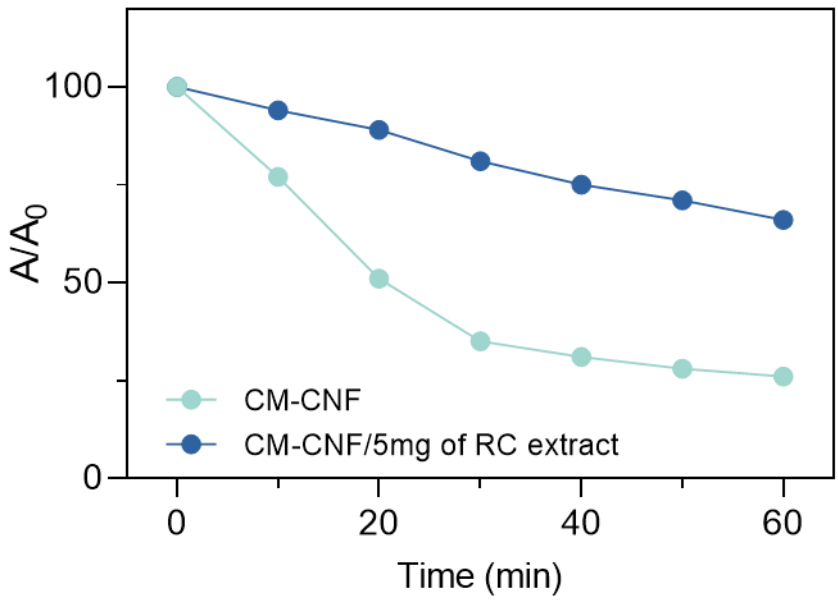

Fig. 29 The absorbance difference between CM-CNF film with CM-CNF/$CaCl_2$/ RC extract film with photocatalytic activity of TiO_2 against RhB solution within 60 min.

4.4.3. Enhancing the stability with RC extract -metal ion complex

DC solution not only enhances the property of CNF film but also contributes to increasing the stability of RC extract (Fig. 30A). RC extract contained the natural dye, so it is easily graded by temperature, pH, humidity, and contact with oxygen. To prevent this, DCs can be stabilized through RC extract and chelation [161]. This can be seen by observing the color changes of the film. The non-treated film and CM-CNF/NaCl film had a higher L* value (Fig. 30B) after one day, and the values of a* (Fig. 30C) and b* (Fig. 30D) changed to positive and negative, respectively. CM-CNF/$CaCl_2$ film, on the other hand, maintains the color relatively long because it is a multivalent state capable of chelating with RC extract. Maintainability is very important to serve as a film that requires food to be stored for a long period of time. Based on these experiments, the film, which was soaked in $CaCl_2$, confirmed that RC extract s retention could be increased. Through this, DC solution predicted two reinforcement effects.

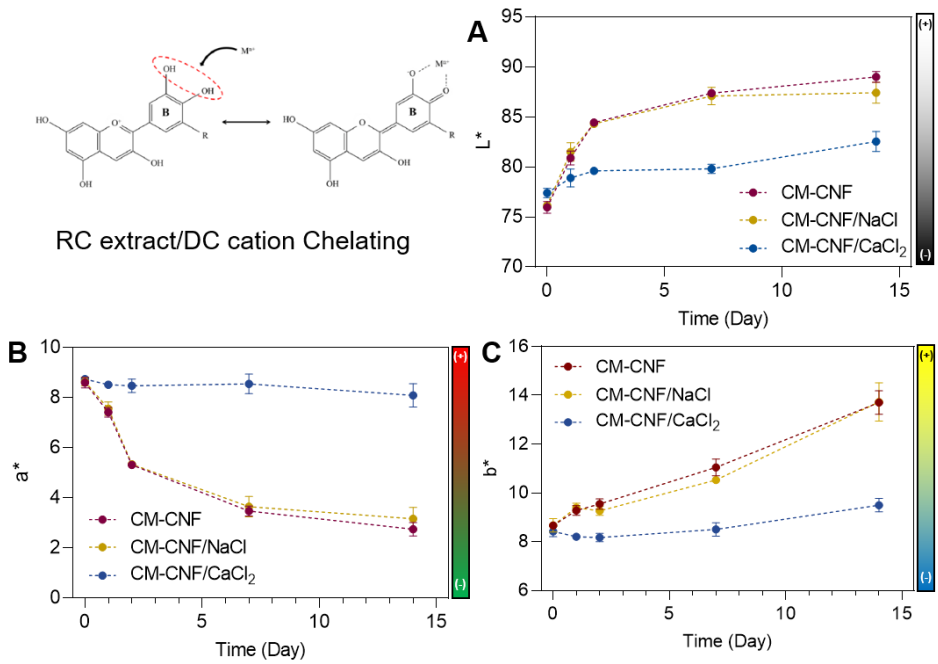

Fig. 30 A) The mechanism of chelating between RC extract with DC. B) The Lightness* distribution CM-CNF film within 14 days. C) The a* distribution CM-CNF film within 14 days. D) The b* distribution CM-CNF film within 14 days. (n=3)

4.4.4. Cell proliferation test of CNF- RC extract film

AlamarBlue assay was conducted to check the cell proliferation of film. NIH-3T3 cells were used for a week for elution [130]. Experiments show that both CM-CNF film and CM-CNF/$CaCl_2$/ RC extract film showed no difference in error range compared to control for about a week (Fig. 31). Carboxymethyl cellulose is a food preservation material included in the U.S. FDA's orbit. CM-CNF, on the other hand, has no exact standard to date. Experiments have shown that there is no toxicity to the substances added to CM-CNF. As a result of the experiment, the cell proliferation rate was the same in all samples on the 7th day. Through this, it is predicted that we indirectly demonstrate the utilization of the food preservation film.

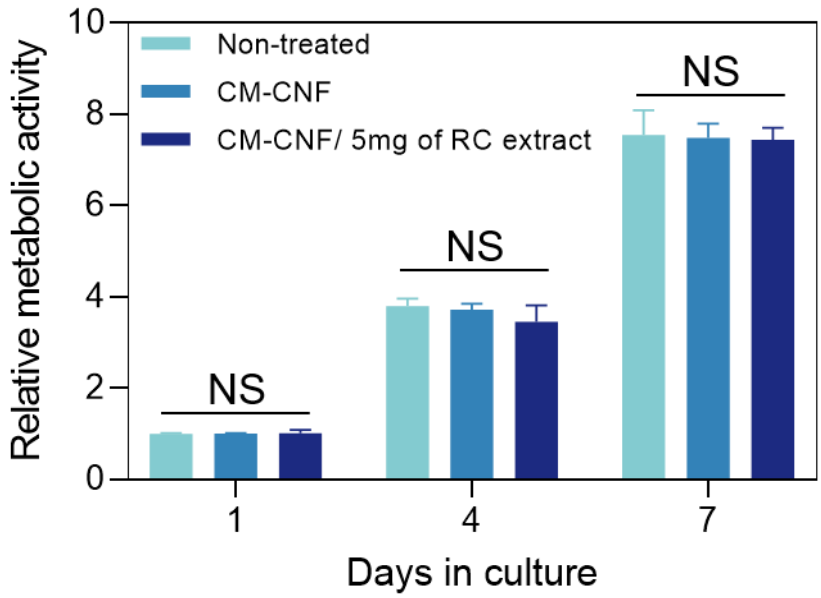

Fig. 31 The cell prolifeation test of CM-CNF films with alamarBlue assay. (n=3) NS indicates no significance, and statistical analysis was performed using one-way ANOVA test.

4.5. Application of non-climacteric fruits

Non-climatic fruits do not produce ethylene by respiration system. Depending on the amount of respiration rate, senecence is received in turn. Therefore, respiration rate could be changed the senecence of non-climacteric fruits. Coating a uniform film throughout the non-climatic fruit and controlling the amount of respiration would be significant. Also, if moisture evaporation is suppressed by film, it will help keep the fruit much longer.

4.5.1. Optimization of coating method

The viscosity of CNF was optimized by evaluating the coating uniformity. If the concentration of CNF is too low, the coating solution will peel off the food surface. On the other hand, if the concentration of CNF is too high, the coating solution will be applied unevenly. As shown in fig.32A, the coating solution was uniformly applied at a concentration of about 1%. Grapes were coated with CNF solution with rhodamine added. The distribution of rhodamine was confirmed through UV ramp. CNFs with too low a viscosity fall off the surface of the fruit. Therefore, the intensity of rhodamine is weak. On the other hand, CNF with too high viscosity adheres unevenly to the surface of the fruit. Therefore, the intensity of rhodamine is formed non-uniformly. Through these results, 1% of CNF viscosity was suitable. Drying time is also a consideration when fabricating a film. This is because prolonged exposure to moisture increases the risk of infection and defect. In this experiment, the drying conditions were about 25 ℃ and the relative humidity was 60%. The drying time under this condition was about 24 hours. In general, drying time is carried out under the conditions of 12 to 48 hours [162]. Depending on the type of food, conditions such as temperature and humidity will have to be controlled. On the other hand, in industrial scale, relative humidity or temperatures are controlled to reduce drying time [163].

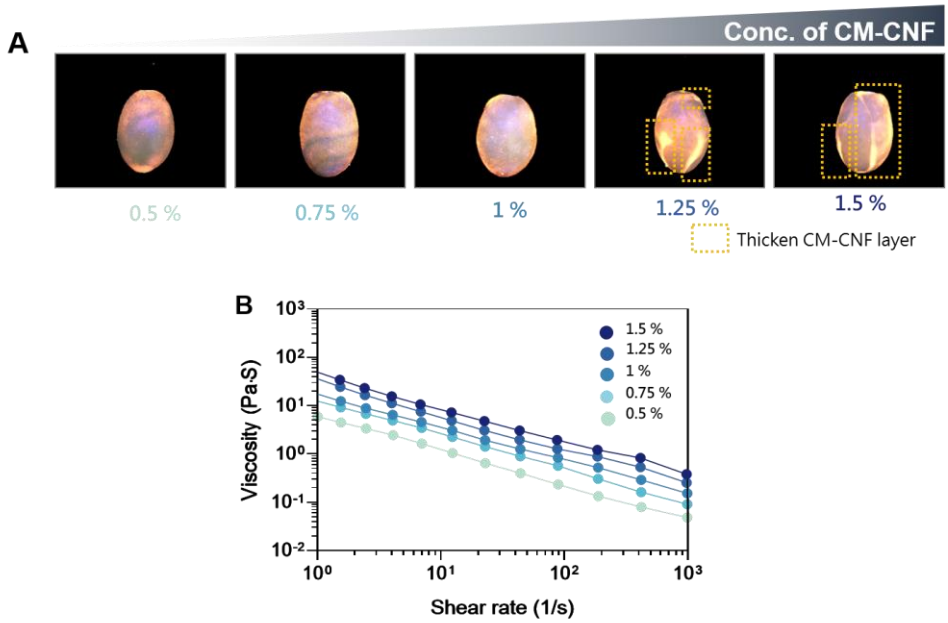

Fig. 32 A) The images of coated surface of grape with concentration from 0.5 % to 1.5 % added fluorescence powder on the CNF solution. B) The viscosity of CNF solution with shear rate from 10^0 to 10^3 (1/S). (n=3)

Strawberry divided into three parts in order to ensure the uniformity of the coating was determined the thickness of the film. Strawberries are prone to detachment from the middle part when set vertically (Fig. 33A). The concentration of CM-CNF was set to 0.5, 0.75, 1, 1.25 and 1.5 %. As a result, when the concentration of CM-CNF was coated at a lower concentration based on the concentration of 1 % CM-CNF, the solution was shown to flow to the ground by gravity. On the other hand, when coating at a concentration higher than 1 %, the coating thickness tended to be densed without constant coating. In particular, the denser portions seem opaque, and when coated with 0.5 % CM-CNF, the lower part of strawberry was confirmed to flow in a dense manner. In addition, the concentration of 1.25 % or more was coated with a constant thickness, and when coated with 1.5 %, the overall irregular coating of strawberry was observed. To confirm the coating thickness accurately, the thickness of strawberries was divided into three parts to confirm the thickness change (Fig. 33B). As a result, it was confirmed that the thickness of the lower part was less affected by the concentration than the thickness of the middle and upper parts. The thicker the concentration of CM-CNF, the thicker the overall thickness tends to be, and the thickness of coatings of 1.25 % and 1.5 % were relatively irregular.

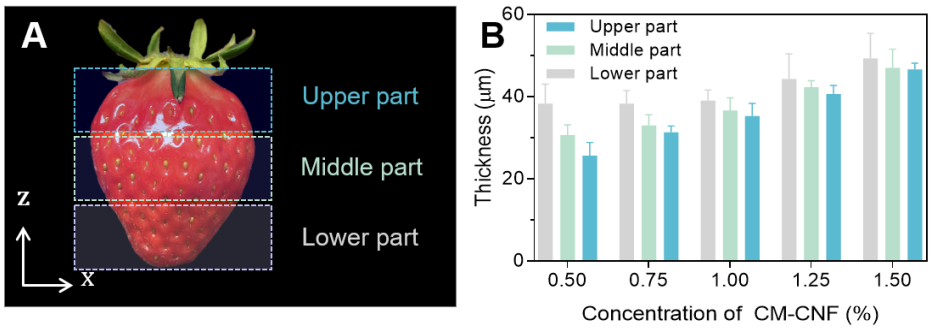

Fig. 33 A) The image of CM-CNF coated strawberry with 3 sections (upper part, middle part and lower part) to measure thickness of film. B) Thickness of CM-CNF film. Each part was selected randomly and measured three times. (n=3)

4.5.2. Evaluation of decay rate and weight loss

The purpose of CM-CNF/DC film is to protect the surface of fruit and prevent external influence. In addition, it suppresses moisture drying and controls respiratory volume to suppress senecence and improve food quality. The efficiency of film was evaluated using strawberries to confirm the applicability. Strawberries are very susceptible fruits, especially after harvesting, because they are highly environmentally affected, both consumers and producers should pay attention to storage. The fraction of original weight, response rate, firmness, total soluble solids and acidity were measured for the comprehensive evaluation. Non-treated strawberry was observed to have mold on the surface from the 4th day of storage and the moisture was dried (Fig. 34). On the other hand, it was confirmed that the sample coated with pristine CM-CNF, CM-CNF/NaCl, CM-CNF/$MgCl_2$ and CM-CNF/$CaCl_2$ film was better conditioned. In particular, CM-CNF/$MgCl_2$ and CM-CNF/$CaCl_2$ films were found to be the relative good condition after 7 days. In addition, it was confirmed that both samples did not cause damage by mold, which proves that the outside air was effectively blocked by coating the surface of the fruit. Moreover, it was confirmed that the softness of the surface of strawberries rarely occurred.

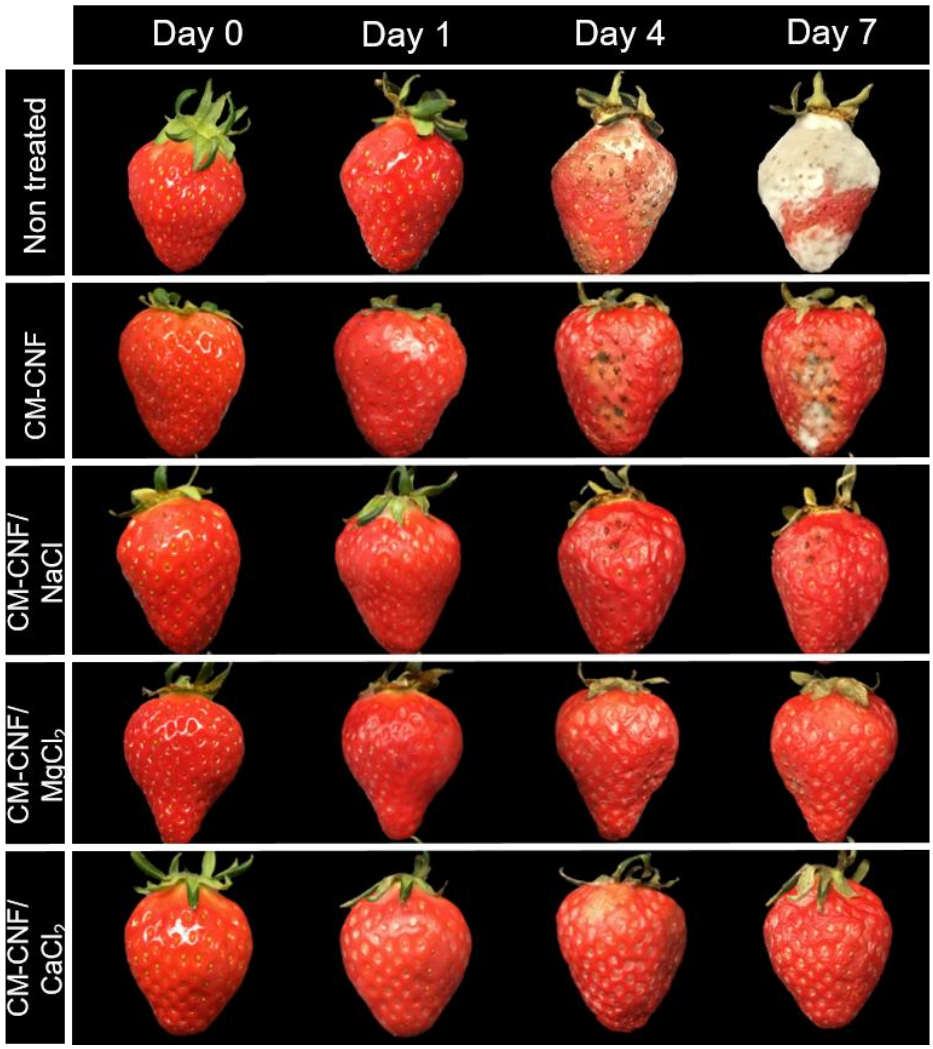

Fig. 34 Microbial contamination of strawberries stored at ambient condition for 7 days. (a) Picture of strawberries. Non-treated strawberries showed the start of microbial growth on Day 4 and CM-CNF coated strawberries without salt treatment showed significant microbial growth on Day 7. CM-CNF/NaCl, CM-CNF/$MgCl_2$ and CM-CNF/$CaCl_2$ film coatings protected the strawberry surface from microbial growth.

Dehydration of Strawberry occurs by water evaporation and microbial decay. Strawberries are perishable fruit, which causes rapid dehydration compared to other fruits. Therefore, it is very important to prevent dehydration. As shown in Fig. 35A, the weight change for each sample was measured by equation 13. Non-treated strawberry was dehydrated after 7 days of storage and 51.98 % of original weight. The relatively low dehydration of the CM-CNF coated strawberry was confirmed. In particular, 73.20 % of original weight was dehydrated after 7 days of the strawberry coated with CM-CNF/$CaCl_2$ film. Compared with non-treated sample, it was confirmed that there was a difference of more than 21.22 %. These results suggest that CM-CNF film prevents the dehydration of strawberry. In addition, the film combined with DC effectively prevented dehydration and CM-CNF/$CaCl_2$ film was the most effective. Also, as shown in Fig.35 B and C, the cross section of the strawberry varies significantly after seven days depending on the type of film. CM-CNF film appears to contract because it does not prevent moisture evaporation and respiration relatively well. CM-CNF/$CaCl_2$ film, on the other hand, shows that moisture is preserved and relatively fresh.

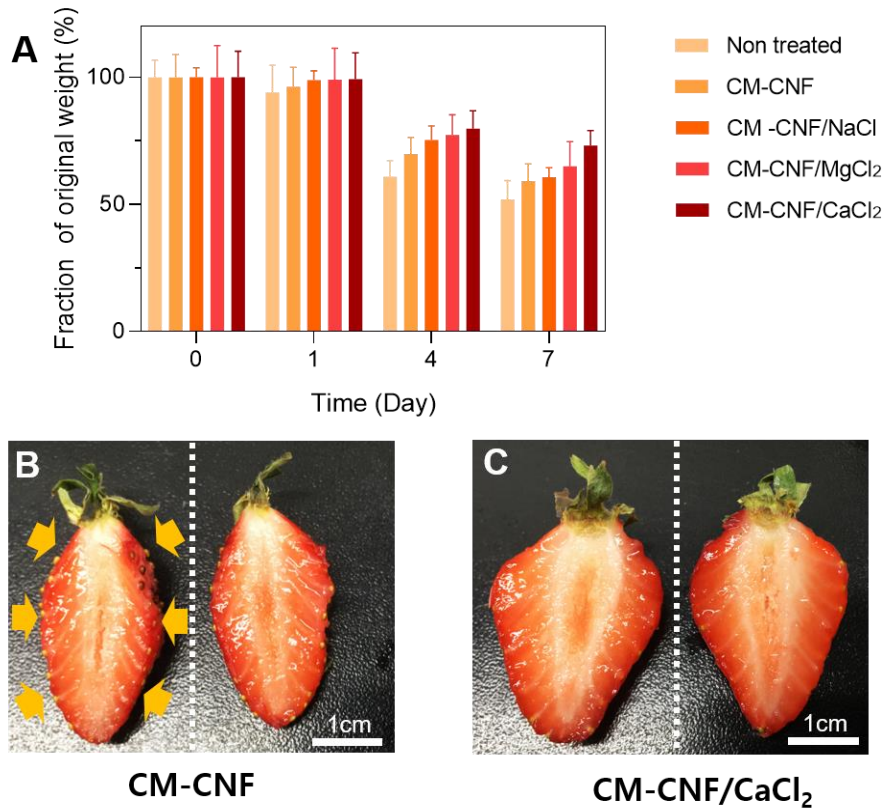

Fig. 35 A) The fraction of original strawberry weight within 7 days. (n=3) B) The cross section image of strawberry coated into CM-CNF film in 7 days C) The cross section image of strawberry coated into CM-CNF/$CaCl_2$ film in 7 days.

4.5.3. Feasibility of control the respiration rate

The respiration rate was calculated by quantifying the CO_2 released through gas chromatography (Fig. 36, equation 14) [144]. The respiration rate was lower than the control of the strawberry coated with CM-CNF/DC film. In particular, the Strawberry coated with CM-CNF/$CaCl_2$ film showed the lowest respiration rate. The performance of film combined with divalent cations was better than that of Na^+ bonded monovalent cations. Moreover, the film performance combined with Ca^{2+} was more effective than Mg^{2+}. This suggests that entangled CNF fiber by Ca^{2+} is the best way to prevent the respiration of fruits. Ca^{2+} has greater binding power than Mg^{2+}, which is the best way to control respiration rate of strawberry. Fruits are known to inhibit quality deterioration by suppressing respiration. The results showed that the freshness of strawberries was preserved by controlling the respiration rate as well as the dehydration of CM-CNF/DC film.

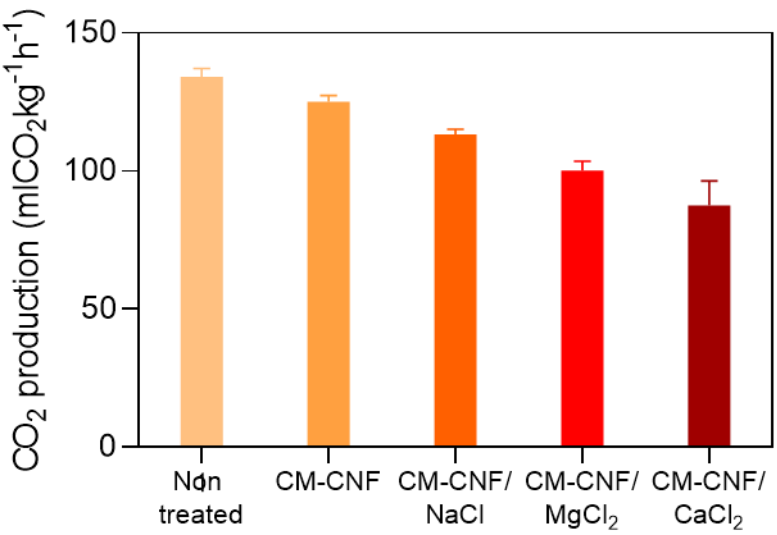

Fig. 36 CO_2 released from strawberries coated with different CNF films in 7 days. (n=3)

4.5.4. Evaluation of texture and ingredient contents

It is important to control the senecence process because the longer the storage period and the product quality increases as the senecence process is delayed. In order to confirm the change of product quality during this process, the firmness, total soluble solids, and acidity were measured. Strawberries quickly cause softening and have a significant impact on the decline of texture. As shown in Fig.37, non-treated strawberry showed a 24.45 % decrease in firmness in just one day of storage. Also, on the 4th day, it was confirmed that the quality was very low due to a sharp decrease. On the other hand, in the case of strawberries coated with CM-CNF/$CaCl_2$ film, the firmness preservation was maintained longer than non-treated sample. In particular, the firmness was twice as high as all other samples on the 4th day of storage. Generally, the decrease in Firmness occurs due to the destruction of the fruit structure by enzymes. Maintaining Firmness inhibits the senecence, which is the most effective CM-CNF/$CaCl_2$ film.

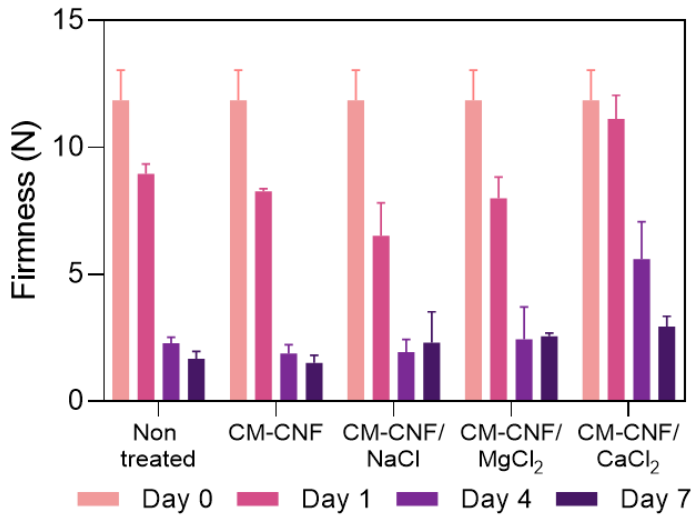

Fig. 37 The firmness of strawberry coated with CM-CNF film within 7 days. (n=3)

Total soluble solids (TSS) exhibit total amounts such as sugar, amino acids, and pectin. Especially in the senecence process, the soluble solids decrease by the respiration of fruit. In other words, the decrease of the TSS leads to the senecence process. Non-treated strawberry showed the highest TSS at 13.65 % on the 4th day (Fig. 38A). On the 7th day, it showed a decrease, which is senecence process through ripening. Strawberries coated on CM-CNF, CM-CNF/NaCl and CM-CNF/$MgCl_2$ film showed the highest TSS value in the 7th day. On the other hand, strawberries coated on CM-CNF/$CaCl_2$ showed TSS value of 11.9 % on the 7th day. This means that the range of senecence is relatively slow compared to other sample. In other words, CM-CNF/$CaCl_2$ film is most effective in reducing the senecence process and maintaining freshness of strawberry. The results of the Acidity measurement also showed that the time of the sequence was similar. Non-treated strawberry showed the highest at 0.50 % on the fourth day (Fig. 38B), which was rather decreased on the seventh day. Strawberries coated with CM-CNF, CM-CNF/NaCl and CM-CNF/$MgCl_2$ film showed the highest acidity value at the 7th day. On the other hand, the strawberry coated on CM-CNF/$CaCl_2$ showed 0.29% acidity value on the 7th day. During the ripening of fruit, acidity increases because of the increase in the concentration of non-dissociated organic acids [164]. At the end of ripening, TA decreases, and this phenomenon is known as one of the indicators for senecence process. The results of the experiment confirmed that CM-CNF/$CaCl_2$ film effectively delayed the senecence process.

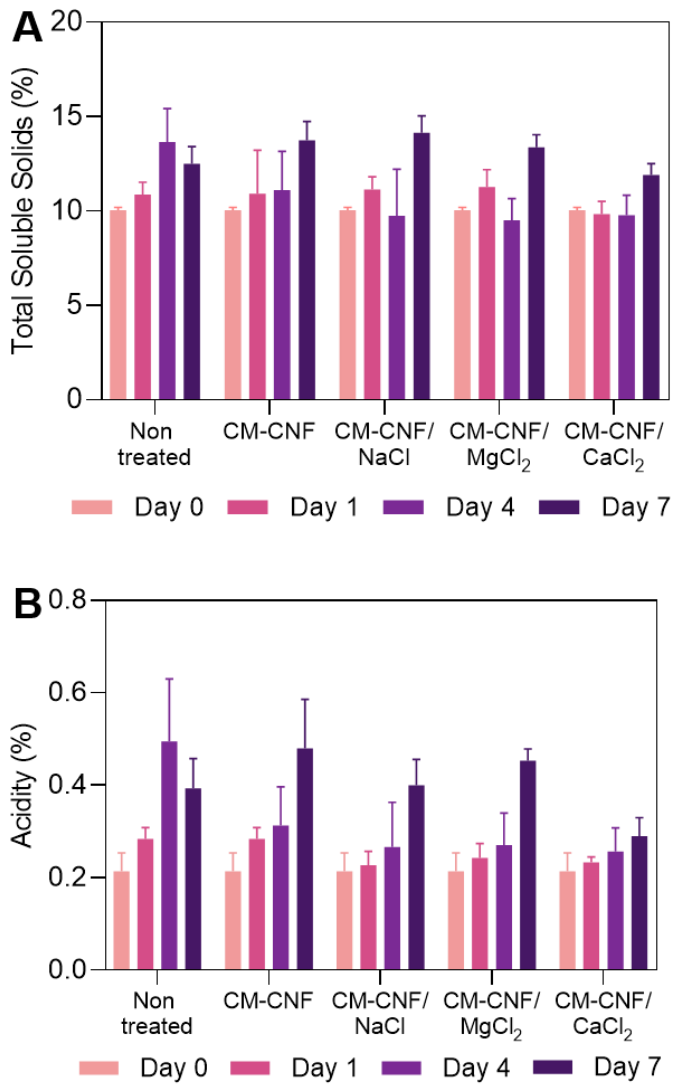

Fig. 38 A) The total soluble solids and B) Acidity of strawberry coated into CM-CNF film within 7 days. (n=3)

4.6. Application of climacteric fruits

Fruits are divided into climacteric fruits and non-climatic fruits according to their process of senecence. The climacteric fruit is caused by ethylene gas, which leads to increase the rate of senecence. In particular, they are also affected by ethylene gas, accelerating their growth rate. This phenomenon has a significant effect on keeping the fruits for a long time in store. The respiration rates are accelerated by absorbing the ethylene gas produced on the surface of fruits. It does not occur because it is quickly consumed afterwards. If the respiration rates were controlled by food preservation film, the concentration of ethylene gas also could be regulated.

4.6.1. Evaluation of decay rate and weight loss

Banana was selected as the experimental sample represented climacteric fruits. It appears the green color before harvesting on the tree. As the senecence in progress, the color of banana was converted green into yellow in nature. When arrive at senecence, the surface of banana was happened black dot all over the body. It was caused by enzymatic degradation as known as browning effect [165]. The process of browning effect was occurred by polyphenol oxidase (or PPO). In the presence of O_2, the PPO was transformed to substances known as phenolic compounds by oxidation process. Quinone was changed to melanin by auto oxidation [166]. Melanin is dark brown pigment that colors skin, hair and iris of eyes. This process, however, generally does not happen within fresh fruits because the PPO and the phenolic compounds are separated in the cells.

In the 4th day of storage, it was considered that CM-CNF/$CaCl_2$ and CM-CNF/$CaCl_2$/ RC extract film influenced to the banana (Fig. 39). There was less browning effect than non-treated sample. After 10 days started experiment, the banana coating with CNF/$CaCl_2$/RC extract film was observed the freshest sample than others. The film acted as a barrier to prevent contact with oxygen. And also, RC extract was known as anti-browning compound because of strong anti-oxidant effect. It was expected that the two reasons were effected with preventing the browning effect on the surface of banana.

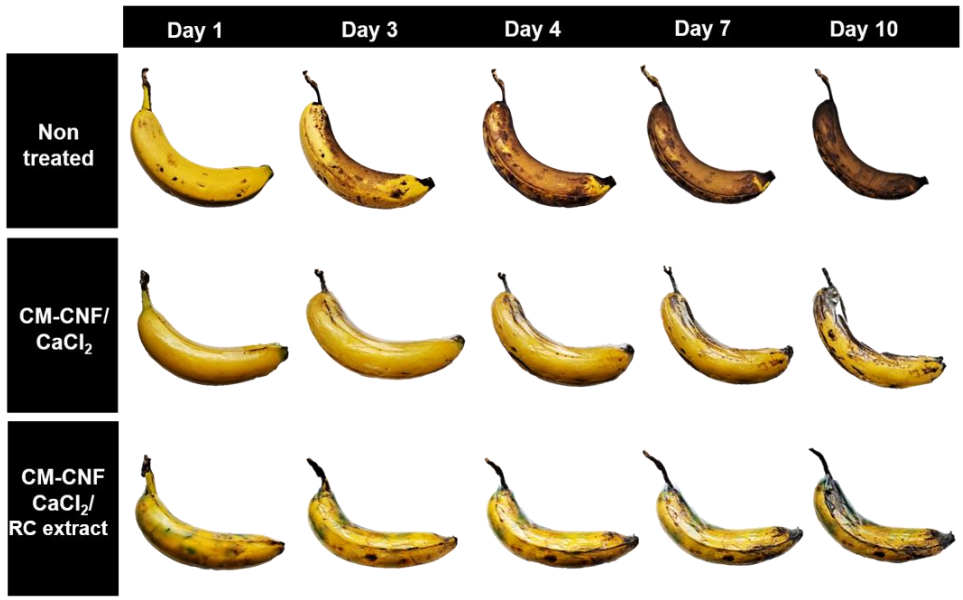

Fig. 39 The representative images of banana, coated with CM-CNF/$CaCl_2$ and coated with CM-CNF/$CaCl_2$/RC extract. Each sample were stored at room temperatures in 10 days. All the samples were hanged with steel bar.

Dehydration of banana was caused by water evaporation and browning effect. Bananas are vulnerable to dehydrate compared to other climacteric fruits. Therefore, it is necessary that protect the dehydration. As shown in Fig. 40, the weight change for each sample was measured by equation 13. Non-treated banana was dehydrated after 10 days of storage and 36.96 % of original weight. In particular, 68.77 % of original weight was dehydrated after 10 days of the banana coated with CM-CNF/$CaCl_2$/RC extract film. Compared with non-treated sample, it was confirmed that there was the difference about 31.81 %. It was suggested that CM-CNF film prevents the dehydration of banana. In addition, the film bonded with Ca^{2+} prevented effectively dehydration. RE acted as the compound of anti-browning effect, which protect the dehydration by enzymatic degradation of PPOs. It helped phenolic compound to prevent converted into quinones with oxidation [167].

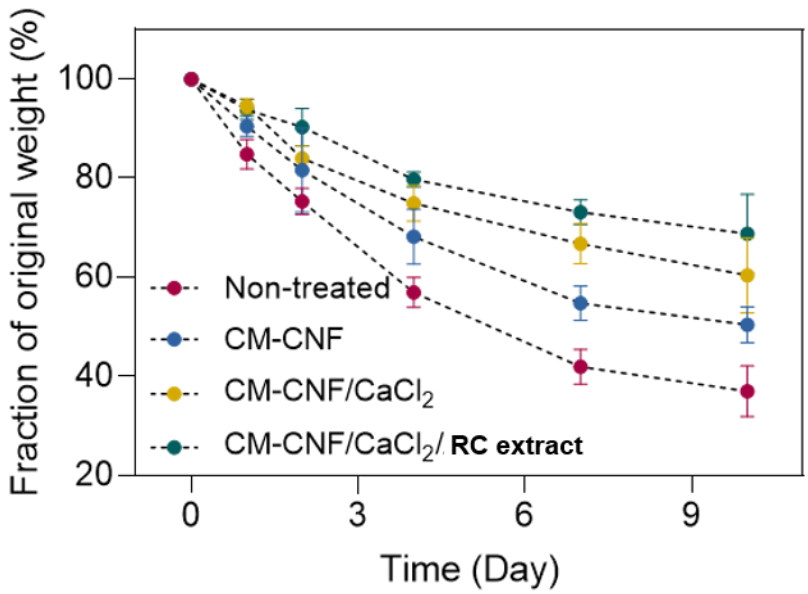

Fig. 40 Fraction of the original weight of banana coated with CM-CNF, CM-CM-CNF/$CaCl_2$ and CM-CNF/$CaCl_2$/RC extract film within 10 days. (n=3)

4.6.2. Feasibility of control the respiration rate

The respiration rate is one of critical reason the how preserve fruits by thin barrier fabricated by CNF. It was evaluated by quantifying the CO_2 released through gas chromatography (Fig. 41A, equation 14). Non treated banana was the highest value among the samples. On the other hands, Both CM-CNF/$CaCl_2$ film and CM-CNF/$CaCl_2$/RC extract film showed the lowest respiration rate. There were 10.58, 10.54 ml·CO_2/kg·h each other. The efficacy of film bonded with Ca^{2+} was higher than only CM-CNF coated. There was no significance both CM-CNF/$CaCl_2$ film and CM-CNF/$CaCl_2$/RC extract film. Ethylene gas is known as excellent mature hormone for almost fruits and vegetables. It could promote to convert amylose into sucrose by accelerating activation of amylase [168]. And also, Pectinase is rapidly activated by ethylene, which accelerating degradation of pectin known as one of structural components [169]. Therefore, it is necessary that the protection of emitting the ethylene gas to atmosphere. At 4 days after coated with film, there were significant difference between non-treated and CM-CNF/$CaCl_2$/RC extract film (Fig. 41B). CM-CNF/$CaCl_2$/RC extract film was determined that the barrier property against ethylene gas were excellent with 18.25 mV·sec. There was no significance both CM-CNF/$CaCl_2$ film and CM-CNF /$CaCl_2$/RC extract film.

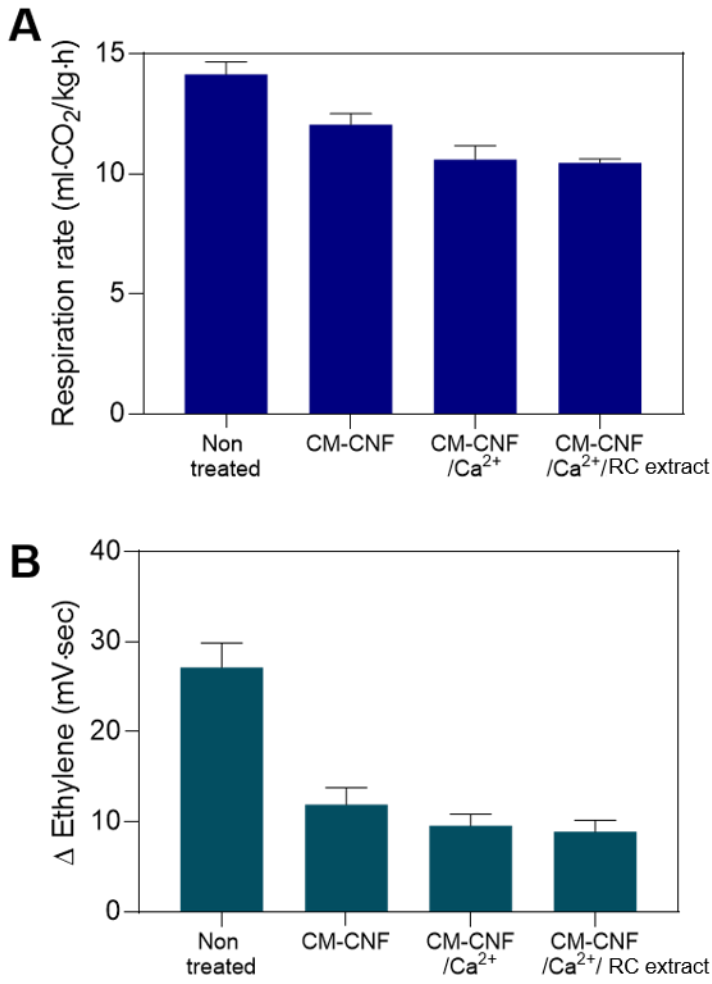

Fig. 41 A) Respiration rate of banana coated with different CNF films in 10 days. B) The integrated area of ethylene emitted in banana coated with CNF films in 4 days. (n=3)

4.6.3. Evaluation of texture and ingredient contents

Senecence process is caused to destroy the structure of fruits by accelerating pectinase to decompose pectin. In addition, as increasing the contents of sugar, both organic acids and lipids were converted to sugar by variant cycle. It caused to decrease the texture around senecence process [170]. As shown in Fig. 42A, there were visually difference each samples. All the sample was measured the firmness by texture analyzer with random point in triplicates (Fig. 42B). As a results of measurement, the difference of firmness was observed after the day coated with film (Fig, 42C). In particular, CM-CNF /$CaCl_2$/RC extract film was calculated at the difference of firmness about 56.49 % in 10 days. On the other hands, Non-treated was calculated at the difference of firmness about 81.56 % in 10 days. It was determined that CM-CNF /$CaCl_2$/RC extract film has the effect to impede the senecence process. There was no significance both CM-CNF/$CaCl_2$ film and CM-CNF /$CaCl_2$ RC extract film.

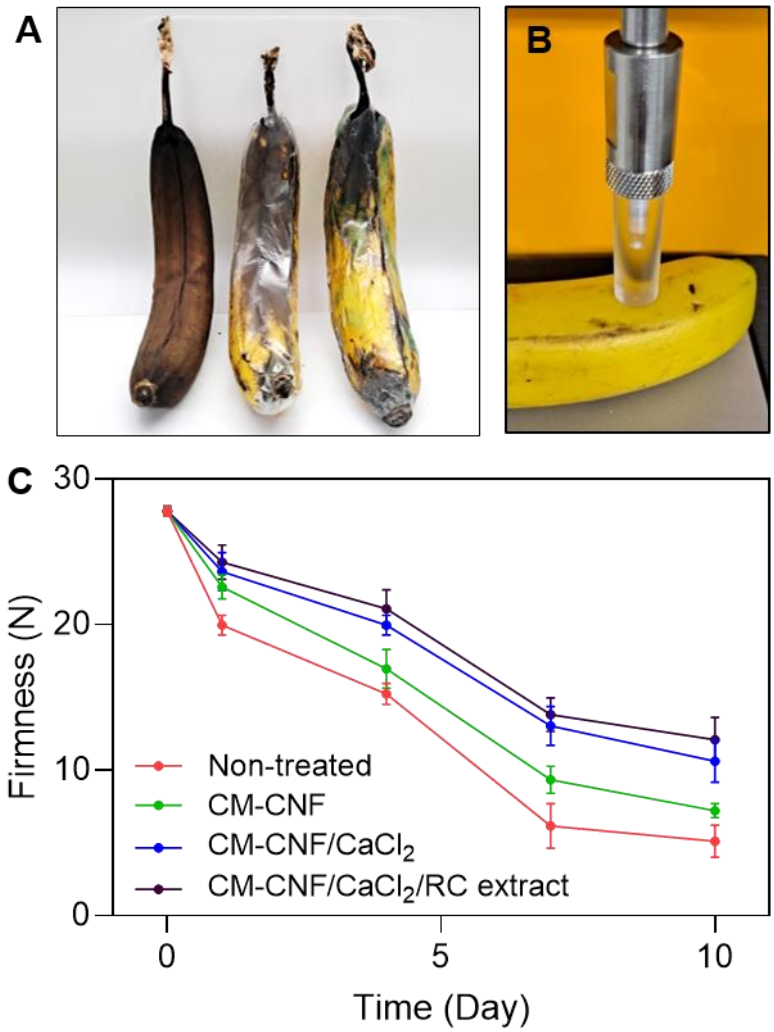

Fig. 42 A) The image of banana stored in 10 days. B) Firmness was measured by texture analyzer in three random point. C) The firmness of banana coated with CM-CNF film within 10 days. (n=3)

TSS value of all sample was measured by refractometer within 10 days. (Fig. 43A) Non treated sample was the highest value at 13.65 % in day 4. After then, TSS value has tendency to descend convulsively. On the other hands, CM-CNF /$CaCl_2$/RC extract film was the highest value at 13.47 % in day 10. It was slowly increased from 10.03 % to 13.47 % all over the day. It was determined that non treated sample was arrived at senecence in 4 days after staring experiments. It was identified that CM-CNF /$CaCl_2$/RC extract film acted as a protective barrier to impede the senecence process. Acidity was evaluated after 10 days (Fig. 43B). Non treated sample was the highest value at 0.57 % in day 4. After then, Acidity has tendency to increase. On the other hands, CM-CNF /$CaCl_2$/RC extract film was the lowest value at 0.61 % in day 7. It was slowly decreased from 0.45 % to 0.61 % all over the day. It was confirmed that non treated sample was arrived at senecence in 4 days after staring experiments. Both CM-CNF /$CaCl_2$ film and CM-CNF /$CaCl_2$/ RC extract film has an impact to preserve banana against the senecence process. It was clearly showed the feasibility of the method to preserve banana coated with film. There was no significance both CM-CNF/$CaCl_2$ film and CM-CNF /$CaCl_2$/RC extract film at day 10.

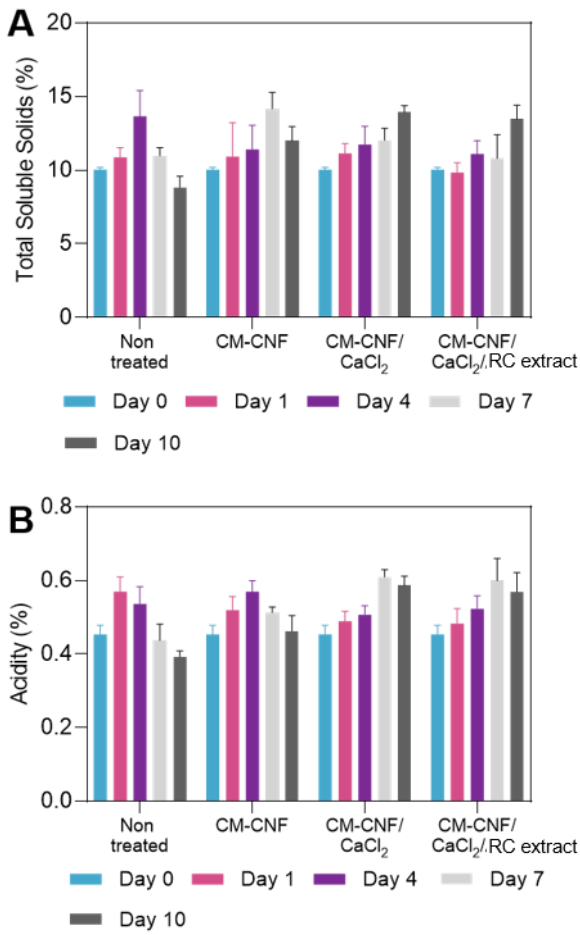

Fig. 43 A) The total soluble solids and B) Acidity of banana coated with CM-CNF film within 10 days. (n=3)

4.6.4. Anti-browning effect

To confirm the anti browning effect by RC extract, a tyrosinase inhibition assay was performed (Fig. 44). In general, enzymatic browning occurs in bananas due to the destruction of cell walls and tissues during the ripening stage. Through this, polyphenol oxidase (tyrosinase) is released and comes into direct contact with oxygen. In this process, the substrate (L-tyrosine) is oxidized to melanin by tyrosinase. Browning dots lower the product value and damage the aesthetics. For this reason, the degree to which oxidation is prevented by RC extract was measured. As a result of the experiment, it was confirmed that the higher the RC extract concentration, the higher the anti-browning effect. When the concentration of RC extract increased from 0 to 3%, it increased to 0.49%, 15.32%, 39.66% and 61.47% (Equation 15). The activity of tyrosinase is inhibited through competitive inhibition by RC extract. Inhibited tyrosinase does not proceed with the oxidation reaction, and eventually melanin production is inhibited. RC extract contained in the CNF film is expected to have an anti-browning effect on the banana peel.

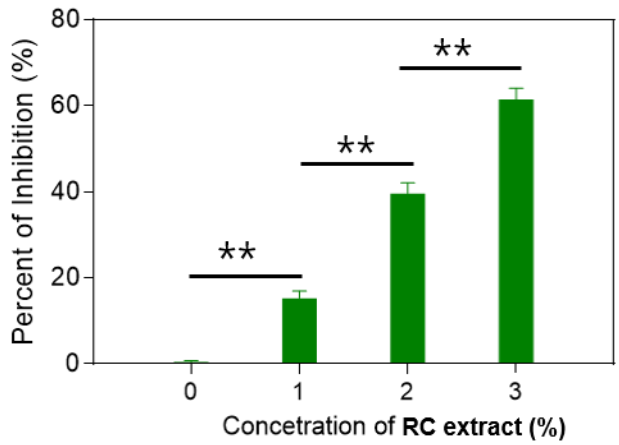

Fig. 44 Tyrosinase inhibition assay for evaluating the anti-browning effect by RC extract. (n=3), ** indicates a p-value of <0.01 and statistical analysis was performed using one-way ANOVA test.

V. Conclusion

In this study, CM-CNF film was introduced on the surface of fruits to enhance the preservation of fruits. CM-CNF films could be formed through electrostatic interactions with divalent cations. In addition, it was possible to improve the mechanical properties of the CM-CNF film and suppress the gas permeation. The prepared CM-CNF film was applied to climacteric fruits and non-climacteric fruits, and its applicability was evaluated as a coating material for fruit to enhance preservation.

As the carboxymethylation reaction time increased, the carboxyl group content, degree of substitution and surface area of CM-CNF gradually increased. There was no significant change in these properties at reaction times greater than 90 min. As the reaction time increased, the surface of CM-CNF showed an increasing negative charge, and improved dispersibility and transparency in the colloidal phase. In addition, as the reaction progressed, the degree of crystallinity increased, and it was found that the thermal stability increased.

The tensile strength of the CM-CNF film in which the network structure was formed with divalent cations increased from 4.15 Mpa to 5.15 Mpa. The contact angle between the CM-CNF film and water increased from 42.7° to 69.8°, showing the relatively enhanced hydrophobicity on the surface of the

film. The water vapor permeability was also reduced through the change of the surface properties. Also, through surface thermal measurement, it was confirmed that fruits coated with CM-CNF film showed relatively low thermal change due to a large amount of moisture content. In addition, it was determined that the fruit coated with the CM-CNF film showed low thermal change through surface thermal measurement because the moisture content was relatively higher than non coated fruit.

CM-CNF film was applied to strawberry, which are representative non-climacteric fruit, and banana, which are climacteric fruit. The CM-CNF film crosslinked with calcium ions suppressed the evaporation of strawberries, and the loss rate of firmness was rapidly reduced during the experiment. The emission of carbon dioxide, a respiration product of fruits, was reduced by the introduction of the CM-CNF film. In addition, considering that the rate of change of total soluble solid and acidity was reduced, it was determined that the CM-CNF film contributed to the improvement of preservation of strawberries.

Bananas also showed excellent storage properties when coated with CM-CNF. As in the case of strawberries, the loss of weight was low because evaporation was prevented, and the decrease in firmness was also suppressed. The emission of carbon dioxide and ethylene was prevented, which reducing the ripening rate of bananas. Additionally, the browning inhibitory properties of bananas were observed by adding the extracts of red cabbage. Considering

that the rate of change of total soluble solid and acidity was relatively low, it was determined that the CM-CNF film contributed to the improvement of preservation of bananas.

The CM-CNF film decreased the ripening rate for both non-climacteric fruits and climacteric fruits, and it was dertermined that improvement in preservation of fruits. Cellulose is one of the most abundant natural resources, and it has been increasing interest of researchers because it is low-cost, eco-friendly materials. Recently, CNF has been actively researched on mass manufacturing processes and its applications. Currently, there are few cases that have been applied and studied in the food field. In this study, CM-CNF was applied to improve the storage of fruits, and it is expected that it can be effectively used in the field of fresh foods such as vegetables and dairy products.

VI. References

[1] Reisch, L., Eberle, U., & Lorek, S. (2013). Sustainable food consumption: an overview of contemporary issues and policies. Sustainability: Science, Practice and Policy, 9(2), 7-25.

[2] Headey, D., & Fan, S. (2008). Anatomy of a crisis: the causes and consequences of surging food prices. Agricultural economics, 39, 375-391.

[3] McMichael, P. (2009). A food regime analysis of the 'world food crisis'. Agriculture and human values, 26(4), 281-295.

[4] Baldwin, Elizabeth A., Robert Hagenmaier, and Jinhe Bai, eds. Edible coatings and films to improve food quality. CRC press, 2011.

[5] Cazón, P., Velazquez, G., Ramírez, J. A., & Vázquez, M. (2017). Polysaccharide-based films and coatings for food packaging: A review. Food Hydrocolloids, 68, 136-148.

[6] Debeaufort, F., Quezada-Gallo, J. A., & Voilley, A. (1998). Edible films and coatings: tomorrow's packagings: a review. Critical Reviews in food science, 38(4), 299-313.

[7] Shendurse, A. M., Gopikrishna, G., Patel, A. C., & Pandya, A. J. (2018). Milk protein based edible films and coatings–preparation, properties and food applications. J Nutr Health Food Eng, 8(2), 219-226.

[8] Miller, K. S., & Krochta, J. M. (1997). Oxygen and aroma barrier properties of edible films: A review. Trends in food science & technology, 8(7), 228-237.

[9] Wróblewska-Krepsztul, J., Rydzkowski, T., Borowski, G., Szczypiński, M., Klepka, T., & Thakur, V. K. (2018). Recent progress in biodegradable polymers and nanocomposite-based packaging materials for sustainable environment. International Journal of Polymer Analysis and Characterization,

23(4), 383-395.
[10] Shit, S. C., & Shah, P. M. (2014). Edible polymers: challenges and opportunities. Journal of Polymers, 2014.
[11] Krochta, J. M. (2017). Edible protein films and coatings. Food proteins and their applications, 529-550.
[12] Chiralt, A., González-Martínez, C., Vargas, M., & Atarés, L. (2018). Edible films and coatings from proteins. In Proteins in Food Processing (pp. 477-500). Woodhead Publishing.
[13] Embuscado, M. E., & Huber, K. C. (2009). Edible films and coatings for food applications (Vol. 9). New York, NY, USA: Springer.
[14] Debeaufort, F., & Voilley, A. (2009). Lipid-based edible films and coatings. In Edible films and coatings for food applications (pp. 135-168). Springer, New York, NY.
[15] Mohanty, A. K., Misra, M. A., & Hinrichsen, G. I. (2000). Biofibres, biodegradable polymers and biocomposites: An overview. Macromolecular materials and Engineering, 276(1), 1-24.
[16] Štefelová, J., Slovák, V., Siqueira, G., Olsson, R. T., Tingaut, P., Zimmermann, T., & Sehaqui, H. (2017). Drying and pyrolysis of cellulose nanofibers from wood, bacteria, and algae for char application in oil absorption and dye adsorption. ACS Sustainable Chemistry & Engineering, 5(3), 2679-2692.
[17] Sharma, A., Thakur, M., Bhattacharya, M., Mandal, T., & Goswami, S. (2019). Commercial application of cellulose nano-composites–A review. Biotechnology Reports, 21, e00316.
[18] Zhang, Y., Nypelö, T., Salas, C., Arboleda, J., Hoeger, I. C., & Rojas, O. J. (2013). Cellulose nanofibrils. Journal of Renewable Materials, 1(3), 195-211.
[19] Chen, C., Mo, M., Chen, W., Pan, M., Xu, Z., Wang, H., & Li, D. (2018). Highly conductive nanocomposites based on cellulose nanofiber networks via

NaOH treatments. Composites Science and Technology, 156, 103-108.
[20] Fu, L. H., Qi, C., Ma, M. G., & Wan, P. (2019). Multifunctional cellulose-based hydrogels for biomedical applications. Journal of materials chemistry B, 7(10), 1541-1562.
[21] Xie, B., Zhang, X., Luo, X., Wang, Y., Li, Y., Li, B., & Liu, S. (2020). Edible coating based on beeswax-in-water Pickering emulsion stabilized by cellulose nanofibrils and carboxymethyl chitosan. Food Chemistry, 331, 127108.
[22] Salas, C., Nypelö, T., Rodriguez-Abreu, C., Carrillo, C., & Rojas, O. J. (2014). Nanocellulose properties and applications in colloids and interfaces. Current Opinion in Colloid & Interface Science, 19(5), 383-396.
[23] Zhang, X. F., Feng, Y., Huang, C., Pan, Y., & Yao, J. (2017). Temperature-induced formation of cellulose nanofiber film with remarkably high gas separation performance. Cellulose, 24(12), 5649-5656.
[24] Shimizu, M., Saito, T., & Isogai, A. (2016). Water-resistant and high oxygen-barrier nanocellulose films with interfibrillar cross-linkages formed through multivalent metal ions. Journal of Membrane Science, 500, 1-7.
[25] Cai, J., Chen, J., Zhang, Q., Lei, M., He, J., Xiao, A., & Xiong, H. (2016). Well-aligned cellulose nanofiber-reinforced polyvinyl alcohol composite film: mechanical and optical properties. Carbohydrate polymers, 140, 238-245.
[26] Wang, W., Zhang, X., Li, C., Du, G., Zhang, H., & Ni, Y. (2018). Using carboxylated cellulose nanofibers to enhance mechanical and barrier properties of collagen fiber film by electrostatic interaction. Journal of the Science of Food and Agriculture, 98(8), 3089-3097.
[27] Wang, T., & Zhao, Y. (2021). Fabrication of thermally and mechanically stable superhydrophobic coatings for cellulose-based substrates with natural and edible ingredients for food applications. Food Hydrocolloids, 120, 106877.
[28] Zhao, K., Wang, W., Teng, A., Zhang, K., Ma, Y., Duan, S., & Guo, Y.

(2020). Using cellulose nanofibers to reinforce polysaccharide films: Blending vs layer-by-layer casting. Carbohydrate polymers, 227, 115264.
[29] Gould, G. W. (2012). New methods of food preservation. Springer Science & Business Media.
[30] Hanjra, M. A., & Qureshi, M. E. (2010). Global water crisis and future food security in an era of climate change. Food policy, 35(5), 365-377.
[31] Butler, P. (2012). Smarter packaging for consumer food waste reduction. In Emerging Food Packaging Technologies (pp. 409-434). Woodhead Publishing.
[32] Leistner, L. (1992). Food preservation by combined methods. Food research international, 25(2), 151-158.
[33] Nout, M. J. R. (1994). Fermented foods and food safety. Food Research International, 27(3), 291-298.
[34] Bhat, R., Alias, A. K., & Paliyath, G. (2012). Progress in food preservation. John Wiley & Sons.
[56] Rahman, M. S. (Ed.). (2007). Handbook of food preservation. CRC press.
[35] Ali, A. A. (2010). Beneficial role of lactic acid bacteria in food preservation and human health: a review. Research Journal of Microbiology, 5(12), 1213-1221.
[36] Leistner, L., & Gorris, L. G. (1995). Food preservation by hurdle technology. Trends in food science & technology, 6(2), 41-46.
[37] Parfitt, J., Barthel, M., & Macnaughton, S. (2010). Food waste within food supply chains: quantification and potential for change to 2050. Philosophical transactions of the royal society B: biological sciences, 365(1554), 3065-3081.
[38] Mannheim, C. H., & Soffer, T. (1996). Permeability of different wax coatings and their effect on citrus fruit quality. Journal of Agricultural and Food Chemistry, 44(3), 919-923.
[39] Cuq, B., Gontard, N., & Guilbert, S. (1995). Edible films and coatings

as active layers. In Active food packaging (pp. 111-142). Springer, Boston, MA.

[40] Petracek, P. D., Dou, H., Mourer, J., & Davis, C. (1997). Measurement of gas exchange characteristics of waxes applied to citrus fruit. In International Symposium on Growth and Development of Fruit Crops 527,73-84.

[41] Umaraw, P., & Verma, A. K. (2017). Comprehensive review on application of edible film on meat and meat products: An eco-friendly approach. Critical Reviews in Food Science and Nutrition, 57(6), 1270-1279.

[42] Dehghani, S., Hosseini, S. V., & Regenstein, J. M. (2018). Edible films and coatings in seafood preservation: A review. Food chemistry, 240, 505-513.

[43] Cagri, A., Ustunol, Z., & Ryser, E. T. (2004). Antimicrobial edible films and coatings. Journal of food protection, 67(4), 833-848.

[44] Sánchez-Ortega, I., García-Almendárez, B. E., Santos-López, E. M., Amaro-Reyes, A., Barboza-Corona, J. E., & Regalado, C. (2014). Antimicrobial edible films and coatings for meat and meat products preservation. The Scientific World Journal, 2014.

[45] Bhagath, Y. B., & Manjula, K. (2019). Influence of composite edible coating systems on preservation of fresh meat cuts and products: a brief review on their trends and applications. International Food Research Journal, 26(2).

[46] Baldwin, E. A. (1994). Edible coatings for fresh fruits and vegetables: past, present, and future. Edible coatings and films to improve food quality, 1, 25.

[47] Dhall, R. K. (2013). Advances in edible coatings for fresh fruits and vegetables: a review. Critical reviews in food science and nutrition, 53(5), 435-450.

[48] Shubik, P., Saffiotti, U., Lijinsky, W., Pietra, G., Rappaport, H., Toth, B., & Ramahi, H. (1962). Studies on the toxicity of petroleum waxes. Toxicology

and applied pharmacology, 4, 1-62.
[49] Hagenmaier, R. D., & Baker, R. A. (1997). Edible coatings from morpholine-free wax microemulsions. Journal of agricultural and food chemistry, 45(2), 349-352.
[50] Hagenmaier, R. D., & Baker, R. A. (1994). Wax microemulsions and emulsions as citrus coatings. Journal of Agricultural and Food Chemistry, 42(4), 899-902.
[51] Grant, L. A., & Burns, J. (1994). Application of coatings (pp. 189-200). Technomic Publishing: Lancaster, PA.
[52] Byun, M. W., Lee, J. W., Jo, C., & Yook, H. S. (2001). Quality properties of sausage made with gamma-irradiated natural pork and lamb casing. Meat Science, 59(3), 223-228.
[53] Kita, A., Lachowicz, S., & Filutowska, P. (2020). Effects of package type on the quality of fruits and nuts panned in chocolate during long-time storage. LWT, 125, 109212.
[54] Nout, M. J. R. (1994). Fermented foods and food safety. Food Research International, 27(3), 291-298.
[55] Bhat, R., Alias, A. K., & Paliyath, G. (2012). Progress in food preservation. John Wiley & Sons.
[56] Hassan, B., Chatha, S. A. S., Hussain, A. I., Zia, K. M., & Akhtar, N. (2018). Recent advances on polysaccharides, lipids and protein based edible films and coatings: A review. International journal of biological macromolecules, 109, 1095-1107.
[57] Cerqueira, M. A., Lima, A. M., Souza, B. W., Teixeira, J. A., Moreira, R. A., & Vicente, A. A. (2009). Functional polysaccharides as edible coatings for cheese. Journal of Agricultural and Food Chemistry, 57(4), 1456-1462.
[58] Pan, H., Jiang, B., Chen, J., & Jin, Z. (2014). Blend-modification of soy protein/lauric acid edible films using polysaccharides. Food chemistry, 151, 1-6.

[59] Vicentini, N. M., Dupuy, N., Leitzelman, M., Cereda, M. P., & Sobral, P. J. A. (2005). Prediction of cassava starch edible film properties by chemometric analysis of infrared spectra. Spectroscopy Letters, 38(6), 749-767.

[60] Orozco-Parra, J., Mejía, C. M., & Villa, C. C. (2020). Development of a bioactive synbiotic edible film based on cassava starch, inulin, and Lactobacillus casei. Food hydrocolloids, 104, 105754.

[61] Agulló, E., Rodríguez, M. S., Ramos, V., & Albertengo, L. (2003). Present and future role of chitin and chitosan in food. Macromolecular bioscience, 3(10), 521-530.

[62] Wu, C., Sun, J., Chen, M., Ge, Y., Ma, J., Hu, Y., & Yan, Z. (2019). Effect of oxidized chitin nanocrystals and curcumin into chitosan films for seafood freshness monitoring. Food hydrocolloids, 95, 308-317.

[63] Venkatachalam, K., & Lekjing, S. (2020). A chitosan-based edible film with clove essential oil and nisin for improving the quality and shelf life of pork patties in cold storage. Rsc Advances, 10(30), 17777-17786.

[64] Kester, J. J., & Fennema, O. (1989). An edible film of lipids and cellulose ethers: barrier properties to moisture vapor transmission and structural evaluation. Journal of Food Science, 54(6), 1383-1389.

[65] Azeredo, H. M., Mattoso, L. H. C., Wood, D., Williams, T. G., Avena-Bustillos, R. J., & McHugh, T. H. (2009). Nanocomposite edible films from mango puree reinforced with cellulose nanofibers. Journal of food science, 74(5), N31-N35.

[66] Ghanbarzadeh, B., & Almasi, H. (2011). Physical properties of edible emulsified films based on carboxymethyl cellulose and oleic acid. International journal of biological Macromolecules, 48(1), 44-49.

[67] Paunonen, S. (2013). Strength and barrier enhancements of cellophane and cellulose derivative films: a review. BioResources, 8(2), 3098-3121.

[68] Zhang, H., & Mittal, G. (2010). Biodegradable protein-based films from

plant resources: A review. Environmental Progress & Sustainable Energy, 29(2), 203-220.
[69] De Pilli, T. (2020). Development of a vegetable oil and egg proteins edible film to replace preservatives and primary packaging of sweet baked goods. Food Control, 114, 107273.
[70] López, D., Márquez, A., Gutiérrez-Cutiño, M., Venegas-Yazigi, D., Bustos, R., & Matiacevich, S. (2017). Edible film with antioxidant capacity based on salmon gelatin and boldine. Lwt, 77, 160-169.
[71] Zhang, S., Wang, Y., Herring, J. L., & Oh, J. H. (2007). Characterization of edible film fabricated with channel catfish (Ictalurus punctatus) gelatin extract using selected pretreatment methods. Journal of food science, 72(9), C498-C503.
[72] Al-Hassan, A. A., & Norziah, M. H. (2012). Starch–gelatin edible films: Water vapor permeability and mechanical properties as affected by plasticizers. Food hydrocolloids, 26(1), 108-117.
[73] Cao, N., Fu, Y., & He, J. (2007). Preparation and physical properties of soy protein isolate and gelatin composite films. Food Hydrocolloids, 21(7), 1153-1162.
[74] Kokoszka, S., Debeaufort, F., Hambleton, A., Lenart, A., & Voilley, A. (2010). Protein and glycerol contents affect physico-chemical properties of soy protein isolate-based edible films. Innovative Food Science & Emerging Technologies, 11(3), 503-510.
[75] Yu, Z., Dhital, R., Wang, W., Sun, L., Zeng, W., Mustapha, A., & Lin, M. (2019). Development of multifunctional nanocomposites containing cellulose nanofibrils and soy proteins as food packaging materials. Food Packaging and Shelf Life, 21, 100366.
[76] Zareie, Z., Yazdi, F. T., & Mortazavi, S. A. (2020). Development and characterization of antioxidant and antimicrobial edible films based on chitosan and gamma-aminobutyric acid-rich fermented soy protein.

Carbohydrate Polymers, 244, 116491.
[77] Lee, J. E., & Kim, K. M. (2010). Characteristics of soy protein isolate-montmorillonite composite films. Journal of Applied Polymer Science, 118(4), 2257-2263.
[78] Baysal, T., Bilek, S. E., & Apaydin, E. (2010). The effect of corn zein edible film coating on intermediate moisture apricot (Prunus Armenica L.) quality. Gida, 35(4), 245-249.
[79] Lai, H. M., Padua, G. W., & Wei, L. S. (1997). Properties and microstructure of zein sheets plasticized with palmitic and stearic acids. Cereal Chemistry, 74(1), 83-90.
[80] Wang, Q., & Padua, G. W. (2005). Properties of zein films coated with drying oils. Journal of agricultural and food chemistry, 53(9), 3444-3448.
[81] Morillon, V., Debeaufort, F., Blond, G., Capelle, M., & Voilley, A. (2002). Factors affecting the moisture permeability of lipid-based edible films: a review. Critical reviews in food science and nutrition, 42(1), 67-89.
[82] Olivas, G. I., & Barbosa-Cánovas, G. (2009). Edible films and coatings for fruits and vegetables. In Edible films and coatings for food applications, 211-244.
[83] Bravin, B., Peressini, D., & Sensidoni, A. (2004). Influence of emulsifier type and content on functional properties of polysaccharide lipid-based edible films. Journal of Agricultural and Food Chemistry, 52(21), 6448-6455.
[84] Banis, G. E., Beardslee, L. A., Stine, J. M., Sathyam, R. M., & Ghodssi, R. (2020). Capacitive sensing of triglyceride film reactions: a proof-of-concept demonstration for sensing in simulated duodenal contents with gastrointestinal targeting capsule system. Lab on a Chip, 20(11).
[85] Vukić, M., Grujić, S., & Odzaković, B. (2017). Application of edible films and coatings in food production. In Advances in Applications of Industrial Biomaterials (pp. 121-138). Springer, Cham
[86] Fritz, A. R. M., de Matos Fonseca, J., Trevisol, T. C., Fagundes, C., &

Valencia, G. A. (2019). Active, eco-friendly and edible coatings in the post-harvest–a critical discussion. Polymers for Agri-Food Applications, 433-463.
[87] Ayranci, E., & Tunç, S. (1997). Cellulose-based edible films and their effects on fresh beans and strawberries. Zeitschrift für Lebens-mitteluntersuchung und-forschung A, 205(6), 470-473.
[88] Pareta, R., & Edirisinghe, M. J. (2006). A novel method for the preparation of starch films and coatings. Carbohydrate polymers, 63(3), 425-431.
[89] Gutiérrez, T. J. (Ed.). (2019). Polymers for Agri-Food Applications (pp. 1-622). Switzerland: Springer International Publishing.
[90] Park, H. J., Weller, C. L., Vergano, P. J., & Testin, R. F. (1993). Permeability and mechanical properties of cellulose-based edible films. Journal of Food Science, 58(6), 1361-1364.
[91] Fischer, S., Thümmler, K., Volkert, B., Hettrich, K., Schmidt, I., & Fischer, K. (2008). Properties and applications of cellulose acetate. In Macromolecular symposia, 262, 89-96
[92] Gardner, K. H., & Blackwell, J. (1974). The structure of native cellulose. Biopolymers: Original Research on Biomolecules, 13(10), 1975-2001.
[93] Finkenstadt, V. L., & Millane, R. P. (1998). Crystal structure of Valonia cellulose Iβ. Macromolecules, 31(22), 7776-7783.
[94] Liu, D., Chen, X., Yue, Y., Chen, M., & Wu, Q. (2011). Structure and rheology of nanocrystalline cellulose. Carbohydrate Polymers, 84(1), 316-322.
[95] Battista, O. A., & Smith, P. A. (1962). Microcrystalline cellulose. Industrial & Engineering Chemistry, 54(9), 20-29.
[96] Bhatnagar, A., & Sain, M. (2005). Processing of cellulose nanofiber-reinforced composites. Journal of Reinforced Plastics and Composites, 24(12), 1259-1268.
[97] Abe, K., & Yano, H. (2012). Cellulose nanofiber-based hydrogels with

high mechanical strength. Cellulose, 19(6), 1907-1912.
[98] Nobuta, K., Teramura, H., Ito, H., Hongo, C., Kawaguchi, H., Ogino, C., & Nishino, T. (2016). Characterization of cellulose nanofiber sheets from different refining processes. Cellulose, 23(1), 403-414.
[99] Ahmed-Haras, M. R., Kao, N., Islam, M. S., & Ward, L. (2020). An Overview of Recent Developments in Hetero-Catalytic Conversion of Cellulosic Biomass. Research Communication in Engineering Science & Technology, 4, 43-54.
[100] Trache, D., Tarchoun, A. F., Derradji, M., Hamidon, T. S., Masruchin, N., Brosse, N., & Hussin, M. H. (2020). Nanocellulose: From fundamentals to advanced applications. Frontiers in Chemistry, 8.
[101] Gardner, D. J., Oporto, G. S., Mills, R., & Samir, M. (2008). Adhesion and surface issues in cellulose and nanocellulose. Journal of Adhesion Science and Technology, 22(5-6), 545-567.
[102] Liu, X., Jiang, Y., Song, X., Qin, C., Wang, S., & Li, K. (2019). A bio-mechanical process for cellulose nanofiber production–Towards a greener and energy conservation solution. Carbohydrate polymers, 208, 191-199.
[103] Zhai, L., Kim, H. C., Kim, J. W., & Kim, J. (2020). Simple centrifugal fractionation to reduce the size distribution of cellulose nanofibers. Scientific reports, 10(1), 1-8.
[104] De Lima, C. F., Ahmed, S., Ghaemmaghami, A. M., Wilmoth, J. L., Carey, M., & Venkataraman, A. (2019). Advances in Cellulose Nano Crystals. Advances in Cellulose Nano Crystals, 357.
[105] Zhu, H., Luo, W., Ciesielski, P. N., Fang, Z., Zhu, J. Y., Henriksson, G., & Hu, L. (2016). Wood-derived materials for green electronics, biological devices, and energy applications. Chemical reviews, 116(16), 9305-9374.
[106] Khalil, H. A., Bhat, A. H., & Yusra, A. I. (2012). Green composites from sustainable cellulose nanofibrils: A review. Carbohydrate polymers, 87(2), 963-979.

[107] Kalia, S., Dufresne, A., Cherian, B. M., Kaith, B. S., Avérous, L., Njuguna, J., & Nassiopoulos, E. (2011). Cellulose-based bio-and nanocomposites: a review. International journal of polymer science, 2011.
[108] Siró, I., & Plackett, D. (2010). Microfibrillated cellulose and new nanocomposite materials: a review. Cellulose, 17(3), 459-494.
[109] Wang, D. (2019). A critical review of cellulose-based nanomaterials for water purification in industrial processes. Cellulose, 26(2), 687-701.
[110] Rol, F., Belgacem, M. N., Gandini, A., & Bras, J. (2019). Recent advances in surface-modified cellulose nanofibrils. Progress in Polymer Science, 88, 241-264.
[111] Li, T., Chen, C., Brozena, A. H., Zhu, J. Y., Xu, L., Driemeier, C., & Hu, L. (2021). Developing fibrillated cellulose as a sustainable technological material. Nature, 590(7844), 47-56.
[112] Missoum, K., Belgacem, M. N., & Bras, J. (2013). Nanofibrillated cellulose surface modification: a review. Materials, 6(5), 1745-1766.
[113] Zhang, Y., Nypelö, T., Salas, C., Arboleda, J., Hoeger, I. C., & Rojas, O. J. (2013). Cellulose nanofibrils. Journal of Renewable Materials, 1(3), 195-211.
[114] Lee, H., Sundaram, J., & Mani, S. (2017). Production of cellulose nanofibrils and their application to food: a review. Nanotechnology, 1-33.
[115] Im, W., Lee, S., Abhari, A. R., Youn, H. J., & Lee, H. L. (2018). Optimization of carboxymethylation reaction as a pretreatment for production of cellulose nanofibrils. Cellulose, 25(7), 3873-3883.
[116] Naderi, A., Lindström, T., & Sundström, J. (2014). Carboxymethylated nanofibrillated cellulose: rheological studies. Cellulose, 21(3), 1561-1571.
[117] Yue, L., Zheng, Y., Xie, Y., Liu, S., Guo, S., Yang, B., & Tang, T. (2016). Preparation of a carboxymethylated bacterial cellulose/polyaniline composite gel membrane and its characterization. Rsc Advances, 6(73), 68599-68605.
[118] Rodionova, G., Eriksen, Ø., & Gregersen, Ø. (2012). TEMPO-oxidized

cellulose nanofiber films: effect of surface morphology on water resistance. Cellulose, 19(4), 1115-1123.
[119] Mousavi, S. M., Afra, E., Tajvidi, M., Bousfield, D. W., & Dehghani-Firouzabadi, M. (2017). Cellulose nanofiber/carboxymethyl cellulose blends as an efficient coating to improve the structure and barrier properties of paperboard. Cellulose, 24(7), 3001-3014.
[120] Guo, J., Filpponen, I., Su, P., Laine, J., & Rojas, O. J. (2016). Attachment of gold nanoparticles on cellulose nanofibrils via click reactions and electrostatic interactions. Cellulose, 23(5), 3065-3075.
[121] Valencia, L., Nomena, E. M., Monti, S., Rosas-Arbelaez, W., Mathew, A. P., Kumar, S., & Velikov, K. P. (2020). Multivalent ion-induced re-entrant transition of carboxylated cellulose nanofibrils and its influence on nanomaterials' properties. Nanoscale, 12(29), 15652-15662.
[122] Benselfelt, T., Nordenström, M., Hamedi, M. M., & Wågberg, L. (2019). Ion-induced assemblies of highly anisotropic nanoparticles are governed by ion–ion correlation and specific ion effects. Nanoscale, 11(8), 3514-3520.
[123] Ajdary, R., Tardy, B. L., Mattos, B. D., Bai, L., & Rojas, O. J. (2020). Plant nanomaterials and inspiration from nature: Water interactions and hierarchically structured hydrogels. Advanced Materials, 2001085.
[124] Khanjani, P., Ristolainen, M., Kosonen, H., Virtanen, P., Ceccherini, S., Maloney, T., & Vuorinen, T. (2019). Time-triggered calcium ion bridging in preparation of films of oxidized microfibrillated cellulose and pulp. Carbohydrate polymers, 218, 63-67.
[125] Damar, İ., & Ekşi, A. (2012). Antioxidant capacity and anthocyanin profile of sour cherry (Prunus cerasus L.) juice. Food chemistry, 135(4), 2910-2914.
[126] Satoskar, R. R., Shah, S. J., & Shenoy, S. G. (1986). Evaluation of anti-inflammatory property of curcumin (diferuloyl methane) in patients with postoperative inflammation. International journal of clinical pharmacology,

therapy, and toxicology, 24(12), 651-654.
[127] Pan, L. H., Liu, F., Luo, S. Z., & Luo, J. P. (2019). Pomegranate juice powder as sugar replacer enhanced quality and function of set yogurts: Structure, rheological property, antioxidant activity and in vitro bioaccessibility. LWT, 115, 108479.
[128] Emam-Djomeh, Z., Moghaddam, A., & Yasini Ardakani, S. A. (2015). Antimicrobial activity of pomegranate (Punica granatum L.) peel extract, physical, mechanical, barrier and antimicrobial properties of pomegranate peel extract-incorporated sodium caseinate film and application in packaging for ground beef. Packaging Technology and Science, 28(10), 869-881.
[129] Zhang, C., Sun, G., Cao, L., & Wang, L. (2020). Accurately intelligent film made from sodium carboxymethyl starch/κ-carrageenan reinforced by mulberry anthocyanins as an indicator. Food Hydrocolloids, 108, 106012.
[130] Jung, S., Cui, Y., Barnes, M., Satam, C., Zhang, S., Chowdhury, R. A., ... & Ajayan, P. M. (2020). Multifunctional Bio-Nanocomposite Coatings for Perishable Fruits. Advanced Materials, 32(26), 1908291.
[131] Moghadam, M., Salami, M., Mohammadian, M., Khodadadi, M., & Emam-Djomeh, Z. (2020). Development of antioxidant edible films based on mung bean protein enriched with pomegranate peel. Food Hydrocolloids, 104, 105735.
[132] Lee, H., Kim, S., Shin, S., & Hyun, J. (2021). 3D structure of lightweight, conductive cellulose nanofiber foam. Carbohydrate Polymers, 253, 117238.
[133] Im, W., Abhari, A. R., Youn, H. J., & Lee, H. L. (2018). Morphological characteristics of carboxymethylated cellulose nanofibrils: the effect of carboxyl content. Cellulose, 25(10), 5781-5789.
[134] Ilyas, R. A., Sapuan, S. M., & Ishak, M. R. (2018). Isolation and characterization of nanocrystalline cellulose from sugar palm fibres (Arenga Pinnata). Carbohydrate polymers, 181, 1038-1051.

[135] Abral, H., Pratama, A. B., Handayani, D., Mahardika, M., Aminah, I., Sandrawati, N., & Ilyas, R. A. (2021). Antimicrobial Edible Film Prepared from Bacterial Cellulose Nanofibers/Starch/Chitosan for a Food Packaging Alternative. International Journal of Polymer Science, 2021.

[136] Yang, C. H., Wang, M. X., Haider, H., Yang, J. H., Sun, J. Y., Chen, Y. M., & Suo, Z. (2013). Strengthening alginate/polyacrylamide hydrogels using various multivalent cations. ACS applied materials & interfaces, 5(21), 10418-10422.

[137] Kwak, H., Shin, S., Lee, H., & Hyun, J. (2019). Formation of a keratin layer with silk fibroin-polyethylene glycol composite hydrogel fabricated by digital light processing 3D printing. Journal of Industrial and Engineering Chemistry, 72, 232-240.

[138] Bedane, A. H., Eić, M., Farmahini-Farahani, M., & Xiao, H. (2015). Water vapor transport properties of regenerated cellulose and nanofibrillated cellulose films. Journal of Membrane Science, 493, 46-57.

[139] Francis, F. J. (1982). Analysis of anthocyanins. Anthocyanins as food colors, 1, 280.

[140] Prietto, L., Mirapalhete, T. C., Pinto, V. Z., Hoffmann, J. F., Vanier, N. L., Lim, L. T., ... & da Rosa Zavareze, E. (2017). pH-sensitive films containing anthocyanins extracted from black bean seed coat and red cabbage. Lwt, 80, 492-500.

[141] Rapisarda, P., Fanella, F., & Maccarone, E. (2000). Reliability of analytical methods for determining anthocyanins in blood orange juices. Journal of Agricultural and Food Chemistry, 48(6), 2249-2252.

[142] Goupy, P., Bautista-Ortin, A. B., Fulcrand, H., & Dangles, O. (2009). Antioxidant activity of wine pigments derived from anthocyanins: Hydrogen transfer reactions to the DPPH radical and inhibition of the heme-induced peroxidation of linoleic acid. Journal of agricultural and food chemistry, 57(13), 5762-5770.

[143] Bang, J., Lim, S., Yi, G., Lee, J. G., & Lee, E. J. (2019). Integrated transcriptomic-metabolomic analysis reveals cellular responses of harvested strawberry fruit subjected to short-term exposure to high levels of carbon dioxide. Postharvest Biology and Technology, 148, 120-131.

[144] Marelli, B., Brenckle, M. A., Kaplan, D. L., & Omenetto, F. G. (2016). Silk fibroin as edible coating for perishable food preservation. Scientific reports, 6(1), 1-11.

[145] Aramwit, P., Bang, N., & Srichana, T. (2010). The properties and stability of anthocyanins in mulberry fruits. Food Research International, 43(4), 1093-1097.

[146] Zhu, Y. S., Xiao, S. Y., Li, M. X., Chang, Z., Wang, F. X., Gao, J., & Wu, Y. P. (2015). Natural macromolecule based carboxymethyl cellulose as a gel polymer electrolyte with adjustable porosity for lithium ion batteries. Journal of Power Sources, 288, 368-375.

[147] Onyianta, A. J., Dorris, M., & Williams, R. L. (2018). Aqueous morpholine pre-treatment in cellulose nanofibril (CNF) production: comparison with carboxymethylation and TEMPO oxidisation pre-treatment methods. Cellulose, 25(2), 1047-1064.

[148] Radakisnin, R., Abdul Majid, M. S., Jamir, M. R. M., Jawaid, M., Sultan, M. T. H., & Mat Tahir, M. F. (2020). Structural, Morphological and Thermal Properties of Cellulose Nanofibers from Napier fiber (Pennisetum purpureum). Materials, 13(18), 4125.

[149] Xie, J., Hse, C. Y., Cornelis, F., Hu, T., Qi, J., & Shupe, T. F. (2016). Isolation and characterization of cellulose nanofibers from bamboo using microwave liquefaction combined with chemical treatment and ultrasonication. Carbohydrate polymers, 151, 725-734.

[150] Habibi, N. (2014). Preparation of biocompatible magnetite-carboxymethyl cellulose nanocomposite: characterization of nanocomposite by FTIR, XRD, FESEM and TEM. Spectrochimica Acta Part A: Molecular

and Biomolecular Spectroscopy, 131, 55-58.
[151] Sofla, M. R. K., Brown, R. J., Tsuzuki, T., & Rainey, T. J. (2016). A comparison of cellulose nanocrystals and cellulose nanofibres extracted from bagasse using acid and ball milling methods. Advances in Natural Sciences: Nanoscience and Nanotechnology, 7(3), 035004.
[152] Yildirim, N., & Shaler, S. (2017). A study on thermal and nanomechanical performance of cellulose nanomaterials (CNs). Materials, 10(7), 718.
[153] Shimazaki, Y., Miyazaki, Y., Takezawa, Y., Nogi, M., Abe, K., Ifuku, S., & Yano, H. (2007). Excellent thermal conductivity of transparent cellulose nanofiber/epoxy resin nanocomposites. Biomacromolecules, 8(9), 2976-2978.
[154] Piskorz, J., Radlein, D. S. A., Scott, D. S., & Czernik, S. (1989). Pretreatment of wood and cellulose for production of sugars by fast pyrolysis. Journal of Analytical and Applied Pyrolysis, 16(2), 127-142.
[155] Edington, S. C., Gonzalez, A., Middendorf, T. R., Halling, D. B., Aldrich, R. W., & Baiz, C. R. (2018). Coordination to lanthanide ions distorts binding site conformation in calmodulin. Proceedings of the National Academy of Sciences, 115(14), E3126-E3134.
[156] Jouhara, A., Dupré, N., Gaillot, A. C., Guyomard, D., Dolhem, F., & Poizot, P. (2018). Raising the redox potential in carboxyphenolate-based positive organic materials via cation substitution. Nature communications, 9(1), 1-11.
[157] Oun, A. A., & Rhim, J. W. (2015). Preparation and characterization of sodium carboxymethyl cellulose/cotton linter cellulose nanofibril composite films. Carbohydrate Polymers, 127, 101-109.
[158] Razavi, S. M. A., Amini, A. M., & Zahedi, Y. (2015). Characterisation of a new biodegradable edible film based on sage seed gum: Influence of plasticiser type and concentration. Food Hydrocolloids, 43, 290-298.
[159] Rolle, L., & Guidoni, S. (2007). Color and anthocyanin evaluation of

red winegrapes by CIE L*, a*, b* parameters. OENO One, 41(4), 193-201.
[160] Lee, D. W., & Gould, K. S. (2002). Anthocyanins in leaves and other vegetative organs: an introduction.
[161] Somaatmadja, D., Powers, J. J., & Hamdy, M. K. (1964). Anthocyanins. VI. Chelation Studies on Anthocyanins and Other Related Compounds. Journal of Food Science, 29(5), 655-660.
[162] Otoni, C. G., Avena-Bustillos, R. J., Azeredo, H. M., Lorevice, M. V., Moura, M. R., Mattoso, L. H., & McHugh, T. H. (2017). Recent advances on edible films based on fruits and vegetables—a review. Comprehensive Reviews in Food Science and Food Safety, 16(5), 1151-1169.
[163] De Moraes, J. O., Scheibe, A. S., Sereno, A., & Laurindo, J. B. (2013). Scale-up of the production of cassava starch based films using tape-casting. Journal of Food Engineering, 119(4), 800-808.
[164] Vargas, M., Albors, A., Chiralt, A., & González-Martínez, C. (2006). Quality of cold-stored strawberries as affected by chitosan–oleic acid edible coatings. Postharvest biology and technology, 41(2), 164-171.
[165] Nguyen, T. B. T., Ketsa, S., & van Doorn, W. G. (2003). Relationship between browning and the activities of polyphenoloxidase and phenylalanine ammonia lyase in banana peel during low temperature storage. Postharvest Biology and Technology, 30(2), 187-193.
[166] Mowlah, G., Takano, K., Kamoi, I., & Obara, T. (1983). Browning Phenomenon by Banana Polyphenoloxidases. Nippon Shokuhin Kogyo Gakkaishi, 30(4), 245-251.
[167] Glagoleva, A. Y., Shoeva, O. Y., & Khlestkina, E. K. (2020). Melanin pigment in plants: Current knowledge and future perspectives. Frontiers in Plant Science, 11, 770.
[168] Norastehnia, A., Sajedi, R. H., & Nojavan-Asghari, M. (2007). Inhibitory effects of methyl jasmonate on seed germination in maize (Zea mays): effect on α-amylase activity and ethylene production. Gen. Appl. Plant

Physiol, 33(1-2), 13-23.
[169] Sawamura, M., Knegt, E., & Bruinsma, J. (1978). Levels of endogenous ethylene, carbon dioxide, and soluble pectin, and activities of pectin methylesterase and polygalacturonase in ripening tomato fruits. Plant and cell physiology, 19(6), 1061-1069.
[170] Mulas, M., Fadda, A., & Angioni, A. (2013). Effect of senecence and cold storage on the organic acid composition of myrtle fruits. Journal of the Science of Food and Agriculture, 93(1), 37-44.

초 록

카르복시메틸화 (Carboxymethylation, CM) 및 그라인딩을 통하여 셀룰로오스 펄프를 나노섬유화 (Cellulose nanofiber, CNF)하며, 제조된 CNF를 과일 표면에 도포하여 저장성의 향상을 모색한다. CM-CNF 는 2가 양이온과 정전기적 상호작용으로 이온성 가교를 형성하며 이로 인하여 재료의 물성이 향상되고 기체 차단 효과를 보이게 된다. CM 시간이 증가함에 따라 CNF의 직경이 감소하고 표면적이 증가하며, CM 치환도가 증가한다. CM 치환도의 증가는 CM-CNF 표면의 음전하를 높이고 CM-CNF 간에 정전기적 반발력을 형성하여 현탁 용액의 분산성 및 콜로이드 안정성을 향상시킨다. 우수한 CM-CNF의 분산성은 필름 제조시에 투명성 및 물성을 향상시키는 주요 요인이 된다. 마그네슘과 칼슘 이온의 첨가는 가교 형성으로 CM-CNF 필름의 인장강도를 향상시키고, 카르복실기의 이온성을 낮추어 필름의 친수성을 감소시킨다. 친수성이 감소된 CM-CNF 필름은 고습도 환경에서 투습도의 감소를 보인다.

CM-CNF 필름의 과일 저장성 향상은 호흡 비급등형 과일인 딸기와 호흡 급등형인 바나나에 적용하여 확인한다. 과일은 호흡을 통하여 숙성이 진행되기 때문에 호흡에 필요한 산소의 유입을 막고, 이와 함께 과일 내부의 수분 증발을 방지하는 것이 중요하다. CM-CNF 필름은 과일의 호흡에 필요한 산소의 유입을 차단하여 호흡과정에서 발생하는 이산화탄소의 양을 현저히 감소시키고 과일의 수분 증발을 방지하여 중량 감소를 억제한다. 과일 저장성의 향상은 과일의 경도 하강 시점이 늦춰지고 당도 및

산도의 변화 속도가 지연되는 것을 관찰함으로써 확인할 수 있다. CM-CNF 필름으로 코팅된 과일은 숙성 속도가 감소하고, 신선도가 상대적으로 유지된다. 이와 더불어, 보관 온도의 변화에 대한 과일 표면의 민감도, 항산화 물질의 첨가에 따른 과일의 숙성도 변화를 통하여 과일 코팅 소재로서 CM-CNF의 응용 가능성을 평가하고자 한다.

주요어: 셀룰로오스 나노섬유, 카르복시메틸화, 정전기적 상호작용, 식품저장법.
학 번: 2017-32983

감사의 글

입학을 위한 면접을 떨면서 본 것이 엊그제 같은데, 벌써 4년이라는 시간을 거쳐 소중한 박사학위를 받게 되었습니다. 지난 시간 동안 저에게 많은 분들의 도움이 없었더라면, 이러한 큰 영광을 얻기 힘들었을 것입니다. 아직 많이 부족하지만 박사학위를 받는데 도움을 주신 분 들께 감사의 인사 전합니다.

우선, 4년동안 깊은 가르침과 참된 뜻을 일깨우게 해주려 노력해주신 저의 지도 교수님, 현진호 교수님께 가장 깊은 감사를 드립니다. 교수님께서 말씀해 주셨던 뜻대로 모든 것을 이행하지 못했지만, 쫓아가기위해 애썼기에 지금의 자리에 설 수 있었다고 생각합니다. 앞으로도 교수님께서 해주셨던 조언과 따뜻한 마음 모두 기억하며, 어렵고 힘든 순간 다시 일어날 수 있는 원동력으로 삼겠습니다.

또한, 지금은 퇴임하셨지만, 퇴임 전 까지 열정적으로 가르침을 주셨던 박영환 교수님과 항상 학생들의 부족한 부분을 메워주고자 하셨던 박종신 교수님께도 깊은 감사의 말씀 드립니다. 그리고 학과의 단합을 이끌어주시고, 부족했던 제 논문의 심사 위원장을 역임하셨던 이기훈 교수님, 적응이 어려웠던 저에게 먼저 다가와 주셨던 김태일 교수님, 연구를 할 때의 마음가짐과 태도에 대한 모범을 보이셨던 기창석 교수님, 그리고 학위논문 작성 시 따뜻한 조언을 많이 해주셨던 곽선영 교수님께 감사의 말씀 드립니다. 아울러 부족한 저의 논문에 진중한 조언과 응원을 주셨던 가천대학교 윤규식 교수님께 감사의 말씀 드립니다. 선생님들의 가르침은 앞으로도 얻지 못할 소중한 자산으로 생각하며, 한 걸음 한 걸음 나아가는데 추진력으로 삼겠습니다.

그리고, 다사다난 했던 나노바이오연구실 생활에서 같이 정을 나누었던, 경아 누나, 신성철, 신동혁, 신종현, 이현지, 김성아, 김재환, 이동한, 이화련, 최준식, 디피카 에게도 감사의 말씀 드립니다. 부디 모두가 곧게 뻗어 뜻한 바를 이룰 수 있기를 간절히 소망합니다. 또한 바이오소재

공학 학우 모두의 건승을 기원합니다.

약 36년 간 뒷바라지 해주시고 항상 용기와 지지를 보내주셨던 아버지, 어머니, 그리고 동생 은임 에게도 감사의 말씀 드립니다. 앞으로의 시작을 하기 위해 오랜 시간이 걸렸지만, 조용한 촛불과 같이 오랫동안 타기 위한 과정이었다고 생각합니다. 앞으로도 바람을 두려워하지 않는 심지 깊은 촛불이 되기 위해 부단히 노력하겠습니다. 또한, 항상 부족한 사위를 위해 항상 기도해주시는 장인어른, 장모님께도 감사의 말씀 드립니다. 아직은 이루지 못한 것이 많이 있지만, 조언 해 주셨던 대로 하나씩 꾸려 나가기 위해 천천히 정진 하겠습니다. 두 분의 성원이 없었더라면, 저의 지금도 없다고 생각합니다. 항상 새기며 나아가겠습니다.

마지막으로, 저의 배우자 성은과 아들 예준이 에게도 감사의 말씀드립니다. 막막한 대해의 등불이 되기 위한 노력은 모두 그대들을 위함입니다. 저라는 사람을 믿고 의지하는 성은, 가족을 위해 헌신하고 매사 최선을 다하는 모습이 존경스럽고, 평생동안 의지가 될 수 있도록, 겸손하고 노력하겠습니다. 그리고 복덩이 우리 아들 예준이, 항상 생각하면 가슴이 따뜻해지고, 기쁨이 차오르게 해줘서 감사합니다. 그대 덕분에 부모님의 마음을 조금이나마 이해 할 수 있고, 삶의 의미를 알아나가고 있습니다. 우리 가족의 행복을 위해 기어코 헌신하겠습니다. 모두 사랑합니다.

2021년 8월 11일

곽호정 올림